ROLE OF RAT NEURONAL OSCILLATIONS IN ACQUISITION AND DISRUPTION OF WORKING MEMORY WITH ACUTE ETHANOL

DISSERTATION

Presented in partial fulfillment of the requirements for the degree Doctor of Philosophy in the Graduate School of The Ohio State University

By

Kristin Edwards Supe, M.A.

Graduate Program in Psychology

The Ohio State University

2014

Dissertation Committee:

Dr. Ben Givens, Advisor

Dr. John Bruno

Dr. Derick Lindquist

Abstract

The set of experiments within this dissertation were designed to characterize neural oscillations within *in vivo* local field potentials recorded simultaneously from the hippocampus, medial prefrontal cortex, and anterior cingulate cortex of rats while performing a goal maintenance operant working memory task. Detailed behavioral and neurophysiological analyses were performed during the course of learning the task and after pharmacological challenge with acute ethanol. The primary goal was to enhance understanding of how the theta and gamma rhythms interact in the hippocampal-frontal cortex circuit to mediate successful and unsuccessful working memory performance.

First, detailed behavioral analyses were performed on the operant variable delayed non-match to position goal maintenance working memory task. Most animals were able to learn the task over time. The task had sufficient simplicity and complexity to avoid most floor and ceiling effects. Results indicate that as delay increased, performance generally decreased thus validating this task as assessing working memory function.

Next, neurophysiological analyses were performed on animals that eventually became fast or slow learners of the task to see if there were any early indicators predictive of good performance. Animals in the fast learning group had higher baseline theta in the medial prefrontal cortex and anterior cingulate cortex than animals in the slow group. The medial prefrontal cortex also elicited stronger stimulus-evoked

potentials than the anterior cingulate cortex. Both the medial prefrontal cortex and the anterior cingulate were more highly correlated with the ventral hippocampus in the early sessions compared to the late recording sessions, suggesting that the role of the hippocampus in the delayed non-match to position operant task may change over time.

Next, performance was disrupted by administering an acute pharmacological challenge with low to moderate doses of ethanol. Ethanol was found to predictably and dose-dependently impair several aspects of performance in the task including accuracy, rate of extraneous lever pressing, and rate of omissions.

Finally, the physiological correlates to the behaviorally disrupting effects of acute ethanol were investigated. In general we observed a slight increase in spectral power and hippocampal to frontal coherence at low doses and a decrease in these measures at high doses. Theta and gamma power were stronger in the medial prefrontal cortex but coherence with the ventral hippocampus was stronger in the anterior cingulate cortex.

In conclusion, the operant protocol used in these experiments is a viable tool for assessing working memory in animal models. The medial prefrontal cortex, the anterior cingulate cortex, and the ventral hippocampus are all brain regions that are involved in mediating working memory. Rhythmic activity in the theta and gamma frequency ranges demonstrates changes over the course of learning and after disruption with acute ethanol. Therefore, theta and gamma rhythms remain potentially fruitful neurophysiological correlates of working memory function and dysfunction.

KEYWORDS: Working Memory, Delayed Non-Match to Position, Local Field Potentials, Oscillations, Theta, Gamma, Power, Coherence, Ethanol

Dedication

This dissertation is dedicated to my tiny co-author, L.E.S.

You have grown alongside this dissertation;

I hope that you continue to grow and to learn something new every day.

Acknowledgments

I wish to thank my advisor, Dr. Ben Givens, for his guidance and assistance in completing this project. I would also like to thank my committee members, Dr. John Bruno and Dr. Derick Lindquist for their discussions and input.

I also wish to thank the undergraduate research assistants who volunteered their time to assist with many aspects of this project, including Geoffrey Bratsberg, Brendon Fusco, Shawn Herron, Ashley Lynn, and Alexa McGuire. Undergraduate research assistants who have volunteered to work on previous projects include Rochelle Mills, Ben Morgan, Darya Task, John Tucker, Jennifer Vesic, and Kelsey Ward.

I am grateful to the software support team, especially Geoff Horseman, at Cambridge Electronic Design for assistance with creating custom scripts for physiological data analysis functions. I extend my gratitude to the lab of Dr. John Bruno for the use of their cryostat and histological supplies and of Dr. Kathryn Lenz for the use of their microscope. Thank you also to Scott Burch, Paul Merry, and Mary Jones for providing invaluable administrative assistance throughout my time at Ohio State.

I would like to comment a note of appreciation towards all laboratory research animals that participated as subjects in the experiments included in this dissertation and other experiments along the way. Please note that this appreciation does not extend to Rat #12.

Many teachers have inspired me along the way including Patricia Latessa and Roger Yauss at Lakota West High School, Dr. Ryan Tweney at Bowling Green State University, and Dr. Melissa Beers at The Ohio State University. Thank you for modeling what it means to be a good teacher, and I hope to emulate you as I continue teaching others.

I would also like to extend my sincerest appreciations to the close friends and colleagues who provided moral and technical support throughout this project: Katie Alexander, Holly Brothers, Ellen Furlong, Sarah Hopp, Lexie Majorczyk, Michelle Pershing, Jackie von Spiegel, and Sarah Vunck.

Last but certainly not least, I wish to express my sincere thanks and appreciation to my family. Thank you to my grandparents and my numerous extended relatives for your support and understanding why I couldn't visit as much as I would have liked. For their unconditional love, support, and positive attitude, I extend my sincerest thanks to my parents and my husband. To Don Edwards, Carol Edwards, and Kyle Supe: I love you, I could not have done this without you, and I am thankful for each of you every day.

This research was supported by a grant from the National Institute on Alcohol Abuse and Alcoholism and funding from the Psychology Department at the Ohio State University.

Vita

2007……B.S., Psychology,
Bowling Green State University

2007……Distinguished University Fellow,
The Ohio State University

2008-Present……Graduate Teaching Associate,
The Ohio State University

2010……Graduate Associate Teaching Award Winner,
The Ohio State University

2010……Louise B. Vetter Teaching Award Winner,
The Ohio State University

2011……M.A, . Psychology,
The Ohio State University

Publications

Jones, K.L., Smith, R. M., Edwards, K. S., Givens, B. S., & Beversdorf, D.Q. (2010). Combined effect of maternal serotonin transporter genotype and prenatal stress in modulating offspring social interaction in mice. *International Journal of Developmental Neuroscience, 28,* 529-536.

Kinzeler, N. R., &, Edwards, K. S. (2009). Functional Implications for Modulating Neuropeptide Y Gene Expression in the Dorsomedial Hypothalamus. *Journal of Neuroscience. 29* (23) 7389-7391.

Slone, D. J., Gonce, L., Upal, M. A., Edwards, K., & Tweney, R. D. (2007). Imagery effects on recall of minimally counterintuitive concepts. *Journal of Cognition and Culture. 7*, 355-367.

Tweney, R. D., Upal, M. A., Gonce, L., Slone, D. J., & Edwards, K. (2006). The creative structuring of counterintuitive worlds. *Journal of Cognition and Culture, 6*, 483–498.

Fields of Study

Major Field: Psychology

Minor Field: Neuroscience

Table of Contents

List of Figures

List of Tables

Chapter 1: Introduction

The purpose of this general introduction is to provide a broad overview of the topics and relevant literature germane to the experiments included in this dissertation. The cognitive behavior of interest, working memory, is reviewed from both theoretical and experimental perspectives. Next, neuroanatomical regions of interest and connections associated with function and dysfunctional aspects of working memory are identified. Neural oscillations are presented as a general mechanism which could connect distal brain regions for successful and unsuccessful working memory performance. Specific emphasis is placed on the theta rhythm, the gamma rhythm, and synchronous interactions between these two rhythms within the brain regions of interest. Next, there is a brief overview of the potential utility of acute alcohol as a tool to gain further mechanistic understanding of the neuro-oscillatory mechanisms underlying encoding and retrieval of working memory.

1.1. Overview of Working Memory

Everything we have ever experienced has the potential to be encoded into our memory, stored indefinitely, and recalled at will. Memory can be broadly defined as the process by which information is retained over time. Many different subtypes of memory have been identified, but the memory of the moment, generally identified as working memory, has a profound impact over daily life. Working memory refers to the system or

systems that are assumed to be necessary in order to keep things in mind while performing complex tasks such as reasoning, comprehending, and learning (Baddeley, 2010). Working memory has a rich theoretical history, many clinical implications, and a rapidly developing body of research on the specific neuroscientific mechanisms. Performance on working memory tasks generally improves over development and peaks in early adulthood. The capacity and duration of working memory is thought to decline as people age, are diagnosed with certain neurological or psychological disorders, or have impaired brain functioning. Notably, performance on working memory tasks gradually declines starting in about the sixth decade of life, creating a cognitive struggle in the elderly population. Working memory is also closely related to many measures of intelligence (Ma et al., 2014). Working memory function and dysfunction have been areas of increasing interest because they have an undeniably profound impact upon daily life.

The term working memory was originally coined in 1960 by Miller, Glanter and Pribam in their book 'Plans and the Structure of Behaviour.' The concept of working memory gained popularity as an elaboration of the multi-modal memory model developed by Atkinson and Shiffrin (1968). According to this model, memory involved a sequence of three dissociable but highly related stages: the very brief and limited sensory memory, the slightly longer lasting and larger capacity short-term memory, and the potentially limitless long-term memory. Many researchers saw a connection between the capacity and duration of the short-term memory store and the concept emerging as working memory. Working memory refers to information held online with active maintenance during performance of a task (e.g., remembering a telephone number while

dialing a phone). Baddeley and Hitch (1974) introduced the popular multicomponent model of working memory. In this theoretical model, a central executive supervises multiple slave systems depending on the modality of information to be processed. Verbal or auditory information is processed in a theoretical phonological loop whereas visual information is processed in a theoretical visuospatial sketchpad. More recently, this model has been updated to include a third slave system for autobiographical information processed in a theoretical episodic buffer (Baddeley, 2000). Additional interpretations of working memory emphasize the "working" aspect and say that it is one specific type of short-term memory that involves active manipulation of information by the individual (Eichenbaum and Cohen, 2001). Cowan defines working memory as a cognitive process that retains information in an unusually accessible state, likely due to the narrow focus of attention (Cowan, 2005). Ma and colleagues define working memory as the short-term storage and manipulation of sensory information lasting on the order of seconds (Ma et al., 2014). If all of these definitions are combined, then it could be said that working memory refers to a specific subtype of short-term memory that is actively focused on and manipulated over a relatively brief moment of time.

Ideas about the capacity of information manipulated and maintained within working memory have also changed over time. The classic view has been that working memory is limited in capacity and holds a finite, small number of discrete items. George Miller first posited the "magic number" 7 ± 2 chunks of information for the limits of working memory capacity (Miller, 1956). Somewhat controversially, Nelson Cowan has recently argued that mental storage capacity should be revisited and that a "magic number" of 4 might be more appropriate (Cowan, 2001). More recently, it has been

suggested that the specific numerical limits of working memory capacity might not be as important and may change based on contextual demands. In a recent review, Ma et al. (2014) suggest that a better way of thinking about working memory might be to think of it as a limited resource that is flexibly distributed among various items to be maintained, and that the quality rather than the quantity of working memory representations is what determines performance.

Executive functions, including working memory, are frequently affected in patient populations. Deficits in working memory have been reported in many different psychological and neurological conditions, including schizophrenia, Alzheimer's disease, alcoholism and related conditions such as Korsakoff's syndrome, and many others (Schnitzler & Gross, 2005). In particular, working memory impairments have been described as a core feature of schizophrenia (Lewis, 2012). Working memory impairments within the schizophrenic population are one of the most reliable indicators of a person's overall prognosis, but they typically fail to respond to traditional antipsychotics. A consortium of researchers and clinicians, called the Cognitive Neuroscience Treatment Research to Improve Cognition in Schizophrenia (CNTRICS), has started identifying specific constructs of working memory impaired in patients with schizophrenia including goal maintenance, memory capacity, and interference control (Barch and Smith, 2008). Goal maintenance is especially thought to represent prefrontal cortex mediated proactive control, which is a form of cognitive processing in which goal relevant information is actively maintained in a form that biases attention, perception and action towards the achievement of that goal (Barch and Ceasar, 2012). Goal maintenance is further defined as "the processes involved in activating task-related goals or rules

based on endogenous or exogenous cues, actively representing them in a highly accessible form, and maintaining this information over an interval during which that information is needed to bias and constrain attention and response selection" (Barch and Smith, 2008, p. 13). Goal maintenance taps into key aspects of working memory that have been explored in animal models of working memory.

1.2. Working Memory Tasks in Animal Models

The term 'working memory' was first applied to animal cognition in the now-classic radial arm maze experiments of Olton and Honig in the 1970's. In these experiments, during a single session rats were seemingly able to remember which arms they had already visited and avoid futile repeat entries. Honig (1978) defined working memory as a representation of a cue over a delay period in which the cue is not present, in order to make a subsequent response. According to Honig's definition, working memory would function only on a particular trial, but then must be forgotten or ignored for successful performance on subsequent trials. In this terminology, "working memory" essentially and incorrectly refers to episodic-like memory of previous responses and misses the critical component of active manipulation, such as maintenance of a specific goal. Other researchers have since tried to improve the definition of working memory as applied to animal cognition. Dudchenko defines working memory as a short term memory for an object, stimulus, or location that is used within a testing session, but not typically between sessions (Dudchenko, 2004). As far as animals are concerned, working memory is typically a delay-dependent representation of stimuli that is used to guide behavior within a task towards a specific goal. This is contrasted with reference memory

which is a longer-term memory for the rules of a given task. Reference memory generally possesses more episodic-like qualities and less active manipulation of information.

Many different animal behavioral tasks have been developed to assess working memory function and dysfunction (Dudchenko, 2004 for review). Maze tasks to assess spatial working memory are among the most commonly used. These include radial arm maze tasks, delayed alternation tasks, and the Morris Water Maze. Radial arm mazes and delayed alternation tasks, such as the T maze and Y maze paradigms, capitalize on rodents' tendency to explore novel territories within a maze rather than revisit previous areas. In these tasks, the initial exposure is separated by a delay, and the animal must remember the initial response to select the alternative novel response. The Morris water maze task requires rats to find and remember the location of a submerged platform in order to escape from a large, circular pool of water. Other tasks that have a goal maintenance component that have been used in animal models include contextual control of response task (also known as an operant rodent Stroop task), touch-screen based visual discriminations, discrimination reversal learning, and 8-arm delayed win-shift mazes (Dudchenko et al., 2012). Notably, the majority of these commonly used tasks tap into highly spatial components of working memory and require the animal to actively traverse through the experimental apparatus. This creates potential locomotive confounds as well as cognitive confounds from spatial navigation.

Delayed matching or non-matching to sample tasks (D(N)MTS) comprise another category of commonly used working memory tasks. D(N)MTS tasks have been used with a variety of stimuli, such as objects, odors, or locations. Delayed matching to sample tasks require an animal to remember a sample stimulus over a delay in which the stimulus

is no longer present with the goal of selecting the same stimulus in the choice phase. Conversely, delayed non-matching to sample tasks require an animal to remember a stimulus over a delay in which the stimulus is no longer present with the goal of selecting a novel or unfamiliar stimulus in the choice phase. D(N)MTS tasks have been successfully used in rodents, non-human primates, humans, and various patient populations to assess goal-maintenance working memory. The translational potential of using a similar task across so many different subject populations, and less confounds from spatial processing and locomotion, are noteworthy advantages of this task.

1.3. Brain Regions associated with Working Memory

A large body of evidence suggests that the hippocampus (HPC) and the medial prefrontal cortex (mPFC) are critical structures in successful working memory performance (Preston & Eichenbaum, 2013). Functional connectivity between these areas has been implicated in the dynamics of working memory in both healthy and diseased human brain states (Poch and Campo, 2012). In animal models, when plasticity of direct connections from the HPC to the mPFC was disrupted, working memory performance was impaired (reviewed in Laroche *et al*., 2000; Hyman *et al*., 2010). Furthermore, lesions that cause reductions in local field potential activity (LFP) in the bilateral HPC or mPFC, or ipsilateral cross combinations of the two regions, significantly impaired spatial working memory performance of rats in a delayed spatial alternation task (Wang and Cai, 2006). It has been suggested that the HPC and the PFC process qualitatively different components associated with working memory tasks and act in a synergistic manner (Yoon *et al*., 2008). These authors hypothesize that the mPFC is

primarily engaged in the temporary storage and processing of information in the range of a sub second to several seconds, while the hippocampal function becomes more critical as the working memory demand extends into longer temporal scales.

The Hippocampus

Influential early neuroanatomists Santiago Ramon y Cajal and Rafael Lorente de Nó first noticed differences in anatomical input along the dorsal-to-ventral axis of the hippocampus. Cajal noticed that the superior path from the entorhinal cortex terminated on what is now known as the dorsal hippocampus, and the inferior path from the entorhinal cortex terminated on what is now known as the ventral hippocampus. Lorente de Nó divided the *Cornu Ammonis* (CA) field into 3 main segments along the longitudinal axis according to different afferent inputs. Despite these early anatomical observations, the hippocampus has historically been thought of as a highly integrated structure that functioned as a single unit during memory processes. Based on three lines of evidence, Moser and Moser (1998) suggested that the hippocampus was not a unitary structure but instead was functionally differentiated along its dorsoventral axis. The first line of evidence was that the dorsal HPC and the ventral HPC have distinct inputs and outputs. Second, spatial memory appears to depend on the dorsal HPC, but not ventral HPC. Third, behaviors related to emotional regulation appear to depend on the ventral HPC, but not the dorsal HPC. Recent behavioral, anatomical and gene expression evidence supports a functional segmentation of the HPC into three distinct zones: dorsal, intermediate, and ventral (Fanselow and Dong, 2010).

The dorsal hippocampus (also known as rostral, septal, or posterior sub-region in primates) is associated with cognitive functions, especially spatial navigation. It is well known that lesions to the dorsal hippocampus, but not ventral, drastically impair functioning on spatial memory tasks such as the Morris water maze or radial arm maze. As reviewed by Fanselow and Dong (2010), anatomical features of the dorsal hippocampus suggest that it is particularly suited for this role in spatial memory. First, the dorsal hippocampus receives information from the caudolateral band of the entorhinal cortex. The caudolateral band receives predominately visual information from the adjacent perirhinal and postrhinal cortices and projects specifically to the dorsal hippocampal region. Interestingly, the dorsal hippocampus contains the greatest density of place cells, including the cells that are the most sensitive to location. Place cells are those that exhibit a high rate of firing whenever an animal is in a specific location in an environment corresponding to the cell's specific place field. The dorsal CA1 sends sequential, multi-synaptic, excitatory projections to other dorsal regions of the hippocampal formation including the subiculum, presubiculum, and the postsubiculum. Similar to the hippocampus proper, the dorsal fields of the subiculum contain the more head direction cells than any other region. Head direction cells fire when the head is oriented a particular way, thus encoding the head's position in space. In rats, the most prominent cortical projections from the dorsal CA1/subiculum are to the retrosplenial and anterior cingulate cortices (Cenquizca & Swanson, 2007). These cortical regions have been associated with the processing of visuospatial information and memory processing. The dorsal subiculum sends massive parallel projections through the post-commissural fornix to the medial and lateral mammillary nuclei and the anterior thalamic complex.

The dorsal CA1—dorsal subiculum —mammillary body—anterior thalamic nuclei pathway provides an important circuit implicated in the mediation of cognitive processes including learning, spatial memory, and navigation.

In contrast, the ventral hippocampus (also known as caudal, temporal, or anterior sub-region in primates) is associated with regulation of stress, emotion, and affect. The ventral hippocampus, but not dorsal, is required for anxiety-like behavior and shows increased synchronization with cortical areas during exploration of anxiogenic environments (Adhikari *et al*., 2010). As reviewed by Fanselow and Dong (2010), anatomical features of the ventral hippocampus suggest that it is particularly suited for this role in emotional regulation. The ventral hippocampus receives information from the medial band of the entorhinal cortex. The medial band receives primarily olfactory, visceral, and gustatory inputs and projects specifically to the ventral hippocampal region. In rats, ventral CA1 projects strongly to the ventral subiculum and to olfactory areas including olfactory bulb, anterior olfactory nucleus, piriform cortex, and endopiriform nucleus. Ventral CA1 and ventral subiculum share large bi-directional connections with amygdala and agranular insular cortices and indirectly connects with the hypothalamus. The connections with the amygdala and hypothalamus further support a role in emotional regulation. In particular, the hypothalamus relates to neuroendocrine, autonomic, and somatic activities associated with motivated behaviors that have strong emotional components, such as eating, drinking, and reproducing. One hypothalamic target is the suprachiasmatic nucleus, a region important for pacing circadian rhythms. Notably, the ventral hippocampus also sends a projection through the fimbria and fornix to reach the

lateral septum, shell of the nucleus accumbens, pre-limbic/infra-limbic region of the prefrontal cortex, and the medial orbital cortex (Laroche *et al*., 2000)

According to the distinctions by Fanselow and Dong (2010), there is an intermediate zone between the dorsal and ventral regions of the hippocampus. This intermediate zone receives widespread intermixed cortical inputs from the intermediate band of the entorhinal cortex. There is some functional overlap with dorsal and ventral regions and this region may be an area for integration of functions. The intermediate hippocampus sends moderate projections to olfactory areas and prefrontal cortex, but the ventral hippocampus sends stronger projections in all cases.

The Prefrontal Cortex

Similar to the hippocampus, the prefrontal cortex does not function as a unitary structure but can be compartmentalized further. In human studies, the dorso-lateral prefrontal cortex has been strongly implicated in mediating executive functions, including working memory (Goldman-Rakic, 1994) and has also been hypothesized as potential neural manifestation of the central executive in the multicomponent model of working memory (Baddeley and Hitch, 1974). Rodents do not have a dorso-lateral prefrontal cortex per se, but homologous regions exist and support variety of processes associated with executive function including working memory, temporal processing, prospective coding, flexibility, rule learning, and decision making. Based primarily on architectonics and connectivity with other structures, as reviewed by Kesner and Churchwell (2011) the rodent PFC can be categorized broadly into dorsomedial, ventral medial, dorsolateral, and ventral lateral sub-regions. The dorsomedial region has major

connections with the neocortex and includes the precentral cortex, dorsal anterior cingulate cortex, and ventral anterior cingulate cortex. The ventral medial region has major connections with the limbic system and includes the prelimbic, infralimbic, and medial orbital cortices. The dorsolateral region has major connections to neocortical areas, especially for smell and taste, but no connections with the limbic system. It includes dorsal and ventral agranular insular cortex, and lateral orbital cortices. The ventral lateral region also has major connections to neocortical areas, especially for smell and taste, but no connections with the limbic system. It includes the ventral orbital and ventrolateral cortices. Broadly speaking, response information is mediated by the medial PFC, spatial location and visual object information is mediated by the ventromedial PFC, and odor/taste information is mediated by the lateral PFC.

The rodent ventromedial PFC is the closest homolog to the human/primate dorsolateral PFC (Kesner & Churchwell, 2011). Lesions to the prelimbic, infralimbic, or medial orbital areas produce deficits in spatial working memory and visual object working memory (Jones, 2002). Lesions do not produce a deficit in working memory for a food reward indicating that effects are primarily cognitive and not motivational in nature. Primary afferents to the vmPFC include the medial dorsal nucleus of the thalamus, parataenial nucleus of the thalamus, midline thalamic nuclei, the limbic system, limbic association areas such as perirhinal cortex, entorhinal cortex, ventral hippocampus, basal nucleus of the amygdala, and medial basal forebrain. Primary efferent projections of the prelimbic area include the ventromedial part of the caudate putamen and core of the nucleus accumbens; the primary efferent projection of the infralimbic/medial orbital areas includes the medial shell of the nucleus accumbens.

1.4. Anatomical connections between the hippocampus and the prefrontal cortex

Previous anatomical tracing studies describe a direct pathway from the ventral hippocampal CA1/subiculum that progresses through the fimbria and fornix to reach the medial portion of the lateral septum, nucleus accumbens, and the prelimbic and infralimbic regions of the ventromedial PFC (Jay and Witter, 1991; Thierry *et al*., 2000; Cenquizca and Swanson, 2007; Hoover and Vertes, 2007). There are not projections from the CA2/CA3 areas of the ventral hippocampus, nor any areas from the dorsal hippocampus or the dentate gyrus (Laroche *et al*., 2000). The vHPC-PFC pathway originates in the stratum pyrmidale of ventral CA1 (Thierry *et al*., 2000) and terminates in all layers of the mPFC, but terminals are most densely distributed in deep layers V and VI of the prelimbic area (Laroche *et al*., 2000; Parent et al., 2010), where they preferentially form asymmetric, excitatory synapses on dendritic spines of pyramidal cells. The PFC does not send direct projections to hippocampus therefore this direct pathway is unidirectional (Thierry *et al*., 2000). Although the direct HPC-PFC projection is unidirectional, there are several anatomical regions that could allow indirect bidirectional communication between the ventral hippocampus and the prefrontal cortex.

One potential region for indirect interaction between the hippocampus and the prefrontal cortex is the midline thalamus. The classic definition of the prefrontal cortex is the part of the frontal lobe with the strongest reciprocal connections between midline nuclei of the thalamus (Thierry *et al*., 2000). The nucleus reuniens is the largest midline thalamic nucleus and is a major source of afferents to hippocampal and parahippocampal cortical structures, including ventral CA1/subiculum (Vertes, 2006; Varela et al., 2013).

The nucleus reuniens may serve as a relay between the hippocampus and prefrontal cortex. A hypothesized feedback loop would flow from ventral hippocampus (CA1/Subiculum) to the ventromedial prefrontal cortex, then to the nucleus reuniens of the thalamus, and finally back to the ventral hippocampus.

Another potential region for indirect interaction between the hippocampus and prefrontal cortex is the nucleus accumbens. The ventromedial PFC and the ventral CA1/subiculum of the HPC both send direct projections to the nucleus accumbens (Thierry *et al*., 2000). The nucleus accumbens is a region of the ventral striatum particularly implicated in goal-directed behavior and reward. The nucleus accumbens subsequently projects to the pallidum, substantia nigra, and hypothalamus. The nucleus accumbens appears to act as an interface between limbic and motor regions, and may be a major area of indirect communication between the HPC and the PFC. Further support for the nucleus accumbens as an integrative hub is that the PFC, HPC, and nucleus accumbens all have reciprocal connections with the ventral tegmental area (VTA), a major source of dopaminergic modulatory influence (Thierry *et al*., 2000).

As suggested by innervation from the ventral tegmental area, it is likely that dopamine plays a key role in modulating the HPC-PFC circuit. Optimal level of dopamine receptor activation is critical for delay cell function, a hypothesized physiological trace of working memory in the primate DLPFC (Goldman-Rakic, 1994). Dopamine projection from VTA to PFC is critical for normal PFC function and has been shown to modulate attention and working memory (Laroche *et al*., 2000). The highest density of dopamine neurons in the PFC is in layers V and VI of the prelimbic cortex, most of which terminate on dendritic shafts of pyramidal neurons (Laroche *et al*, 2000).

This pattern of termination corresponds with the projections from the ventral hippocampus discussed above and it is likely that these projections are in close proximity to each other and may even terminate on the same dendrites. Disrupting mesocortical dopamine projections to the PFC modulates HPC-PFC interaction (Goto and Grace, 2008; Laroche *et al*., 2000). Goto and Grace have suggested that differential dopamine receptor activity in the prefrontal cortex can mediate different cognitive strategies in a radial arm memory task with different memory demands. The authors suggest that D1 and D2 receptor activation in the PFC differentially affects retrospective memory processing within the hippocampus via an indirect pathway. Furthermore, D1 activity is crucial for incorporation of HPC-based retrospective info into the PFC, and D2 activation is required for further processing of info to effect preparation of future actions and shift to a prospective strategy (Goto and Grace 2008). Thus, dopaminergic ascending systems which innervate the HPC, PFC, and nucleus accumbens may modulate or "gate" information processing at different levels of these circuits (Thierry *et al*., 2000)

Several lines of evidence suggest that the HPC-PFC pathway is ipsilateral, monosynaptic, and glutamatergic (Jay *et al*., 1995; Laroche *et al*., 2000; Thierry *et al*., 2000; Parent et al., 2010). Normal neurotransmission at HPC to PFC synapses is AMPA receptor dependent (Jay *et al*., 1992), but long-term potentiation (LTP) at HPC to PFC synapses is NMDA receptor dependent (Jay et al., 2006). Under normal conditions, stimulation of the ventral CA1/subiculum evokes robust LTP in the PFC characterized by significant increase in the amplitude of an evoked response. Animals treated with D-AP5, an NMDA antagonist that selectively binds to the glutamate site, during the tetanus failed to induce LTP. There was no significant difference between the pre-tetanic and

post-tetanic response, and tetanic stimulation 1 hour after D-AP5 administration produced reliable LTP. This indicates that activation of NMDA receptors is required for induction of LTP in this pathway. LTP is widely accepted as a potential means of physiological storage of information.

1.5. Overview of neural oscillations

Neural oscillations appear on recordings as a sinusoidal rhythm of electrical activity in the extracellular field potential. Once mistakenly thought of as an artifact or an epiphenomenon, oscillatory patterns of synchronous activity within the brain have emerged as an area of considerable interest. Oscillation synchrony is an emergent property of networks, generated by temporal coordination between synaptic transmission and firing of individual neuron populations (Buzsàki, 2006). Gross synchronized electrical oscillations in the brain have become very popular as a possible binding mechanism for coordinating many different levels of neural processing (Buzsàki, 2006). Oscillations are highly heritable traits that are less complex and more proximal to gene function than traditional diagnostic labels or cognitive measures, and thus and have been described as a potential "phenotype of cognition" and as a valuable tool for understanding genetic disorders and other pathologies (Porjesz et al., 2005). Changes in oscillatory dynamics have been observed in patients with Alzheimer's disease, bipolar disorders, schizophrenia, mild cognitive impairments, genetic disorders, ADHD, and alcoholism (Başar et al., 2001; Başar and Güntekin, 2008). Schizophrenia, for example, has been described as a "disconnection syndrome" in which several brain areas demonstrate impaired communication with each other altered via oscillatory activity

(Jones et al., 2010). It is worth noting that there is significant overlap in disorders with changes in oscillatory dynamics and disorders in which cognitive deficits, specifically in the domain of working memory, are key symptoms.

Neural activity in the brain produces transmembrane currents that can be measured in the extracellular medium. Electric fields can be monitored by extracellular electrodes with temporal resolution in the sub-millisecond range. Several methodological approaches are available to investigate extracellular electric fields. In electroencephalography (EEG), electrodes are placed at the surface of the scalp to look at the brain's electrical signals. It was through early EEG experiments that neural oscillations were originally discovered. The magnetic field induced by the same electrical activity is recorded through magnetoencephalography. In electrocorticography, subdural grid electrodes are placed directly on the cortical surface. This provides a more accurate reading than EEG, but there are more risks associated with the highly invasive procedure. Local field potentials (LFP) are recorded when metal, glass, or silicon electrodes are placed deep within the brain. LFPs are also known as micro-, depth, or intracranial EEG recordings. Depending on the size of the electrode, LFPs can measure the extracellular field that results from the activity of tens to hundreds of neurons (Kajikawa & Schroeder, 2011). LFP signals have excellent temporal resolution, but multiple electrodes are needed to resolve the precise spatial location of the signal and construct larger circuit models.

Any excitable membrane and all transmembrane currents contribute to the extracellular field potential. The field represents the superposition and aggregation of all ionic processes involving sinks and sources. A sink is a site on a neuronal membrane

where positive charges enter the neuron, while a source is a site where positive charge flows out of the neuron. For negative charges, sinks and sources are inverted. Excitatory postsynaptic currents, and to a slightly lesser extent inhibitory postsynaptic currents, are the most prominent contributors to the field potential (Buzsàki et al., 2012). When an excitatory receptor is activated, an influx of cations such as sodium or calcium flow into the cell and create a local sink. To achieve effective electroneutrality, the sink needs to be balanced by an extracellular source of outward cation movement, known as a passive or return current. This influx and efflux of cations creates an electrical dipole, which can be measured by electrodes. Inhibitory currents are typically assumed to add relatively little to the extracellular field as the equilibrium potential for chloride is very close to the resting membrane potential, so there is less net movement of anions than cations.

Although the transmembrane current is the major contributor to the extracellular field potential, other sources such as action potentials, ionic fluxes through transporters, and intrinsic membrane oscillations, can contribute to the extracellular signal (Buzsàki et al., 2012). Action potentials generate the strongest currents across neuronal membranes, but are often of such short duration (< 2 ms) that an individual action potential will not have a significant bearing on the extracellular field potential. However, synchronous action potentials from many neurons can contribute substantially to LFP signals, particularly higher frequency components of the LFP. To contribute substantially to the LFP, resonant membrane potential fluctuations must occur synchronously in many nearby neurons, a feature that most commonly occurs in networks of inhibitory interneurons (Buzsàki et al., 2012). Additionally, it is worth nothing that all neurons are surrounded by a conducting medium in the extracellular space and can 'sense' the electric

gradients generated during processing by nearby neurons. The extracellular field can influence the transmembrane potential of a neuron via ephaptic coupling, thus the extracellular field environment can influence the extracellular field signal. The environmental influence over a signal can be observed in other phenomena, such as metronomes or large crowds of people applauding at different beats that eventually become coordinated over time.

The magnitude and sign of the individual current sources, their spatial density, and the temporal coordination of the respective current sources shape the extracellular field. The two most important things for determining the strength of the extracellular field are the temporal synchronies of the dipole moments they generate and the spatial alignment of the neurons. When structures are cytoarchitecturally regular, such as in the cortex, the apical dendrites of pyramidal neurons are parallel to each other and the afferent inputs run perpendicular to the dendritic axis. This geometry is ideal for the superposition of synchronously active dipoles, and is a primary reason why LFPs are often largest in the cortex (Buzsàki et al., 2012).

Neural rhythms are a ubiquitous phenomenon across all animals. Every known pattern of oscillations in the human brain is present in other mammals with similar frequencies, duration, temporal evolution, and behavioral correlations (Buzsàki et al., 2013). Despite major differences in brain size, the hierarchy of brain oscillations remains among the most well-preserved phenotypes in mammalian evolution (Buzsàki et al., 2013). The preservation of cortical rhythms despite substantial variability in brain size is unlikely due to an inability of the brain to change its timing mechanisms; instead the similarity across species highlights the importance of precise neural timing mechanisms.

Oscillatory rhythms are an efficient way for large groups of neurons to be in states of maximal depolarization when information arrives (Buzsàki, 2006).

Brain rhythms cover more than four orders of magnitude in frequency, from the infraslow (<0.01 Hz) to the ultrafast (200-600 Hz), with at least 10 interactive classes of oscillations (Buzsàki et al., 2013). The five most common oscillatory rhythms were named as symbols of the Greek alphabet in order of their discovery. The alpha rhythm oscillates at 7-14 Hz in humans and is often correlated with a relaxed, closed-eye state. The beta rhythm oscillates at 15-30 Hz in humans and is often associated with alertness or active concentration. The gamma rhythm oscillates at 30-100+ Hz in humans and is often associated with sensory processing. The delta rhythm oscillates at 1-4 Hz in humans and is associated with slow-wave sleep. The theta rhythm oscillates at 4-7 Hz in humans and is associated with some locomotor tasks and may play a significant role in learning and memory. Interestingly, the mean frequencies of neuronal oscillators form a linear progression on a natural logarithmic scale (Buzsàki & Draguhn, 2004).

1.6. The Theta Rhythm

In particular, the oscillatory rhythm known as theta has been hypothesized as a potential control mechanism of working memory (Sauseng *et al*., 2010). In human studies, there is growing evidence that theta is involved in central executive function, and that the power of theta during encoding in the right temporal and frontal cortex may predict subsequent memory performance (Sederberg *et al*., 2003). Theta power is significantly greater for stimuli that are later remembered than stimuli that are later forgotten and there is an inverse relationship between activation of theta and the default

mode network indicating that theta oscillations may be key in attenuating processes which would otherwise impair encoding (White *et al*., 2012).

The theta rhythm is a relatively large amplitude (1-2 mV) repeating sinusoidal pattern that does show some frequency variation across species. Rodents show theta oscillations at 6-10 Hz, with a peak of prominent activity around 7 Hz (Vanderwolf, 1969; Buzsàki, 2002). Meanwhile, carnivores show theta oscillations 4-6 Hz and humans have the slowest theta frequency observed, typically around 4 Hz (Buzsàki et al., 2013). A potential argument for the decreasing frequency and irregularity of hippocampal theta oscillations in mammals as brain size increases is that the hippocampus processes information as a single cortical module and axon conduction delays limit its growth.

There are two distinct types of theta activity. Type I theta is associated with voluntary locomotor functions, like walking or running. Type II theta is at a slightly lower frequency and is correlated with sensory processing, immobility, or involuntary motor behaviors such as licking, shivering, or scratching. Type I theta is resistant to impairment from atropine, a muscarinic acetylcholine antagonist, but Type II theta is abolished by atropine thus suggesting that Type II is mediated by cholinergic mechanisms, but Type I theta is not (Bland and Oddie, 2001; Givens, 1996).

Voltage-dependent resonance and oscillations at theta frequency have been described in principal neurons of several cortical regions (Buzsàki et al., 2012). The theta rhythm typically has the largest amplitude in the hippocampal formation, but subcortical pathways contribute to the synchronization and maintenance of the hippocampal theta rhythm. The supramammillary nucleus projects to the medial septum / vertical diagonal band of Broca where tonic excitation is converted to phasic, rhythmic firing (Vertes et al.,

2004). The medial septal region is often thought of as a pacemaker that helps coordinate hippocampal theta activity and activates intrinsic theta neurons (Givens et al., 2000). The medial septum communicates with the hippocampus via cholinergic and GABA-ergic projections. Ascending cholinergic pathways terminate predominately on principal cells within the hippocampus and GABA-ergic projections terminate predominately on hippocampal interneurons (Bland and Oddie, 2001). When the hippocampus transitions from large amplitude irregular activity to synchronized theta activity, the medial septum initiates two cellular changes that occur approximately 500 milliseconds before the transition and help synchronize theta activity in the hippocampus. The medial septum inhibits hippocampal theta-off cells, which provides tonic depolarizing inputs that initiate membrane potential oscillations in hippocampal phasic theta-on cells which in turn synchronize membrane potential oscillations of hippocampal phasic theta-on cells and discharge hippocampal tonic theta-on cells (Bland et al., 1999). Each theta cycle is a travelling wave that undergoes a half cycle (180°) phase shift from the septal to the temporal poles in the rat (Lubenov and Siapas, 2009).

Theta rhythm activity is especially interesting in relation to memory because of previously hypothesized involvement in separating encoding and retrieval. Encoding is analogous to storing a memory whereas retrieval is pulling a previously stored memory out for use. In a model proposed by Hasselmo and colleagues, encoding of memory is strongest at the peak of the theta wave whereas retrieval of memory is strongest at the trough (Hasselmo et al., 2002). According to this model, encoding occurs preferentially when excitatory connections from hippocampal region CA3 to CA1 are strong, but inputs to CA3 are week. Conversely, retrieval occurs during the phase when entorhinal

input is weak and inputs from region CA3 are strong (Hasselmo et al., 2002; Kunec et al., 2005; Manns et al., 2007). Some fundamental tasks, particularly those associated with short term or working memory, are performed better if memories are encoded and retrieved at different phases of theta activity (Kunec et al., 2005). For example, separate phases of encoding and retrieval enhance reversal of prior learning (Hasselmo et al., 2002). Theta activity at the hippocampus suggests a physiologically plausible mechanism for the context-dependent retrieval of episodes (Hasselmo & Eichenbaum, 2005) as would occur in working memory. High frequency stimulation at the peak of stimulus reset theta produced LTP whereas stimulation on the trough did not (McCartney et al., 2004). The theta rhythm allows the hippocampus to alternate rapidly between conditions that promote memory encoding and conditions that promote memory retrieval.

If theta phase is responsible for dissociating encoding and retrieval processes, then it would be important for the ongoing theta phase to demonstrate perturbation, such as phase reset, in response to stimuli. The first known report of theta reset found that CA1 hippocampal theta in cats was reset by a visual stimulus early in the stages of learning a visual discrimination task, but disappeared once performance plateaued (Adey, 1967). Recording of theta activity in rodents demonstrates that the onset of visual or auditory stimuli in a working memory task causes ongoing theta rhythm activity to reset such that it becomes temporally phase-locked to the sensory stimuli (Givens, 1996; Williams & Givens, 2003). In other words, mnemonically relevant stimuli reset the theta oscillation to the peak phase of activity. The purpose of hippocampal theta resetting may be to ensure that the hippocampal formation is in a maximal state of depolarization at the time of incoming sensory information from afferent projection sites. Theta rhythm

activity shows stimulus-evoked reset in rats performing a working memory task, but not in rats performing a reference memory task (Givens, 1996). Theta reset follows the presentation of stimuli across different sensory modalities, suggesting theta reset as a viable mechanism for mnemonic processing across different modalities. Consequently, theta reset in the hippocampus produces optimal conditions for long-term potentiation (LTP) (McCartney et al., 2004). Theta reset has also been observed in human participants. Rizzuto et al. (2003) administered a recognition memory task to epileptic patients undergoing intracranial EEG monitoring for seizure localization. They found that theta oscillations exhibited an almost instantaneous stopping and restarting following both encoding and retrieval of consonants. Importantly, the observed theta reset did not correspond with overall increases in oscillatory power, as would be expected from an evoked component of the EEG. The consistent phase of oscillatory activity following the presentation of the stimulus suggests that some stimulus-evoked cognitive process is able to reset the phase of ongoing theta oscillations. In a follow-up study involving similar patients and a verbal Sternberg working memory task, there were consistent theta phase differences between study and test stimuli. At 215 ms after stimulus presentation, theta oscillations showed a 180° phase difference between encoding and retrieval conditions (Rizzuto et al., 2006). Human working memory tasks are thought to be gated by theta oscillations (Raghavachari et al., 2001; Raghavachari et al., 2006) and human cortical circuits for central executive function emerge by theta phase synchronization (Mizuhara & Yamaguchi, 2007).

The hippocampus and prefrontal cortex are regions that are consistently associated with activity in the theta range (Williams and Givens, 2003). The theta

rhythm is often most prominent in the hippocampal formation and thus is associated with hippocampally-dependent memory functions. During consolidation and retrieval of episodic information, hippocampal theta activity is known to synchronize with prefrontal circuits (Siapas et al., 2005; Paz et al., 2008). It is clear that the transfer of information from hippocampal circuits to the medial prefrontal cortex mediates aspects of memory retrieval and consolidation (Wiltgen et al., 2004). The medial prefrontal cortical sites that receive afferents from the hippocampus appear to be particularly involved in task switching (Rich and Shapiro, 2007). In human studies that used subdural recording nets and found theta activity during encoding predicted successful recall, theta activity was clustered in the right temporal lobe and the frontal cortex (Sederberg et al., 2003). The hippocampal-entorhinal axis has population dynamics that allow populations of neurons to discharge in close temporal synchrony and thus communicate rapidly and effectively (Chrobak and Buzsáki, 1998).

Although the theta rhythm is often most prominent in the hippocampal formation, it is also known to show phase coupling with other brain regions. Theta phase synchronization between the hippocampus and PFC has been demonstrated in several studies. A significant portion of rat prefrontal neurons demonstrate a phase locking to hippocampal theta rhythm with a lag of about 50 ms, suggesting directionality to the phase coupling (Siapas *et al*., 2005). Theta phase coupling between the hippocampus and the PFC has also been found to increase in rats during performance of a spatial memory maze task (Jones and Wilson, 2005), and in mice experiencing anxiogenic contexts (Adhikari *et al*., 2010). Working memory performance has been found to correlate with prefrontal-hippocampal theta entrainment, but not necessarily with individual prefrontal

neuron firing rates (Hyman *et al*., 2010), emphasizing the importance of the population activity over the individual neuron activity. Together, this suggests that theta synchronization between the vHPC and pre-limbic/infralimbic region of the medial PFC may be a plausible model for neurophysiological correlates of animal and human working memory function.

1.7. The Gamma Rhythm

Gamma oscillations are thought to be a fundamental mechanism for integrating neural networks within and across brain structures, facilitating coherent sensory registration. The gamma rhythm oscillates at 30-100+ Hz in humans, primates, and rodents. Since gamma occupies a much wider range of frequencies than most neural oscillations, gamma can be broken down into slow (30-50 Hz) mid-frequency (50-90 Hz) and fast gamma or epsilon (90-140 Hz sub-bands) (Belluscio et al., 2012), but it is also common to refer to all of these sub-bands as simply gamma oscillations. Gamma oscillations are short-lived, can be quite variable in frequency, and typically emerge from the coordinated interaction of excitation and inhibition (Csicsvari et al., 2003). Gamma oscillations are typically associated with the neocortex but have also been found in the entorhinal cortex, hippocampus, amygdala, striatum, olfactory bulb, thalamus, and other regions with a high density of inhibitory interneurons and GABA-A synapses (Buzsàki &Wang, 2012). Gamma oscillations are thought to arise from intrinsic membrane properties of inhibitory interneurons or from neocortical excitatory-inhibitory circuits (Sauseng & Klimesch, 2008). Network gamma oscillations may coexist with highly irregular or stochastic firing of pyramidal neurons, but perisomatic inhibition is essential

for gamma oscillations (Buzsàki &Wang, 2012). Perisomatic inhibitory interneurons have a preferred resonance in the gamma frequency range, particularly between 30 and 90 Hz (Buzsàki et al., 2012). Fast-spiking GABAergic interneurons, particularly those that express the calcium-binding protein parvalbumin (PV+) are central to the generation of gamma rhythm (Jones et al., 2010). PV+ neurons are the most abundant interneuron in the brain and they possess the largest dendritic tree, soma surface, and highest density of afferent synapses suggesting the activity level of these cells is higher than other interneuron populations (Timofeeva and Levin, 2011). PV+ interneurons include basket cells which innervate the soma and proximal dendrites of pyramidal cells, and chandelier cells which form axo-axonic connections on the axon initial segment of pyramidal neurons, placing them in an optimal position to regulate the timing of principal neurons (Jones et al., 2010). Furthermore, optogenetic activation of PV+ interneurons in the neocortex is sufficient to trigger emergent gamma frequency activity (Sohal et al., 2009). The timing of a gamma cycle of a cell assembly is closely related to several biophysical properties of neurons including the time constant of GABA-A and AMPA receptors, the membrane time constant of cortical pyramidal cells, and the critical window for spike-timing-dependent plasticity (Buzsàki &Wang, 2012).

Although gamma oscillations are locally generated, they can become synchronized over surprisingly long distances, such as across hemispheres, in a context-dependent way. There are two primary candidates for the mediation of gamma synchronization (Buzsàki et al., 2013). First, reciprocal fast-conducting glutamatergic projections originating from pyramidal cells could affect both inhibitory and excitatory

neurons in the target structure. Second, long-range inhibitory projections could directly link the inhibitory network in one region with another target region.

1.8. Relationships between theta and gamma rhythms

For working memory processes, it has been suggested that the gamma rhythm nests within the theta rhythm and acts as a multi-item working memory buffer within oscillatory sub-cycles (Lisman and Idiart, 1995; Jensen, 2006). This "nesting" would allow items that occurred seconds apart to be represented with a temporal separation of 20-30 ms, bringing 7 $\pm$ 2 items within the ~100 ms theta range typical for induction of LTP (Jensen and Lisman, 2005; Lisman & Buzsáki, 2008). Interestingly, 7 $\pm$ 2 chunks correspond perfectly with Miller's "magic number" for one of the hypothesized known limits of working memory capacity (Miller, 1956). Phase precession occurs in place cells when a rat runs along a well-known path. Precession depends on prior learning and has been interpreted as a cued recall sequence for upcoming places. Phase precession also provides evidence that physiology can represent prospective coding as an animal navigates through the environment (Jensen and Lisman, 2005). In the theta-gamma nesting model, as memory content moves forward, then a new item occupies the first gamma cycle and as it becomes inhibited the contents of subsequent cycles shift to a more competitive point for activation. The theta rhythm of the CA1 is not symmetrical, but it has an asymmetric saw tooth appearance with shorter, steep ascending and longer, gradual descending components of the wave (Belluscio et al., 2012). The implication for this finding with Lisman and Idiart's model is that if gamma period-associated cell assemblies represent separate items or positions, then the items are weighted differently

based on their position in the asymmetrical theta rhythm. This differential weighting of representations may be advantageous for cognition because it may strengthen time-forward connections similar to response chaining.

Coupling between the theta and gamma rhythms has emerged as a potential means of coordinating local and global cell assemblies (Lisman & Jensen, 2013). Entrainment of neocortical neurons and gamma oscillations by the hippocampal theta rhythm is one such example of local and global coordination (Sirota et al., 2008). Fast oscillations, such as the gamma rhythm, are thought to synchronize cell assemblies over relatively localized regions. Spatial integration from a local to global scale requires longer integration times and thus a slower clock mechanism, such as the theta rhythm (Jensen & Colgin, 2007). In humans, successful encoding of verbal stimuli showed increased theta and gamma activity, with the gamma activity observed to increase bilaterally at widespread cortical locations (Sederberg *et al*., 2003), thus supporting an emerging view of gamma as reflecting top-down attentional processes. Theta and gamma oscillations predict encoding and retrieval of declarative memory (Osipova et al., 2006). Recently, cross-frequency theta-gamma coupling has also been observed in the CA1 region of the rat hippocampus during maze exploration and rapid eye movement sleep, and the power of gamma rhythms is phase modulated by theta waves (Belluscio *et al*., 2012). It has also been shown that high gamma power is phase-locked to theta oscillations in the human neocortex (Canolty et al., 2006).

1.9. Measures of Synchrony

Phase synchronization of electrical oscillations reflects the precise timing of communication between distant but functionally related neural populations, the exchange of information between both local and global neural networks, and the sequential activity of neural processes in response to incoming stimuli. Phase synchronization can emerge in three main ways: phase synchronization across frequencies, phase coupling between brain regions, and phase resetting to external events or stimuli (Sauseng and Klimesch, 2008).

Phase synchronization across frequencies (also known as cross frequency coupling) between neuronal oscillations can occur in a variety of complicated ways that often overlap with each other. Examples of cross-frequency relationships include power to power, phase to phase, phase to frequency, and phase to power (Jensen & Colgin, 2007). In power to power coupling, the frequency remains fairly constant but the amplitude of the signal changes over time. In phase-phase coupling, the phase of a faster oscillation is coupled to multiple phases of a slower rhythm. The frequency of the fast oscillation is modulated by the phase of the slower oscillations in phase to frequency coupling (Jensen & Colgin, 2007). In phase to power coupling, the amplitude of a faster oscillation is modulated by the phase of a slower rhythm (Buzsàki &Wang, 2012). In this scenario, the faster rhythm appears nested within the slower rhythm. The phase of a faster oscillation is coupled to multiple phases of a slower rhythm in phase to phase coupling. . Cross-frequency coupling between fast and slow rhythms (e.g. between gamma and theta) may help facilitate the transient coordination of local networks on

short time scales and integrate multiple networks in distal locations across longer time scales (Jensen & Colgin, 2007).

Oscillations are most effective communicators when they can be perturbed by factors in the environment. Phase reset to external events or stimuli is one example of such environmental perturbation. Recording of theta activity in rodents demonstrates that the onset of visual or auditory stimuli in a working memory task causes ongoing theta rhythm activity to reset such that it becomes temporally phase-locked to the sensory stimuli (Givens, 1996; Williams & Givens, 2003). In other words, mnemonically relevant stimuli reset the theta oscillation to the peak phase of activity. The purpose of hippocampal theta resetting may be to ensure that the hippocampal formation is in a maximal state of depolarization at the time of incoming sensory information from afferent projection sites. Theta rhythm activity showed stimulus-evoked reset in rats performing a working memory task, but not in rats performing a reference memory task (Givens, 1996).

1.10. Memory and Alcohol

Drinking is pervasive in many cultures and is part of life for many individuals. According to 2012 data from the National Institute on Alcohol Abuse and Alcoholism, 87.6 percent of people aged 18 or older reported that they drank alcohol at some point in their lifetime; 71 percent reported that they drank in the past year; and 56.3 percent reported that they drank within the past month. Despite this near ubiquity, it is common knowledge that consumption of alcoholic beverages is associated with a variety of harmful cognitive, behavioral, medical, and social effects. The well-known effects of

alcohol on memory are of particular interest for the current studies. In American popular culture, it is commonplace to see characters drink to the point of forgetfulness. In extreme cases of excessive consumption, a person may have no declarative memory for events that occurred while drinking—a phenomenon popularly referred to as a blackout episode. Even though most people are aware of the potential consequences—including memory impairments—alcohol remains one of the most easily accessible and widely used psychoactive compounds.

In chemistry, an alcohol is an organic compound in which the hydroxyl functional group is bound to a carbon atom. There are many types of alcohols, such as methyl and isopropyl alcohol, but these are highly toxic and only ethyl alcohol (ethanol, C_2H_6O) can be used as an intoxicant. Therefore, the terms ethyl alcohol, ethanol (EtOH), and alcohol are often used interchangeably. Ethanol is a short chain, lipid-soluble compound that is classified as a central nervous system depressant. Depressants are substances that can slow down brain activity. The pharmacological effects of ethanol that contribute to these depressant effects are relatively well-understood. Ethanol increases the activity of γ-amino butyric acid (GABA), the chief inhibitory neurotransmitter in the brain, and decreases the activity of glutamate, a major excitatory amino-acid neurotransmitter.

Effects on GABA-ergic and glutamatergic transmission occur primarily through actions on postsynaptic receptors (Weight, 1992; Criswell and Breese, 2005). Alcohol is a GABA agonist / positive allosteric modulator that increases the inhibitory actions of GABA. Alcohol increases the actions of GABA at the receptor by increasing the amount of negatively charged chloride ions that can enter the cell. Alcohol has a specific binding site within the channel on GABA receptors, particularly GABA-A subtypes. The ethanol

binding site is also activated by steroids and by general anesthetics such as propofol and halothane. Barbiturates and benzodiazepines have similar effects to alcohol on GABA receptors. A potential mediating factor for ethanol's effects at hippocampal GABA-A receptors is allopregnanolone, a potent neuroactive steroid that functions as positive modulator of GABA-A receptors and has been shown to increase in the hippocampus with acute ethanol administration (Matthews & Silvers, 2004). Ethanol also acts as an uncompetitive antagonist of the NMDA glutamate channel. Ethanol blocks the NMDA channel so that calcium can no longer enter the neuron, thus reducing excitability.

Ethanol disrupts hippocampal activity, particularly in pyramidal cells, by both direct and indirect mechanisms (White et al., 2000). Ethanol interacts with membrane-bound proteins and ligand gated ion channels at synapses in the hippocampus, potentiating GABA-A receptor subtypes particularly on inhibitory interneurons or perisomatic regions of pyramidal cells. Ethanol increases the excitability of inhibitory interneurons in both CA1 and Dentate Gyrus regions of the hippocampus (Steffensen et al., 1993). Ethanol also affects hippocampal activity by altering cellular activity in afferent brain regions such as the medial septum, ventral tegmental area, and raphe nuclei (White et al., 2000). Ethanol suppresses cellular activity in the medial septum (Givens, 1996), but not the lateral septum (Givens and Breese, 1990). As mentioned previously, the medial septum has been hypothesized as a potential pace-maker region for the theta rhythm. Acute ethanol exposure elevates muscarinic tone in the septohippocampal system (Ericson et al., 2009). Activation of the dopaminergic ventral tegmental area or the serotonergic raphe nucleus inhibits excitatory pyramidal cells and potently excites inhibitory interneurons within the hippocampus (White et al., 2000).

Alcohol's immediate effects can appear within about 10 minutes. Blood alcohol concentration follows an inverted-U trajectory. As the blood alcohol concentration level increases, so does the general level of impairment. Alcohol has different effects on memory encoding and retrieval depending on the memory task, the type of memory involved, and the limb of the blood alcohol concentration curve (Söderlund et al., 2005). Most (90%) of alcohol is broken down by liver enzymes. Alcohol dehydrogenase converts alcohol into acetaldehyde. Accumulation of acetaldehyde causes an unpleasant reaction including skin flush, nausea, and headache. A single low dose (0.20 to 0.25 g/kg) of alcohol is usually completely metabolized within an hour.

The potential harm of alcohol consumption is indisputable and thus continued research on the specific consequences, particularly the physiological and psychological effects, and their underlying neural mechanisms is an important priority for public health. The Independent Scientific Committee on Drugs, an expert panel of researchers from a variety of disciplines, used a multi-criteria decision analysis model to assess the relative harm of many psychoactive compounds typically used for recreational purposes. Based on a combination of factors including physical, psychological, and social harm to both the using individual and to others, this panel scored drugs on a 100-point weighted scale where zero was no harm and 100 was the most harmful. Somewhat surprisingly, alcohol was scored, by far, as the "most harmful drug" with a combined score of 72, followed by heroin with a combined score of 55 , crack cocaine with a combined score of 54, and methamphetamine with a combined score of 33 (Nutt et al., 2010). The overwhelming prevalence and potentially grave consequences of alcohol use and abuse are major issues facing society.

Ethanol is a drug that is widely available, easily administered in a non-invasive fashion, is rapidly absorbed into the bloodstream, is relatively short-lasting, is fully reversible, and produces effects in specific brain regions including the hippocampus (Matthews & Silvers, 2004). Ethanol is associated with highly specific effects on memory functions. Ethanol preferentially blocks memory formation without impairing previously formed memories (Wixted, 2005). Alcohol is known to have effects on both GABAergic and Glutamatergic systems which have both been hypothesized to have an important role in establishing and maintaining neural oscillations such as the theta and gamma rhythms. Therefore, acute ethanol administration is a valuable pharmacological tool that can be used to investigate multiple memory systems and neurophysiological properties.

1.11. Specific Hypotheses

If the variable delayed non-match to position task protocol assesses goal-maintenance working memory, then increasing working memory load will affect performance. Specifically, performance will be best at short delay periods (5 seconds) and will progressively decline in a delay-dependent manner, culminating in near chance-level performance at long delay periods (15 seconds).

If theta and/or gamma oscillations in the ventral hippocampus, pre-limbic/infralimbic sub-region of the medial prefrontal cortex, and the anterior cingulate cortex are important for mediating working memory performance, then these oscillations should show differences between early pre-criterion testing sessions and late post-criterion testing sessions. Furthermore, oscillatory activity in these regions should show

dissociations between animals that become fast learners of the task and those that become slow learners of the task. Differences in oscillatory activity for these two time points and two groups will be investigated by assessing baseline power, waveform averages around task-relevant stimuli, and waveform correlations.

Phase reset and stimulus-evoked potentials will be assessed by peri-stimulus phase histograms and stimulus-triggered waveform averaging. If theta rhythm phase reset in the ventral hippocampal to medial prefrontal cortex pathway is a mechanism of memory retrieval, then phase reset will be seen preferentially at the start of the choice phase in the variable delay non-match to position operant working memory task.

If theta and/or gamma rhythm phase synchronization in the ventral hippocampus-frontal cortex circuit is involved in successful variable delayed non-match to position performance, then it is hypothesized that there will be greater phase coupling between the ventral hippocampus and the medial prefrontal cortex on correct trials but greater coupling between the ventral hippocampus and the anterior cingulate cortex on incorrect trials. Phase coupling between anatomical regions will be assessed via waveform correlation analyses.

It is also hypothesized that working memory performance will be disrupted by acute ethanol injections in both dose-dependent and delay-dependent manners. In addition to disruption in behavioral performance, it is hypothesized that acute ethanol injections will attenuate the observed power in both the theta and gamma frequency bands. Furthermore, it is hypothesized that acute ethanol will disrupt coherence between the ventral hippocampus and the frontal brain regions. If ethanol disrupts performance, power, and coherence in similar ways then it is likely that theta and/or gamma

oscillations in the ventral hippocampus, medial prefrontal cortex, and anterior cingulate cortex are important neural mechanisms underlying working memory.

1.12. Significance

In order to elucidate the neural mechanisms of goal maintenance working memory over a delay, it is necessary to locate specific functional connections between anatomical regions involved. This likely involves the ventral hippocampus and the pre-limbic/infralimbic sub-region of the medial prefrontal cortex and the physiological relationship between those areas during the performance of a working memory task. If the ventral hippocampus (CA1/subiculum) sends afferent projections to the medial prefrontal cortex then electrical stimulation of the vHPC (vHPC) will result in a short latency evoked response in the mPFC. Furthermore, if these areas are functionally connected then they will show synchronization of oscillatory signals and spectral coherence, particularly in the theta and gamma frequency ranges. Once the functional pathway is established, then it must be demonstrated that this physiological coupling is sensitive to discreet phases of the DNMTP working memory task and is predictive of choice accuracy. Understanding the phase reset in this task, the phase coupling between the ventral hippocampus and the medial prefrontal cortex, and the phase relationship between theta and gamma frequencies will be useful for enhancing our understanding of neural oscillations underlying working memory. Acute ethanol intoxication will be used as a tool to compare altered working memory performance and altered oscillatory patterns. This may lay groundwork for future studies looking to identify and potentially treat cognitive deficits in working memory or pathologies in which oscillations are

distorted. Furthermore, additional understanding of the neurophysiological effects of acute ethanol may be used to improve the overall health and well-being of individuals who consume alcohol.

Chapter 2: General Methods

2.1. Subjects

Subjects for all experiments were adult male Long-Evans rats (shipped at postnatal day 56 from Charles River Laboratories, International, Inc. Wilmington Mass). After arrival, animals were habituated to the vivarium and regular handling while access to water was gradually restricted. All animals were single-housed in a clear plastic cage (38.1 cm x 20.3 cm x 17.75 cm) with corncob bedding. The vivarium was humidity- and temperature-controlled and on a 12 hour light-dark cycle with lights on at 6:00 AM. All handling and testing occurred during the animal's light cycle. Behavioral training began on postnatal day 65. All rats had free access to food throughout the study, but access to water was restricted to the water earned during daily training sessions (5-10 mL) and for 1 hour of daily *ad libitum* access to a water bottle in the home cage. If an animal's weight dropped below 85% of normal age-adjusted body weight or experienced any health concerns, then the animal received supplemental water as needed to regain normal weight. All animals underwent regular general health examinations and were handled daily outside of training or testing contexts to minimize stress. All animal procedures were approved by the Ohio State University Institutional Animal Care Use Committee and were performed in accordance with NIH guidelines.

Twenty-four animals were included in the initial experimental design. We intended for all animals to be used in all phases of the experiment, but there was some

attrition in subjects over time (See Table 1). Seven subjects, cohort 1, received electrode implantation surgery after reaching behavioral criterion on Working Memory E (See Section 2.3.5). By design, these animals were not included in experiments involving the acquisition of the working memory task. Seventeen subjects, cohort 2, received electrode implantation surgery after reaching behavioral criterion on Working Memory B (See Section 2.3.2). The highest stage in which each animal achieved criterion performance is listed. Animals that were included in the learning physiology experiment were later divided into "fast learning" and "slow learning" groups (See Section 4.3). Subjects 28, 31, and 33 were excluded from learning physiology experiments due to occluded head stages or poor quality of physiological recordings. Animals in cohort 1 that achieved criterion on Working Memory E (n=4), and Animals in cohort 2 that achieved criterion on Working Memory D (n=8) were advanced to the acute ethanol experiments. Subjects 15, 24, and 25 failed to reach the behavioral criterion necessary for advancement to ethanol experiments. Subject 23 was in cohort 2 but advanced to achieve criterion on Working Memory E. Subject 17 was excluded from ethanol behavior and physiological analyses due to excessively low trial completion rates across multiple doses. Subjects 30 and 31 were included in ethanol behavioral experiments but not physiological experiments due to occluded head stages.

Data from experiments in Chapter 3 were based on the following number of subjects: Working Memory A =24, Working Memory B=24, Working Memory C= 20, Working Memory D= 16, Working Memory E=8. Data from experiments in Chapter 4 were based on the following final number of subjects: Fast learning group = 5, Slow learning group =5. Data from experiments in Chapter 5 were separated for accuracy such

that Working Memory E =4, Working Memory D=8, but groups were collapsed into n=12 for all other analyses. Data from experiments in Chapter 6 were based on a final number of 8 subjects.

Subject	Surgery Time Point	Highest Stage with Criterion	Included in Learning Physiology	Included in Ethanol Behavior	Included in Ethanol Physiology
12	Cohort 1	WM D	N/A	X	X
13	Cohort 1	WM E	N/A	Yes	Yes
14	Cohort 1	WM E	N/A	Yes	No
15	Cohort 1	WM E	N/A	No	No
16	Cohort 1	WM E	N/A	Yes	No
17	Cohort 1	WM E	N/A	Yes #	No
18	Cohort 1	WM E	N/A	X	X
19	Cohort 2	WM C	Slow	X	X
20	Cohort 2	WM B	X	X	X
21	Cohort 2	WM B	X	X	X
22	Cohort 2	WM B	X	X	X
23	Cohort 2	WM E	Fast	Yes	Yes
24	Cohort 2	WM C	Slow	No	No
25	Cohort 2	WM C	Slow	No	No
26	Cohort 2	WM D	Fast	Yes	Yes
27	Cohort 2	WM D	Slow	Yes	Yes
28	Cohort 2	WM D	Slow #	Yes	Yes
29	Cohort 2	WM D	Slow	Yes	Yes
30	Cohort 2	WM D	Fast	Yes	Yes #
31	Cohort 2	WM D	Fast #	Yes	Yes #
32	Cohort 2	WM B	X	X	X
33	Cohort 2	WM C	Slow #	X	X
34	Cohort 2	WM D	Fast	Yes	Yes
35	Cohort 2	WM D	Fast	Yes	Yes

Table 1: Flow of animals between studies

X indicates that an animal died or was removed from the study. # indicates that the animal was tested under this paradigm, but later excluded from analyses for other reasons.

2.2. Operant Chambers

All behavioral experience took place in operant conditioning chambers and shells developed by Med Associates Inc. (East Fairfield, VT). The operant chambers and shells were located in a copper-shielded Faraday Cage room to block external static and non-static electrical signals. Operant conditioning chambers (28 x 20.5 x 42 cm) were housed in a ventilated light and sound attenuating shell that was encased in copper mesh to minimize electrical interference from outside the chamber. The operant chamber walls were made of clear Plexiglas and the floor was parallel stainless steel rods 1 cm apart. The chamber was illuminated by a house light (2.8 Watts) located at the top of the back panel. The front panel contained two signal lights (2.8 Watts, 2.5cm Diameter), two retractable stainless steel response levers, and a central recessed port with a water dispenser (40-80 µl per drop, 20 cc dispenser capacity). Lights, levers, and the water dispenser were grounded to the outer copper shell. All equipment was controlled by Med-PC IV software and custom written Med-PC programs.

Figure 1 Equipment Photos.

A represents an operant box chamber used for behavioral training and neurophysiological recordings. B shows the front panel of the operant box chamber, including two signal lights, two response levers (retracted), and a recessed water port. C shows the pre-amplifier and adaptor that connects to the implanted socket on the animal's head. Penny included for scale.

2.3. Variable Delay Non-match to Position Task Overview

Rats underwent one session of behavioral training per day. Each session lasted for 100 trials or 60 minutes, whichever came first. Animals progressed through a series of up to 5 shaping steps.

2.3.1. Working Memory Stage A: Bar Pressing

In this stage of behavioral training, rats are habituated to the operant chambers and learn to associate bar pressing with a water reward. The house light is on throughout the session, but there are no signal lights illuminated. Each lever press is rewarded, unless the animal shows a side bias. If one lever is pressed 5 more times than the other lever, then the lever with more presses ceases to yield a reward until the other lever is pressed. This stage continued until the animal had 50 rewarded presses on each lever.

2.3.2. Working Memory Stage B: Sample Phase

In this stage of behavioral training, rats learned that only lever presses under an illuminated signal light yielded a reward. The house light turned on 1 second before each randomized signal light illumination. If the lever under the light was pressed within 3 seconds, then a small (40 μL) water reward was earned. If the wrong lever is pressed or no lever was pressed, then the house light is turned off for a 10 second intertrial interval (ITI) and a new trial began. This stage continued until the animal had $\geq$70% accuracy for two consecutive daily sessions.

2.3.3. Working Memory Stage C: DNMTP with 5 second delay

In this stage of behavioral training, rats built on the sample phase learned in the previous stage by adding a delay phase and a choice phase. A trial began and the house light was turned on 1 second before the sample phase signal light illumination. A correct response in the sample phase (under the illuminated light), yielded a small (40 μL) water reward and advanced the trial to the delay phase. An incorrect response or failure to respond within the 3-second response window in the sample phase was counted separately but the trial repeated until a correct response for subsequent encoding. The house light remained illuminated during the delay, but both signal lights were off. In this stage, the delay was fixed at 5 seconds. At the conclusion of the delay, both signal lights were illuminated simultaneously. A correct response in the choice phase was defined as the animal pressing the lever opposite of the one that yielded a correct response in the sample phase. For example, if the left light was illuminated in the sample phase, then the right lever was the correct response in the choice phase. A correct choice response yielded a large (80 μL) water reward, left the house light on for 3 additional seconds, and then started a dark ITI for 10 seconds. An incorrect response or an omission in the choice phase turned off the house light immediately and started a dark ITI for 10 seconds. This stage of training continued until the animal had one day $\geq$70% accuracy for the choice phase responses, and then the animal advanced to stage D.

2.3.4. Working Memory Stage D: DNMTP with 5 and 10 second delays

This stage of behavioral training was very similar to the previous stage, but the working memory load was increased. The delay interval was randomly either 5 or 10

seconds. This stage of training continued until the animal had one day ≥70% accuracy for the choice phase responses, and then the animal advanced to stage E.

2.3.5. Working Memory Stage E: DNMTP with 5, 10, and 15 second delays

Similar to the previous stage, this stage follows the same structure as Working Memory C, but the delay period was randomly 5 ("Short"), 10 ("Medium"), or 15 ("Long") seconds. Behavioral criterion for this stage was defined at one day ≥70% overall accuracy for the choice phase responses, then the animal progressed to ethanol injections if applicable.

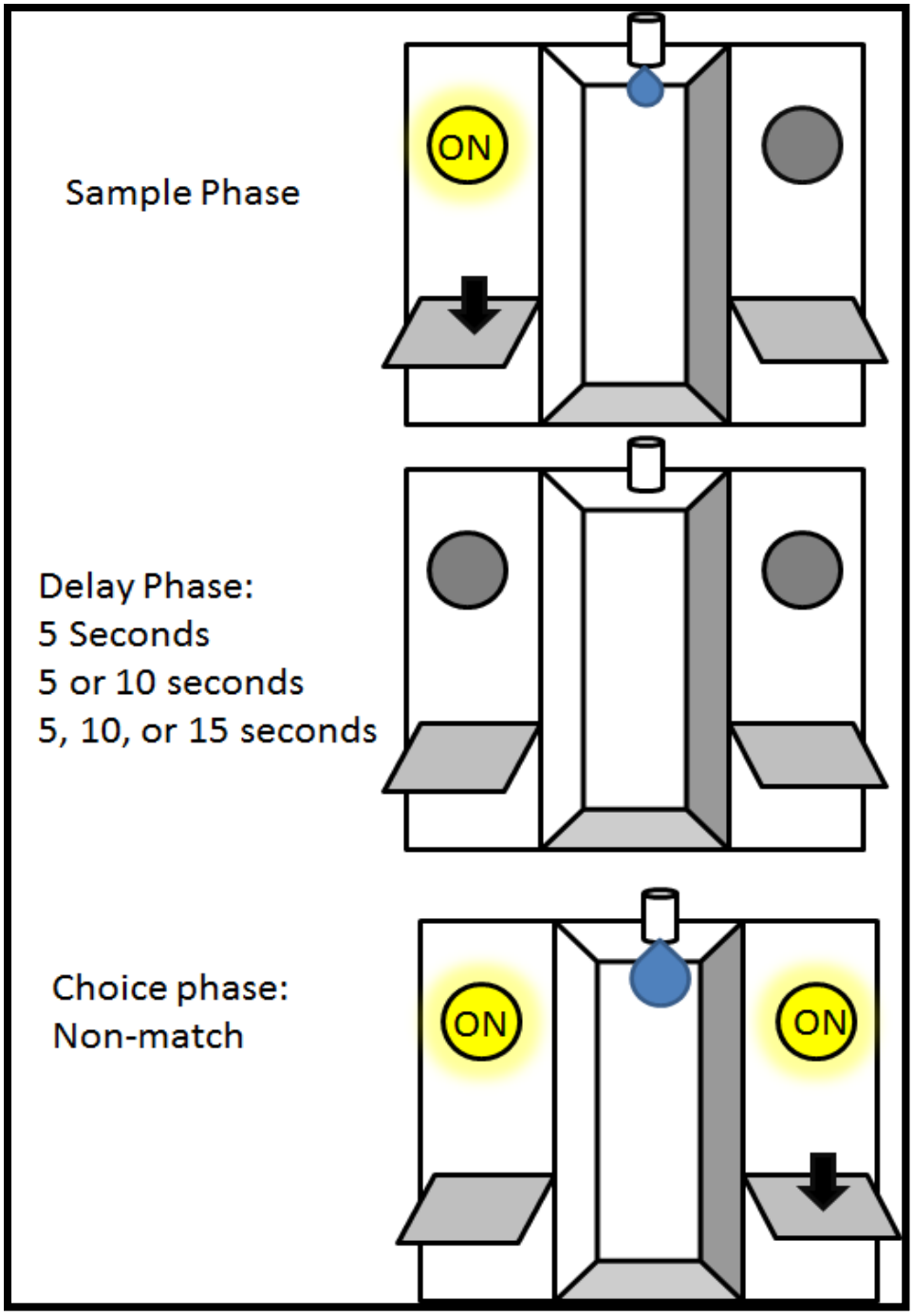

Figure 2 Delayed Non-Match to Position Operant Conditioning Task Schematic.

Representation of sample phase (encoding), delay (goal maintenance), and choice phase (retrieval). Delay phase duration is randomly 5, 10, or 15 seconds randomly interspersed throughout the session.

2.4. Behavioral data analysis

All behavioral data analysis was done on personal computers using MedPC2XL (Med Associates, East Fairfield, VT) software and GraphPad Prism version 6.00 for Windows (GraphPad Software, San Diego, CA). Behavioral dependent measures include sessions to criterion performance, sample phase accuracy & reaction time, responses during the delay interval, choice phase accuracy & reaction time, and responses during the intertrial interval. Choice phase accuracy includes overall performance and each delay interval. Errors of commission and omission were analyzed separately. Data was analyzed via repeated measures within subjects ANOVAs and paired sample t-tests when applicable.

2.5. Electrodes

All electrodes were constructed from stainless steel wires coated in Teflon (A-M Systems Inc. Carlsborg, WA) and had a male gold ITT/Cannon Centi-Lok pin attached to the distal end. Recording wires were 75 μm diameter. Two wires were epoxied together into a stereotrode such that they can be implanted together, but have 1.5mm depth difference between recording sites. Two ground reference wires were 125 μm diameter and had un-insulated 1mm tips that terminated in the brain.

2.6. Surgical Electrode Implantation Methods

Rats were deeply anesthetized with isoflurane gas mixed in oxygen. Body temperature was maintained at approximately 37°C with a deltaphase isothermal pad. Using stereotaxic coordinates from Bregma, a stereotrode was implanted unilaterally into

the PL/IL region of the medial prefrontal cortex (+ 3.2 mm anterior, - 0.8 mm lateral, 3.2-3.4 ventral from dura) and the anterior cingulate cortex (3.2 mm anterior, -0.8 mm lateral, 1.7-1.9 ventral from dura). A signal ground wire was implanted into the contralateral corpus callosum (-1.4 mm posterior, +2.0 mm lateral, -3.1 mm ventral). The prefrontal stereotrode and the corpus callosum ground wires were then fixed with dental cement. Another single electrode was implanted in the ventral hippocampus (6.5 mm posterior, 5.6 mm lateral, 5.2-5.6 mm ventral from dura). Depth of the hippocampal electrode was optimized for each rat during surgery by a single-pulse stimulation protocol (see Electrical Stimulation and Evoked Response methods), and then fixed with dental cement. All electrode pins were securely clamped into an ITT/Cannon Insulator Strip that served as a head stage. Three additional burr holes were drilled into the skull for small stainless-steel machine screws to anchor the dental cement. A ground electrode was wrapped around one of the machine screws. Dental cement secured all electrodes and the headstage to the screws. Lidocaine and topical triple antibiotic ointments were applied to the wound immediately after surgery. Animals were given post-operative access to oral acetaminophen suspension (Children's Tylenol) for 48 hours, and received applications of Lidocaine and triple antibiotic ointment twice daily for 4 days. During the recovery period of 5 days, rats were in their home cages with free access to food and water. Water access was restricted on the 6^{th} day after surgery and on the 7^{th} day the animal then resumed behavioral testing and neurophysiological recordings were started.

2.7. Electrical Stimulation and Evoked Response

The ventral coordinates for hippocampal electrodes was determined for each rat during surgery by delivering a series of small amplitude single square wave electrical pulses (10-100 μA, 0.1 ms, square pulse) via a Grass Instruments S8800 stimulator (Quincy, MA) to the implanted but not fixed ventral hippocampus electrode. Evoked responses in the PL/IL region of the medial prefrontal cortex and anterior cingulate cortex were observed with an oscilloscope to locate the ventral hippocampal coordinates that result in the maximal amount of electrically evoked response in the PL/IL sub-region of the medial prefrontal cortex.

2.8. Local Field Potential Signal Acquisition

All physiological recordings took place in a room with radio frequency shielding and overhead fluorescent lights turned off. All computer monitors were adjusted to refresh at a rate of 60 Hz. The implanted electrodes and insulator strip headstage connected to female gold ITT/Cannon Centi-Lok sockets which were connected to a plastic 8-channel [10 pin] male adaptor, with .050 mm spacing manufactured by Omnetics Connector Corporation (Minneapolis, MN), which in turn connected to a high impedance unity gain head stage with 8 channels (Plexon, Inc., Dallas, TX). The signal was carried by a 36 inch cable from the preamplifier to a freely-movable commutator and differential AC amplifier ((1000x)/filter 1.0-500 Hz with notch for 60 Hz mains hum, A-M Systems, Sequim, WA), to an A-D board for digitization (Power 1401, Cambridge Electronic Design, Cambridge, England), and then to personal computers with Spike 2

Version 7.11 and 7.13 data acquisition and analysis software. All waveform channels were sampled at 1 kHz.

2.9. Neurophysiological Data Analysis

Acquisition and Filtering

Neurophysiological analyses were completed on personal computers with data acquisition and analysis software developed by CED (Spike 2 version 7.13). Initial recordings included a wide-bandwidth but were filtered with a finite impulse response (FIR) digital filter for subsequent analysis. The main advantage to FIR filters is that the position of peaks does not change. An FIR settles to zero at a specified time, whereas an impulse infinite impulse response filter does not. The FIR filter used a low pass band filter to select frequencies between 0 and 90 Hz, with a transition gap of 20 Hz. All files were manually scanned and filtered to eliminate instrumental or environmental noise, movement artifacts, or interference. These irregular events were collectively defined as irregular activity in excess of 5 millivolts across all three recording channels and were removed from subsequent analyses.

Acquired waveform data were additionally processed with DC offset to remove very low frequency noise. DC remove has one argument, a time period in seconds, p. The output at time t is the input value at time t minus the average value of the input data points from time t-p to t+p. The result is equivalent to the original signal minus the result of the smoothing operation. This process does not affect the channel scale, but the channel offset is set to zero. The time constant used for this processing was 0.1 second.

Onset of events from the operant task including all lever presses, light stimuli, incorrect choice responses, and water rewards was recorded simultaneously with the neurophysiological waveforms as event markers. Additional event markers were created via a custom script from Cambridge Electronic Design to indicate the sample and choice phases of the task. These behavioral event markers were used as triggers to gate further analyses around stimuli and responses.

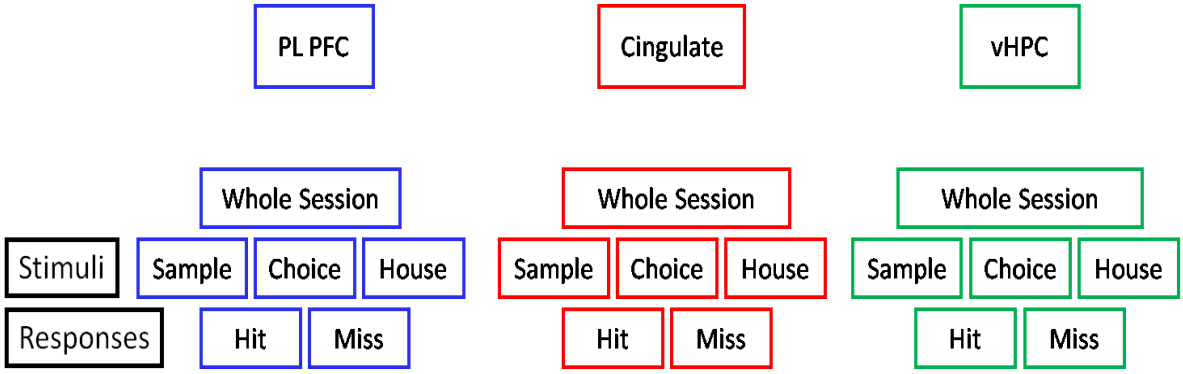

Figure 3 Recording locations and behavioral event markers.

Power Spectrum Analyses

Power spectrum analyses were performed with Spike2 Software from Cambridge Electronic Design. Power Spectrum analyses were performed on the waveform channels representing field potentials in the medial prefrontal cortex, the anterior cingulate cortex, and the ventral hippocampal cortex. A power analysis is a representation of a frequency variable as determined by time. Power analyses are computed by using a Fast Fourier Transform (FFT) to convert the waveform data into a power spectrum. The FFT

transforms a block of data between a waveform and an equivalent representation as a set of cosine (single frequency) components. The output of a power analysis is the amount of energy at a given frequency, measured in units of root-mean-square-power. The term power spectrum means that amplitude is 2/2 versus frequency. Power analyses are useful for determining the frequency content of a signal and help identify dominant repeated frequency patterns within the data. Analyses focused on the power within the theta band (4-10 Hz) and the gamma band (30-90 Hz). To compute the power spectrum, we used an FFT size of 2048 (2.048 seconds) to show frequencies from 0 to 500 Hz in 1024 bins with a resolution of 0.4883 Hz. To avoid sharp discontinuities at the end of one block and the start of the next, the FFTs used standard Hanning windows, also known as raised cosines, for tapering the start and end of each data block to zero so that they join smoothly. Each source data block overlaps the previous, contiguous block by 50%, known as Welch's method for spectral density estimation. This method reduces noise in the estimated power spectra compared to non-overlapping methods.

Waveform Average Analyses

Waveform average analyses were performed with Spike2 Software from Cambridge Electronic Design. Peri-stimulus waveform averages were performed on the recording channels for each anatomical site (medial prefrontal cortex, anterior cingulate cortex, and ventral hippocampus). Waveform averages were calculated by sweeping a specified time interval around the nearest trigger event and then calculating the arithmetic mean of all the sweeps over the span of the time window. A flat waveform average indicates random or unpatterned activity; whereas peaks in the waveform average

indicate patterned activity. Waveform Averages were performed on filtered waveforms. Each waveform average was a width of 2 seconds (2000 bins), with one second occurring prior to stimulus onset ("Pre" condition) and one second occurring after stimulus onset ("Post" condition). Waveform averages were triggered to event markers indicating a correct ("Hit") or incorrect ("Miss") response. Averages were gated to houselight illumination, single light illumination which represented the sample phase, or double light illumination which represented the choice phase. Gate sweeps scanned for 1.5 seconds around the signal onset to acquire the waveform averages that included 1 second before and 1 second after the signal onset. Group differences in mean waveform averages were quantified with an area under the curve analysis. An area under the curve analysis is an integrated measurement where a series of trapezoids are used to compute the total area under both positive and negative peaks. A larger area under the curve generally indicates a more coordinated waveform average.

Waveform Correlation Analyses

Waveform correlation analyses were performed with Spike2 Software from Cambridge Electronic Design. Waveform correlations were performed to assess the degree of synchrony between the different anatomical regions. Waveform correlations measure the similarity of two waveforms with the same sample interval. The first result point is calculated by multiplying all of the data points in one waveform, the "reference," by all of the data points in the second waveform and summing the results. The sum is normalized to allow for waveform amplitudes and the number of points. The reference waveform is moved one sample point to the right and the process repeated for the next

result point until all of the result view bins are filled. The result is scaled so that the Y axis of a waveform correlation ranges from -1 (inversely correlated), through 0 (uncorrelated), to +1 (fully correlated, except for amplitude). DC offsets are removed from the waveforms so that offsets do not change the result. Waveform correlations were performed on waveforms that had been filtered with FIR low band pass processing described above. Waveform correlations were performed on the anterior cingulate cortex waveform and the medial prefrontal cortex waveform with both being referenced to the ventral hippocampus waveform. These were performed on the whole session, or gated to sample and choice phases of the sessions of interest. In each case, the width of the correlation analysis was 1.0 second (1000 bins) and included a 0.5 second pre-trigger offset.

Coherence Analyses

Coherence analyses were performed with Spike2 Software from Cambridge Electronic Design. The custom script for coherence was available for download from the CED website. Coherence of two waveforms is the measure of their similarity in frequency content, or general synchrony. Coherence is a function of frequency and ranges from 0 for totally incoherent waveforms to 1.0. For two waveforms to be perfectly coherent at a particular frequency over a given time range, the phase shift between the waveforms at that frequency must be constant, and the amplitudes of the waves at that frequency must have a constant ratio. Coherence is calculated through Fast Fourier Transform methodology. Cross spectral density between two waveforms is normalized by the power spectral density of each waveform.

Coherence analyses were performed on both the medial prefrontal cortex referenced to the ventral hippocampus, and the anterior cingulate cortex referenced to the ventral hippocampus. Analyses were performed for the entire duration of the recording session and separated coherence into 2048 frequency bins with a resolution of 0.48 Hz per bin. Coherence results were isolated for specific frequency bands of interest for further analyses. Theta band was defined as 4-12 Hz, low gamma band was defined as 50-70 Hz, and high gamma band was defined as 70-90 Hz. The gamma frequencies in close proximity to 60 Hz were avoided for these analyses due to the roll-off effect of the notch filter on the amplifier interfering with coherence values at these frequencies.

2.10. Acute Systemic Alcohol Injections

All systemic injections were administered intraperitoneally 10 minutes before the animal was placed in the operant conditioning recording chamber. We mixed absolute ethanol (200 proof) with physiological saline (0.9% sodium chloride) in a 10% (weight/volume) solution. Injections were given at doses of 0.00 (1.0 ml/kg saline vehicle), 0.25, 0.50, 0.75, or 1.0 g/kg body weight. These doses were chosen based on previous work in the lab assessing changes in blood ethanol concentrations (Williams and Givens, 2000). Blood ethanol content was maximal by the first 15-minute time point and then gradually decreased over the hour long behavioral testing session. The peak blood ethanol concentration for the highest dose used was 120 mg/dL. In the present studies, the order in which doses were received was randomized via a Latin Square design. At least 48 hours separated each injection to minimize any potential residual effects of a previous dosage or potential tolerance.

2.11. Electrolytic Lesion and Histological Site Verification

Final recording sites were marked with a small electrolytic lesion (± 150 μA for 20 seconds at both positive and negative directions). At the end of each series of experiments, the animals were deeply anesthetized with pentobarbital sodium and phenytoin sodium (euthasol: 100 mg/kg, intraperitoneally), transcardially perfused first with heparinized saline and then with formalin. The brains were extracted, cryoprotected with a 30% sucrose solution for two days, frozen, sliced via cryostat into coronal brain sections 50 μm thick, mounted on gelatin-coated microscope slides, and stained with cresyl violet for Nissl stain verification of anatomical placement of the electrodes. Photomicrographs at 2.5x magnification were obtained with a Carl Zeiss Axio Imager M2 microscope using Stereo Investigator software by MBF Biosciences. Electrode placement diagrams and representative histology are shown in Figures 4, 5, and 6. Atlas Images are from Paxinos & Watson (2007). Electrode tip locations are projected onto a single target coronal atlas section in panels A, although their actual anterior/posterior placement varied up to .5 mm from the target section. Several electrode locations are not depicted due to indeterminate final tip locations, but the visible electrode tracks suggested that the final tip was within the target region.

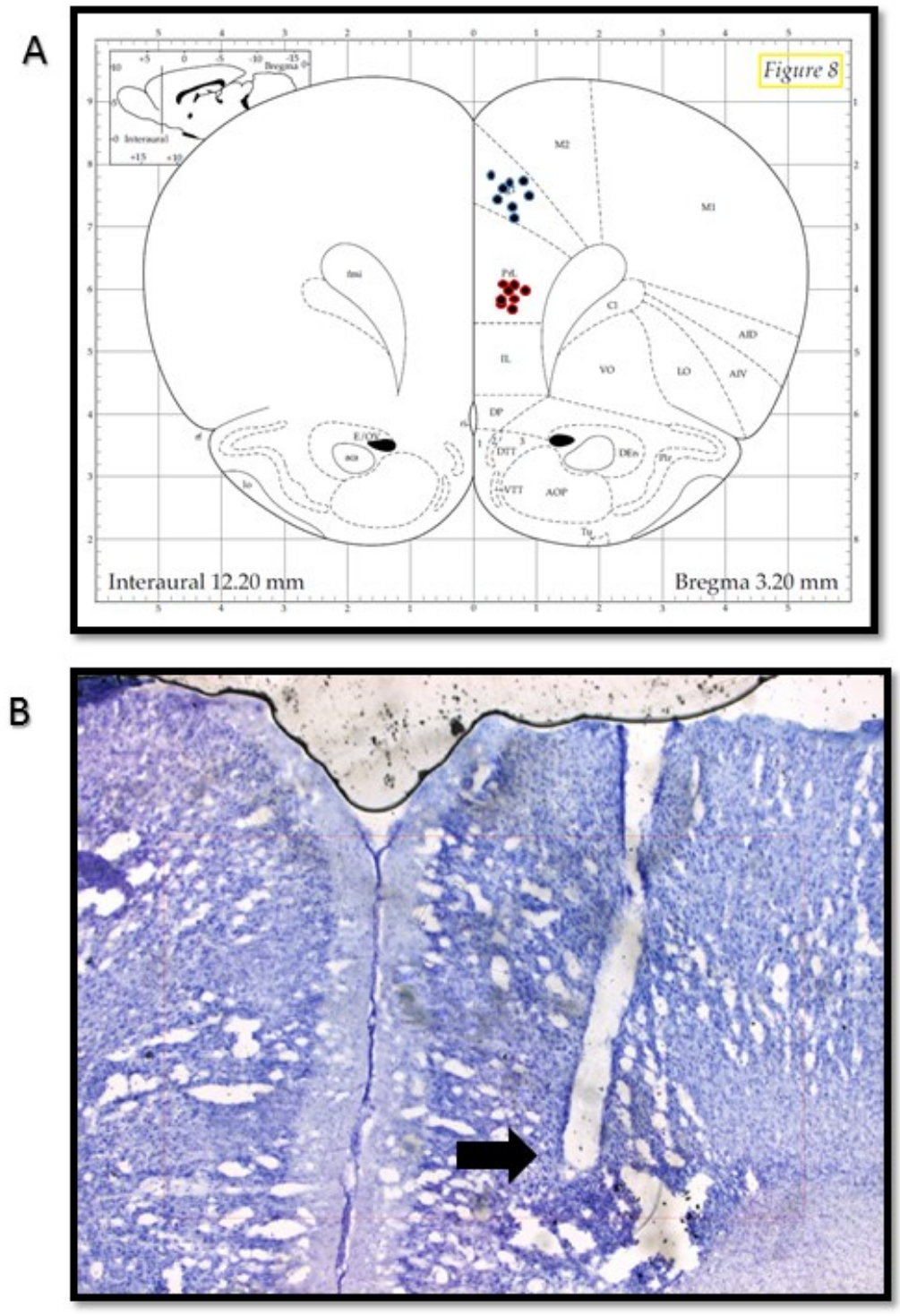

Figure 4 A: Placements of recording electrodes in the anterior cingulate cortex and the Prelimbic/Infralimbic regions of the medial prefrontal cortex.
B: Representative Histology

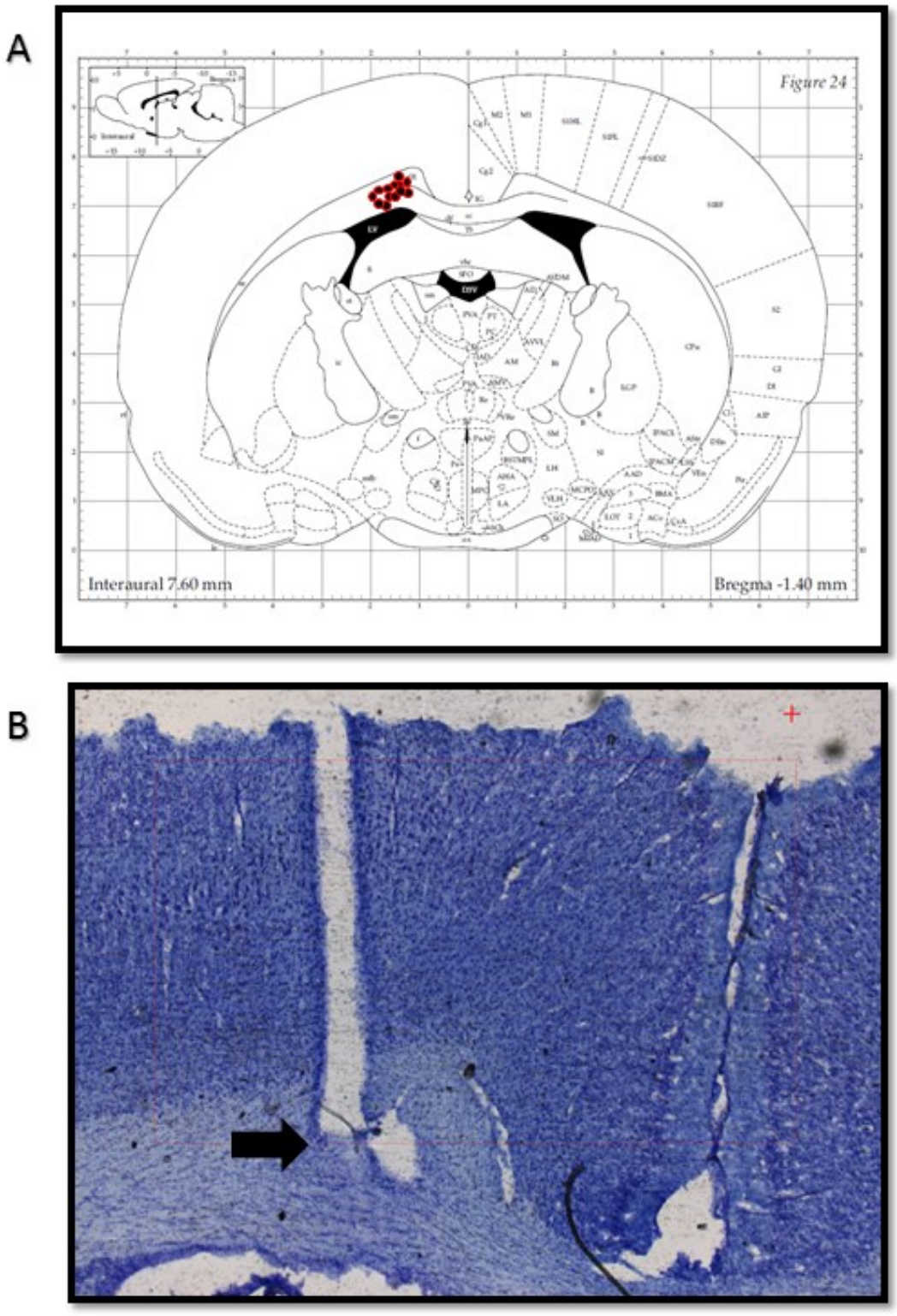

Figure 5 A: Placements of ground electrode in the corpus callosum.
B: Representative Histology

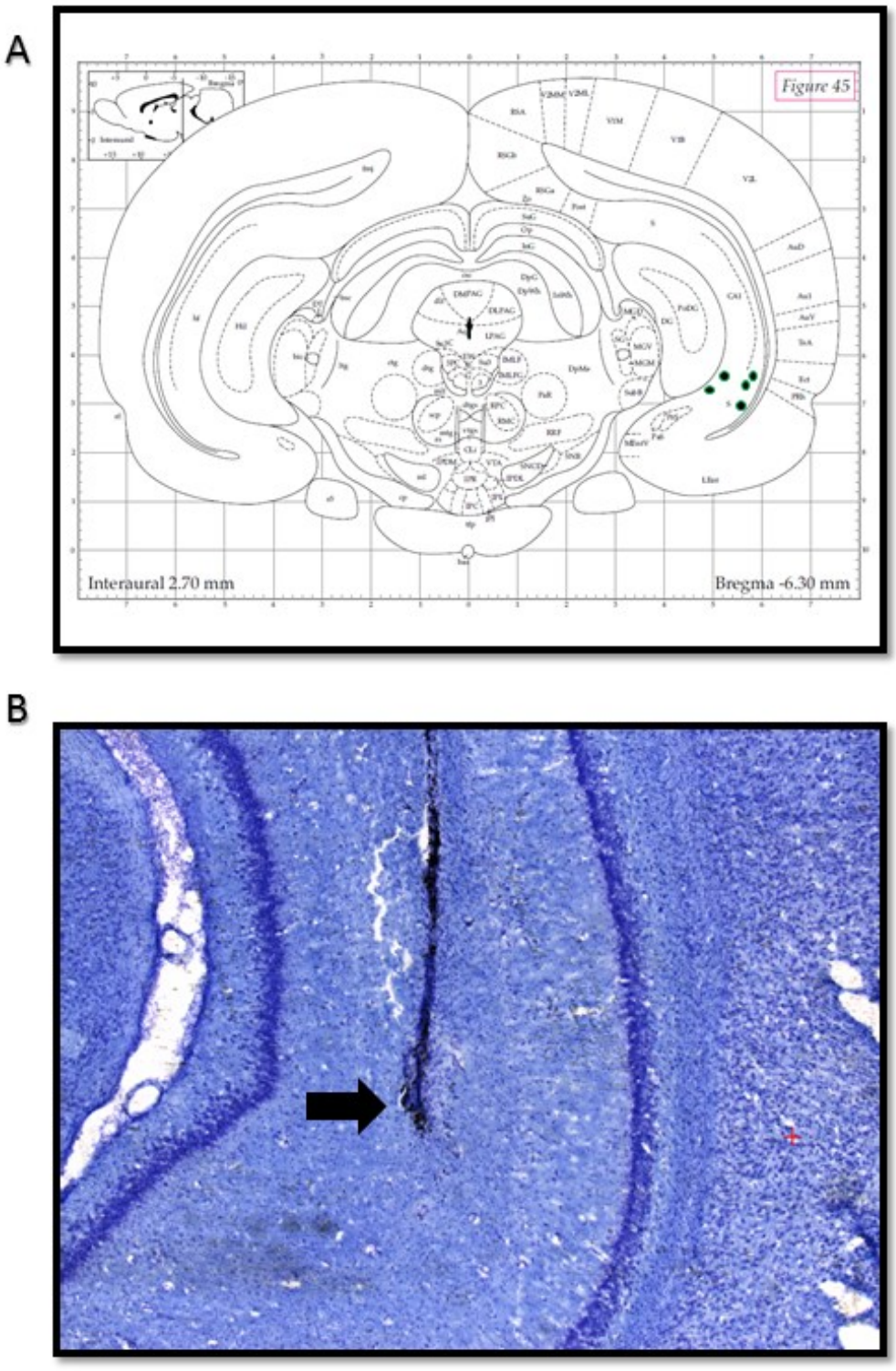

Figure 6 A: Placements of recording electrodes in the ventral hippocampus. B: Representative Histology

Chapter 3: Learning the Delayed Non-Match to Position Task

3.1. Introduction

Operant conditioning adaptations of D(N)MTS tasks are among the most promising behavioral tasks to assess goal maintenance working memory in animal models (Dudchenko et al. , 2012). This version is often referred to as the variable delayed (non-) match to position task (D(N)MTP). In operant environments the type of stimuli is usually limited so the position of stimuli becomes the salient item to be maintained over time and remembered. D(N)MTP involves a visuo-spatial stimulus during a sample phase, such as the location of a light cue or retractable lever, which must be encoded and stored for the duration of a variable delay, and then retrieved in a later choice phase in order to make a correct response on an alternate lever (Dunnett et al., 1988). In delayed matching conditions, the same lever pressed during the sample phase is rewarded during the choice phase. However, in delayed non-matching conditions, the opposite lever than the one pressed during the sample phase is the one that is rewarded during the choice phase. It is not yet clear if rats solve D(N)MTP tasks with egocentric, allocentric, or salient landmark cues within the operant box. Rats with a salient spatial cue, such as an asymmetrical operant box, perform the task with higher accuracy and faster acquisition than those without a similar spatial cue (Ennaceur and Aggleton, 1998).

Most researchers consider delayed match and non-matching paradigms to be approximately equal (Dudchenko et al., 2012), however it should be noted that some

manipulations may appear to preferentially increase or decrease performance in one paradigm or the other if the manipulation influences an animal's tendency to alternate or perseverate behavioral responses (Sahgal, 1987). According to Pache and colleagues (1999), a combination of delayed matching and non-matching is the most sensitive measure for determining a drug effect. Scopolamine, a muscarinic antagonist, caused delay dependent impairments in a matching paradigm but delay-independent impairments in a non-matching paradigm. Conversely, 8-OH-DPAT, a serotonin agonist, was found to slightly improve accuracy in matching paradigms but not non-matching paradigms at low doses, and to impair non-matching but not matching paradigms at high doses (Pache et al., 1999). When only one paradigm is used, non-matching paradigms are slightly preferred by most researchers because there is less likelihood of the animals developing side biases (van Hest & Steckler, 1996)

D(N)MTP tasks require ability to flexibly adopt a rule in response to incoming stimuli and then maintain this information across a delay in order to achieve the goal of a correct matching or non-matching response. Any delay-dependent effects are considered memory effects, whereas delay-independent effects such as increases in response latencies or omissions are considered effects on motivation, attention, motor function, or other non-mnemonic processes (Chudasama and Muir, 1997). Most animals show clear signs of delay-dependent memory, with higher performance at shorter delay intervals than at longer delays. In rats, performance generally declines to chance levels at delays between 20 and 60 seconds (Dudchenko et al., 2012). Therefore, by varying delay intervals D(N)MTP tasks have adequate dynamic range to detect performance enhancements or impairments and may avoid problematic floor or ceiling effects.

Operant D(N)MTP tasks are categorized as either delayed response tasks or delayed comparison tasks (Pontecorvo et al., 1996). Most rodent delayed matching or non-matching paradigms are characterized as delayed response, whereas most primate or human paradigms are characterized as delayed comparison (van Hest & Steckler, 1996). In delayed response tasks, the information for a correct response is available prior to the retention interval and must be maintained over time. In delayed comparison tasks, the answer is not known prior to the retention interval and the subject must compare stimuli before and after the retention interval in order to determine the correct response. Delayed response tasks are much easier for animals to acquire and provide valid assessment of working memory if measures are taken to limit alternative non-mnemonic strategies such as postural mediation of a response during the delay interval (Dudchenko, 2004). In versions of the task when mediating strategies are not prevented, short delays or control animals show more successful mediating strategies than animals at longer delays or after an experimental manipulation (Chudasama and Muir, 1997). Examples of measures taken to limit postural mediation of responses include nose-pokes on the rear panel of the operant box, metal barriers between the levers, or a rewarded sample-phase response that requires the animal to go into a central food or water port. Rats that were rewarded where they responded had significantly faster acquisition than rats that were rewarded in a central port (Ennaceur and Aggleton, 1998), providing support that requiring an animal to go to a centralized reward port is a valid means of reducing postural mediation strategies.

There is also considerable interest in using pharmacological interventions to restore working memory function in the DNMTP task. Blockade of metabotropic

glutamate (mGlu1) receptors improves working memory and reduces impulsive choice at doses that have no effects on time perception but appear to facilitate impulsive action (Sukhotina et al., 2008). Since working memory deficits are one of the most consistently observed symptoms in the schizophrenic population, several anti-psychotic medications have been tested for improvement in DNMTP accuracy (Gemperle et al., 2003). Iloperidone, an atypical neuroleptic, dose-dependently improved choice accuracy but impaired other aspects of task performance. Clozapine, another atypical neuroleptic, did not affect accuracy or motor function, but decreased the number of trials completed. Haloperidol, a typical neuroleptic, did not affect accuracy except at the highest dose tested and only at the longest delay. Haloperidol also caused more task impairment in terms of trials completed than either of the atypical neuroleptics tested.

The main purpose of this chapter is to confirm that rats are able to learn this version of the operant delayed non-match to position task in a manner that is similar to other studies in animal models of goal maintenance working memory. Data presented includes the time to criterion for each stage of behavioral training, the gradual trends of rule acquisition over time, and the delay-dependency of the task under baseline conditions.

3.2. Subject Information and Specific Methods

There were 24 animals that underwent behavioral training and electrode implantation surgery. Seven of these animals were trained up to behavioral criterion ($\geq$70% overall accuracy) on Working Memory E (5, 10, and 15 second delays) before

undergoing electrode implantation surgery. These animals are referred to as Cohort 1. Seventeen animals were trained up to behavioral criterion ($\geq$70% overall accuracy) on Working Memory B (sample phase) before undergoing electrode implantation surgery and then resuming training on Working Memory C (DNMTP with 5 second delay) after recovery. These animals are referred to as Cohort 2. The timing of surgery did not have any statistically significant effects on time to achieve criterion or the course of progression through each behavioral training stage.

3.3. Time to criterion for each stage of behavioral training

Due to the complex nature of the behavioral task and the substantial amount of time necessary to progress through all stages of training, there was some attrition in the number of subjects over time. All 7 animals in Cohort 1 reached behavioral criterion on all working memory stages. Four animals from Cohort 2 were removed from the study prior to reaching criterion on Working Memory C. Seven additional animals from Cohort 2 were removed from the study or failed to reach criterion performance on Working Memory D. Only 1 animal from Cohort 2 was advanced to Working Memory E and subsequently achieved criterion. In other words, the number of subjects represented for time to criterion are Working Memory A =24, Working Memory B=24, Working Memory C= 20, Working Memory D= 16, Working Memory E=8.

All animals that achieved behavioral criterion demonstrated predictable patterns in the amount of time necessary to achieve criterion. For all stages, behavioral criterion for advancement was defined as $\geq$70% overall accuracy. The mean number of sessions necessary to achieve criterion performance is illustrated in Figure 7. All rats had a quick acquisition time and minimal variability while learning the early stages of the task

including bar pressing (Working Memory A) and responding to the sample phase (Working Memory B). The mean time to criterion for Working Memory A was 1.29 days and the mean time to criterion for Working Memory B was 2.95 days. Initial learning of the delayed non-match to position paradigm with a fixed 5-second delay (Working Memory C) required substantially more time to achieve criterion performance and showed more individual variability. The mean number of daily sessions to behavioral criterion for Working Memory C was 20. When an additional delay 10-second delay was incorporated into Working Memory D, animals generally required less sessions to achieve criterion than in Working Memory C. The mean number of daily sessions for Working Memory D was 14.56 days. However, attaining criterion performance after incorporation of the 15-second delay into Working Memory E took the longest of all stages, averaging 23.43 days, and was also the most variable between animals. It typically took an animal a little more than 3 months of daily sessions to progress through all five of the training stages.

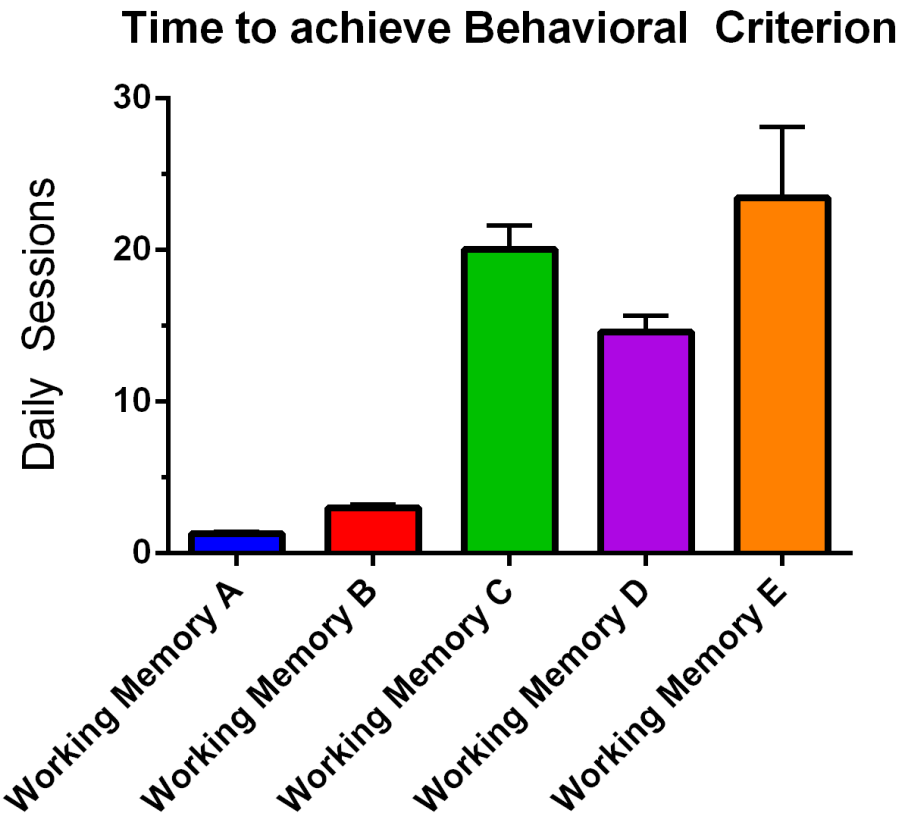

Figure 7 Mean Time to achieve behavioral criterion.

Number of subjects represented for WM A =24, WM B=24, WM C= 20, WM D= 16, WM E=8. Error bars indicate SEM.

3.4. Accuracy Progression over time for each stage of behavioral training

Rats in the delayed non-match to position task generally show a gradual improvement in accuracy over the course of each training stage. The left column of Figure 8 depicts the mean accuracy score for animals as they progress through Working Memory C, Working Memory D, and Working Memory E respectively. The early time point represents scores from the first day experiencing that stage of the task. The criterion time point is when the overall accuracy score is greater than or equal to 70%. Overall accuracy reflects an arithmetic mean of accuracy at all available delay intervals. The midpoint is in the middle of the early and criterion time points.

The mean accuracy for early, mid, and criterion time points for Working Memory C shows a linear progression of gradual increases until criterion is reached. Since 5 seconds is the only delay at this stage, accuracy at this delay is reflective of the overall accuracy. When animals advance from criterion at Working Memory C to the first day of Working Memory D, there is a decrease in mean performance at the short delay and near-chance level performance at the medium delay. In Working Memory D, performance at both short and medium delays gradually increases until the overall criterion is achieved. When animals advance to Working Memory E, performance is relatively high and stable at the short delay, but accuracy at the medium delay initially drops and eventually regains high levels by the time criterion is reached. Performance at the long delay is at near-chance levels for both early- and mid-time points, but increases as criterion is reached.

In the right column of Figure 8, the mean overall session accuracy for all animals over sequential daily training sessions was plotted for each stage and subsequently analyzed via linear regression. In each stage, the line of best fit is indicated by red

dashes. The linear regression for Working Memory C had the highest R^2 value and was significantly non-zero with an upward slope ($R^2 = .68$, $F_{1, 38} = 82.31$, $p < 0.0001$). The linear regression for Working Memory D ($R^2 = .19$, $F_{1, 25} = 6.008$, $p < 0.05$) and Working Memory E ($R^2 = .17$, $F_{1, 39} = 8.127$, $p < 0.01$) were also significantly different from zero with upward slopes over time. Both Working Memory D and E showed more variance over time than was observed for Working Memory C, particularly in late sessions as many animals had already reached behavioral criterion performance and were thus no longer plotted or part of the regression analysis.

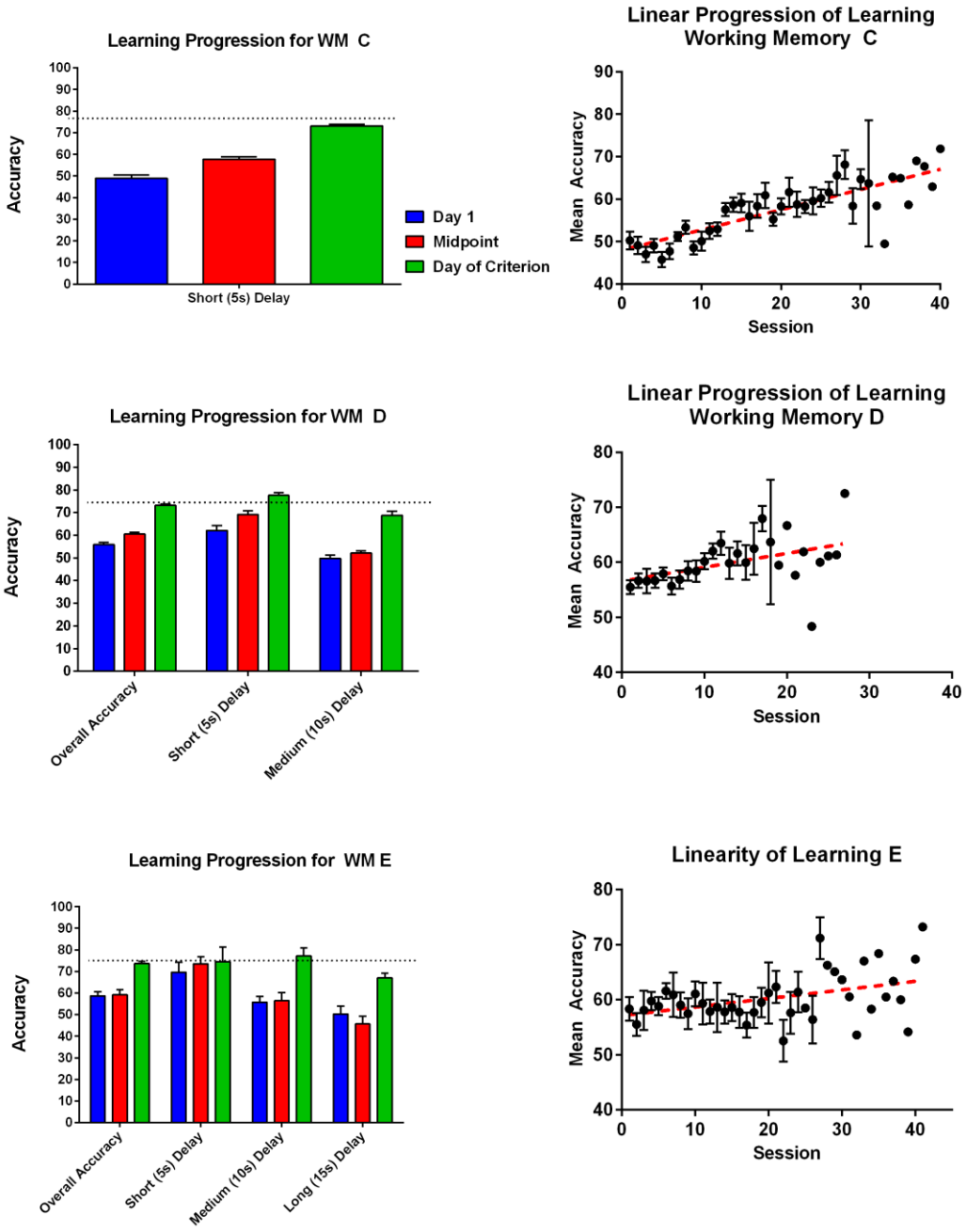

Figure 8 Gradual Learning Progression for Working Memory C, D, and E

Left column shows progression for each delay period at the beginning, midpoint, and criterion for each stage. Black dashed line represents behavioral criterion level performance. Right column shows mean overall accuracy as daily sessions progress. Red dashed line represents line of best fit. All error bars indicate SEM.

3.5. Delay-Dependency of the Operant Working Memory Task

Delay-dependency is a key aspect of validating a task as assessing working memory functions. A task is delay-dependent if performance decreases as delay and putative working memory load increases. As data from the learning progression of each stage of the task shows, performance in the delayed non-match to position operant task is generally best at the shortest delay worst at the longest delay, thus suggesting that this task shows delay dependency.

To further assess the delay-dependency of this task, a subset of Working Memory E sessions was analyzed for seven subjects. Any sessions that had less than 50 out of 100 completed trials, less than 50% overall accuracy, or involved an injection were excluded. Included sessions span from early time points to post-criterion time points and reflect aggregate experience each delay interval. 245 Sessions were included in the analysis.

The mean accuracy score across all sessions resulted in a very linear pattern with highest performance at the shortest delay and gradually decreasing until worst performance at the longest delay. The mean accuracy score for the 5 second delay was 69.90%, for the 10 second delay was 63.04%, and for the 15 second delay was 54.37%. A repeated measures one-way ANOVA showed a significant overall effect of delay ($F_{1.918,468} = 173.3$, $p < 0.0001$. Post-Hoc t-tests with Tukey's correction for multiple comparisons showed that short delay vs. medium delay, short delay vs. long delay, and medium delay vs. long delay were all significantly different with $p < 0.0001$.

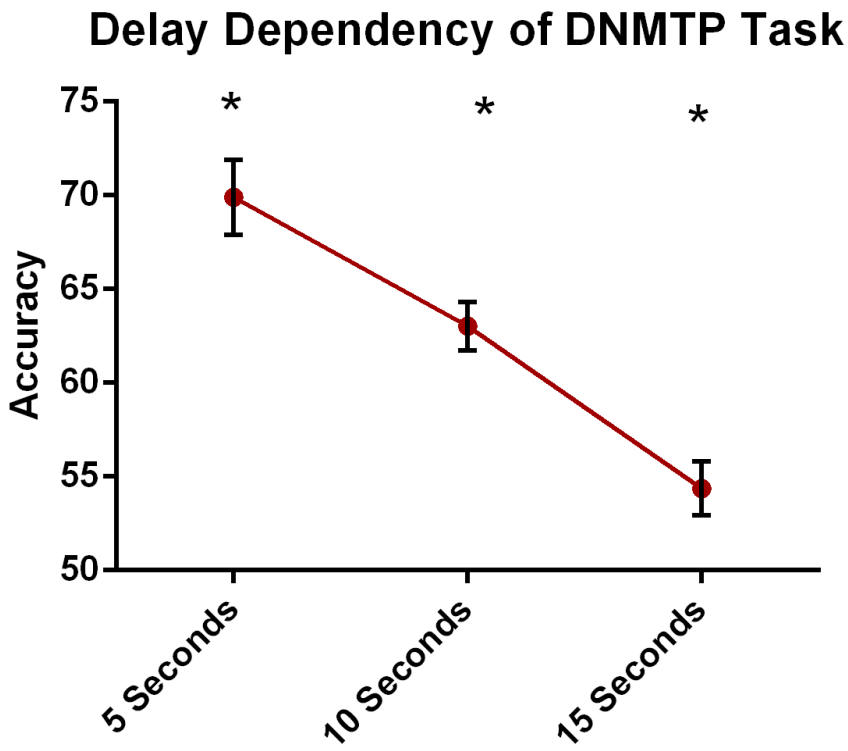

Figure 9 Delay Dependency of the Delayed Non-Match to Position Operant Task.

Points represent mean accuracy for 7 subjects over 245 sessions of Working Memory E. Each delay interval is significantly different from the other two delay intervals with $p < 0.0001$. Error bars indicate SEM.

3.6. Conclusions and Discussion

The results presented in this chapter indicate the validity and utility of the operant delayed non-match to position goal maintenance working memory task protocol. With very few exceptions, animals were able to acquire the rules of the task and gradually improve from chance levels to achieve the pre-defined behavioral criterion at each of the training stages. The 5, 10, and 15 second delays used in this task protocol showed linear delay-dependent effects and avoided potentially problematic floor and ceiling effects.

It is important to note that all training sessions occurred in an operant box optimized for neurophysiological recordings. After correct responses in the sample phase or choice phase, the animals obtained water rewards from a recessed port in the center of the front panel between the two signal lights and response levers. The height of this recessed port was much higher than typical operant box configurations in order to allow for animals with head stages and recording wires to access the port without obstruction. The water drop dispenser was located at the top of this port and although not required, animals often reared upwards in order to obtain their reward. This rearing behavior was an unintended consequence of the physical configuration, but it may have effectively reduced postural mediation strategies requiring more active manipulation of information over the delay period. This would likely manifest as longer times to criterion than animals trained in boxes that did not allow for such rearing behavior to obtain the reward. This observation aligns with data reported by Ennaceur and Aggleton (1998) where rats that were rewarded where they responded had significantly faster acquisition than rats that were rewarded in a centralized port. If the rearing behavior to the sample phase reward prevented postural mediation strategies during the delay period, then the animal

would theoretically need a higher reliance on working memory function thus improving the validity of this specific protocol, although slowing acquisition.

Since the origination of the delayed match to position operant task by Dunnett (1985), delayed match- and non-match to position (or sample) tasks have been an important tool in the behavioral assay repertoire of many researchers interested in working memory. Delayed match-and non-match tasks have been consistently tested in rodents, non-human primates, humans, and among clinical populations under a wide variety of drug and or lesion manipulations. The translational potential of this task is considerable.

While much is understood about the mechanisms underlying DNMTP, there is still more work that needs to be done. DNMTP has great potential as a tool to understand mechanisms underlying goal maintenance working memory. Of all existing methods to assess goal maintenance working memory in animals, variable delayed response DNMTP tasks have the most viability to be used in the screening process for drug treatments to improve performance because it has varying memory load in the multiple randomized delay periods, high throughput, sensitivity to precise timing, and good standardization (Dudchenko et al., 2012). There are many additional advantages of this task, including: capacity for systematic modification of task variables such as intertrial intervals and delay periods, ability to study the retention of information over time, enabling the dissociation between mnemonically-relevant events, having multiple trials over which to average physiological data, controlling precise timing of stimulus onset, recording precise timing of behavioral responses, and dissociating the task into separate short-term encoding and retrieval phases (van Hest & Steckler, 1996; Robinson et al., 2000;

McCartney et al., 2004). The major disadvantage of this task is that training animals to stable criterion performance can reasonably take up to three months and thus is more time-consuming and cost-intensive than many other available behavioral tasks that are used to assess working memory function. In spite of these challenges, the DNMTP task is more amenable to neurophysiological recordings from many neuroanatomical sites than many other tasks. Compared to other common working memory tasks, such as maze tasks, there are considerably fewer locomotive confounds. Considering these logistical advantages as well as the complexity of the cognitive behavior it elicits, the delayed non-match to position task is ideally suited to study the subtle neurophysiological mechanisms underlying working memory function and dysfunction.

Chapter 4: Physiology and Learning

4.1. Introduction

For a task to sufficiently assess goal-maintenance working memory, it must be moderately challenging for the subject to learn. As described in the previous chapter, although the D(N)MTP operant task can be a powerful tool for assessing goal maintenance working memory function, it often requires a significantly larger investment of time, animals, and personnel than similar methodologies. It is not unusual for a rat to take over three months to learn DNMTP to behavioral criterion (Dudchenko et al., 2013). If the task is set up to reduce the likelihood of postural mediation strategies, then this rule acquisition time can be even longer (Ennaceur & Aggleton, 1998). Given that there is often considerable individual variability in time to learn stages of the task, and some rats fail to ever reach behavioral criterion, it would be useful to have an indicator predictive of successful or efficient task acquisition. Such an indicator could be used to screen for subjects that are unlikely to acquire the complex rules of the task and thus avoid investing substantially in an animal that is unlikely to yield fruitful data.

Previous research suggests that hippocampal theta oscillations are a likely physiological indicator predictive of learning success. Novel stimulation triggers hippocampal theta oscillations (Adey, 1967), suggesting a potential role in attentional focusing or early encoding of experiences. Historically it has been shown that hippocampal theta oscillations can also be triggered by several types of learning,

including operant conditioning (Grastyan et al., 1959; Lopes da Silva & Kamp, 1969). In one classic study, recordings from the dorsal hippocampus of rabbits during a baseline period before classical conditioning of the nictitating membrane revealed a predictive relationship between EEG frequency and subsequent rate of learning (Berry & Thompson, 1978). One potential interpretation of this finding is that higher power of hippocampal theta oscillations during baseline conditions could correlate with a stronger response to novelty or additional attention which may create optimal conditions necessary for subsequent learning. In a more recent study with rats, the mean hippocampal theta rhythm frequency observed during baseline periods of immobility had a positive correlation with the rate at which rats learned a simple discrimination operant task (Santos et al., 2008). Interestingly, this relationship was observed during both quiet waking and REM sleep, suggesting that basal theta frequency may relate to basic neurological processes important in the acquisition of operant behavior.

The exact nature of the relationship between neural oscillations and behavioral learning rates has yet to be determined. Intracranial EEG recordings in humans have shown that hippocampal theta power increases with virtual maze difficulty (Kahana et al., 1999). However, in an eight-arm radial maze task, theta power in rat hippocampal CA1 area gradually decreases as learning progresses (Masouka et al., 2006). In cats, the activity of mPFC neurons was modulated by theta during quiet waking and theta power in the mPFC increased as the conditioned stimulus in a trace fear paradigm gained predictive value for reward delivery (Paz et al., 2008). Specifically, conditioned stimulus presentation caused a larger increase in theta power at late vs. early stages of training, especially in PL/IL subregions of the mPFC. These authors suggest that theta oscillations

generally contribute to synchrony of neurons in the mPFC and that the hippocampus may generate stronger theta during learning, thus leading to more synchronization of the mPFC and facilitation of rhinal transfer of activity to the neocortex for consolidation.

According to human EEG studies, episodic memory formation, and thus learning, may occur via the mechanism of neuronal synchronization (Axmacher et al., 2006). Theta-Gamma coupling is stronger during a working memory task compared to a simple vigilance task, but there were no differences in theta or gamma power (Park et al., 2013), suggesting that theta-gamma interactions may be a useful biophysical marker for working memory processes. Human studies on electrophysiological correlates of memory encoding have demonstrated power fluctuations in both theta and gamma frequency bands (Kahana, 2006, Nyhus & Curran, 2010). Although localized increases in theta and gamma activity during encoding predictive of subsequent recall have been demonstrated in the temporal cortex and hippocampus (Sederberg et al., 2003), successful memory encoding is also associated with an extensive decrease in global theta power and increases in gamma power (Sederberg et al., 2007). Such wide frequency band activity is not consistent with a mechanism that relies on precise narrow band phase synchronization and might reflect arrhythmic and intrinsically asynchronous processes. If oscillations bind spatially distributed memory representation, then overall synchrony and power should increase, whereas if asynchronous activity dominates, then synchrony and power should decrease. In a recent human intracranial EEG study, Burke et al. (2013), found that successful encoding was marked by theta synchrony increases and decreases occurring very near each other in time and space. Specifically, they observed an initial transient increase in theta synchrony in posterior regions of interest, followed by

concentration of theta synchrony in the left prefrontal cortex, and then asynchronous gamma activity following synchrony along an anterior to posterior pathway Similar to Paz et al. (2008), and others, these authors suggest that the prefrontal cortex might act as a network hub of theta oscillations during memory formation, potentially providing contextual integration, top-down interactions between cortical structures, or communication between the neocortex and the hippocampus.

In this chapter, the main question under investigation is whether or not neural oscillations in the medial prefrontal cortex, the anterior cingulate cortex, and the ventral hippocampus correlate with the rate at which rats will achieve criterion performance in the DNMTP operant working task. Other questions for investigation include how physiology changes within a subject as learning progresses, and how physiology differs on correct vs. incorrect responses. To answer these questions, rats had a baseline recording session prior to initial training on the 5 second delay version of the DNMTP task. This baseline recording was followed by subsequent recording sessions throughout learning the task. To investigate how physiology changes over the course of learning, emphasis was placed on comparing the recordings from the first session of the DNMTP task to the last available recorded session. Post-hoc analysis of animals that had relatively fast or slow rates of acquisition for the DNMTP task will be used retroactively to compare physiological results and look for a physiological indicator predictive of more efficient learning. These animals will be referred to as the “fast” and “slow” learning groups.

Baseline recording sessions will be analyzed via power spectrum analyses. It is hypothesized that all animals will show peaks of activity in the theta frequency range,

and this effect will be observed in all anatomical recording locations. We expect to observe the strongest power indicated by peak amplitude values in the ventral hippocampus, followed by the medial prefrontal cortex, and then followed by the anterior cingulate cortex. It is hypothesized that animals later divided into the fast learning group will retroactively show higher mean amplitudes of power in the theta (4-12 Hz), low gamma (30-50 Hz), and high gamma (70-90) frequency bands than the animals later divided into the slow learning group.

Early and late learning sessions will be analyzed via waveform averaging and waveform correlations. Waveform averages will be used to look at the coordination of activity in each waveform around visual stimuli. A flat waveform average indicates noise, or random activity; whereas discernible peaks in the waveform average indicate patterned or coordinated activity. Coordinated activity is represented by higher amplitude or patterned responses such as oscillatory resonance or event-related potentials. Observations of patterned oscillatory responses such as theta rhythm reset following light illumination, and event-related potentials around stimulus onsets with different mnemonic roles in the task are expected. The houselight illuminates one second before the sample light and does not have a mnemonic role in the task, so we do not expect to observe coordinated waveform averages or event-related potentials in response to the onset of this light. The location of the sample light represents information to be encoded and maintained, so we expect to observe coordinated waveform averages and event-related potentials in response to this light, especially in the ventral hippocampus and medial prefrontal cortex. The choice lights represent retrieval of information. We expect the ventral hippocampus and medial prefrontal cortex to show the highest coordination

and event-related potentials in response to choice lights that yield correct responses, whereas we expect the anterior cingulate cortex to show the highest coordination and event-related potentials in response to choice lights that yield incorrect responses.

The degree of coordination for the waveform averages will be assessed by performing area under the curve analyses, with more coordinated waveform averages displaying larger areas. We hypothesize that animals in the fast group will have more coordinated waveforms than animals in the slow group, indicated by larger area under the curve. We hypothesize that waveforms will show more coordination as learning progresses, so area under the curves will increase from early to late sessions. It is hypothesized that the ventral hippocampus and the medial prefrontal cortex have more substantial roles in mediating the successful performance of this task, so we expect to observe larger areas under the curve for these waveforms compared to the anterior cingulate cortex. Since the sample light and the choice lights have the most salient mnemonic roles in this task, we expect to observe larger areas under the curve for these lights compared to the non-mnemonic houselight. We expect to observe the largest area under the curve in waveform averages around the choice lights that yield correct responses.

Waveform correlations are a way of quantifying the similarity between two waveforms, or their synchrony. A waveform correlation of -1 indicates an inverse relationship, a value of 0 indicates an uncorrelated relationship, and a value of +1 indicates a perfect correlation where the waveforms demonstrate high phase synchrony with each other. Based on the anatomical literature reviewed in Chapter 1, there is good evidence that the ventral hippocampus projects directly to the pre-limbic/infra-limbic

region of the medial prefrontal cortex, but only projects indirectly to the anterior cingulate cortex. Consequently, we hypothesize that there would be more similarity or synchrony in the waveforms between the ventral hippocampus and medial prefrontal cortex than the ventral hippocampus and the anterior cingulate cortex. We expect to observe higher peak correlation values in the early recording sessions compared to the late recording sessions.

4.2. Subject Information and Specific Methods

Recording Timing

All animals were trained to criterion on Working Memory stages A (Bar Press) and B (Sample Phase). Animals were surgically implanted with electrodes and allowed to recover for one week before a 5 minute baseline recording in the operant box without any stimuli. Immediately following the baseline recording, animals were recorded for their first day of Working Memory C (DNMTP with 5 second delay) training. This recording is considered the "Early" time point. The last recording available for each rat is considered the "Late" time point.

4.3. Post-Hoc creation of "Fast" and" Slow" groups

The number of daily sessions necessary for each animal (n=13) to reach behavioral criterion (> 70% accuracy) for WM C was rank ordered from shortest to longest. The median number of days to achieve criterion was 18. Animals that achieved criterion before the median were divided into the "Fast" learning group; animals that achieved criterion on or after the median were in the "Slow" learning groups for

subsequent physiological analyses. Animals in the fast group (n=6) reached criterion in a mean of 13.8 days with a standard deviation of 2.23. Time to acquisition for the fast group ranged from 10 to 16 days. Animals in the slow group (n=7) reached criterion in a mean of 24 days with a standard deviation of 4.51. Time to acquisition for the slow group ranged from 18 to 31 days. An unpaired two-tailed t-test with Welch's correction for unequal variance confirmed that the groups were significantly different from each other on mean time of acquisition for this initial stage of the DNMTP task (t=5.280, df=9.027, p <0.0005).

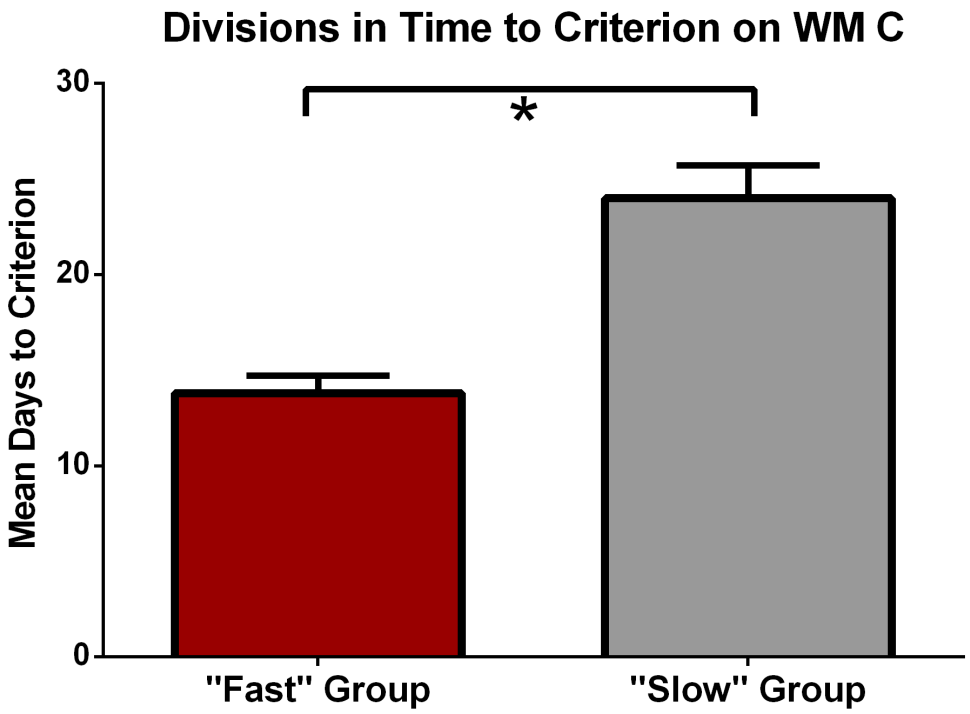

Figure 10 Divisions in Time to Criterion on WM C

Mean days to criterion (≥70% accuracy) for WM C divided by median split into "Fast" (n=6) and "Slow"(n=7) groups. Groups had significantly different time to criterion (p < 0.0005). Error bars indicate SEM.

4.4. Baseline Power Spectrum Results

Five-minute long baseline recordings were acquired for each animal that was part of the learning cohort. Some animals were excluded from physiological analysis due to occluded head stages or recordings that were unusable for any other reason. There were 5 animals/recordings in both the "Fast" and "Slow" groups, for a total N=10. Baseline recordings were acquired in the same operant box as all subsequent recordings. During the baseline period, the houselight was illuminated but no other stimuli or response levers were activated.

A power spectrum analysis was performed on the entire 5-minute baseline session and included frequencies from 0 to 90 Hz with a resolution of 0.48 Hz. All animals showed comparable power spectrums with dominant power occurring within the theta frequency band (4-12 Hz). Specifically, the mean frequency at which maximum power occurred across all animals and all recording locations was 6.77 Hz. The frequency with the most power ranged between 6.5 and 7.0 Hz in all animals and in all recording sites. The mean frequency with maximum power was not different between the fast group (mean = 6.9 Hz) and the slow group (mean = 6.6 Hz), with a substantial overlap in ranges (See Figure 11).

The strongest power was observed in the medial prefrontal cortex and was especially prominent in the fast group. An unpaired two-tailed t-test was performed on mean power spectrum curves for fast versus slow learning groups at each recording location (See Figure 12). In the medial prefrontal cortex, the fast group had significantly more overall power than the slow group $t(372)=6.38$, $p<0.0001$. Also, the anterior cingulate cortex power spectrum showed a highly significant effect $t(373)=4.929$,

p<0.0001. The ventral hippocampus power spectrum was also significant t(378)=2.038, p<0.05.

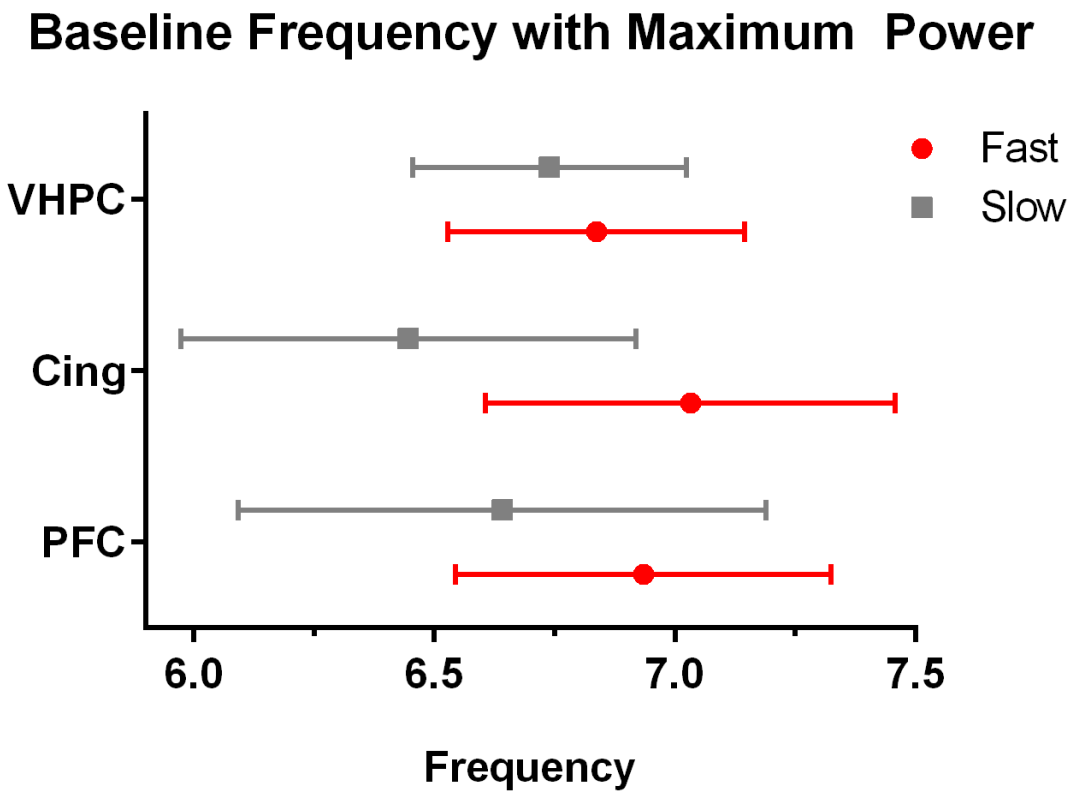

Figure 11 Baseline Frequency with Maximum Power

Mean frequencies with maximum power for fast versus slow group at each recording location. Error bars indicate SEM.

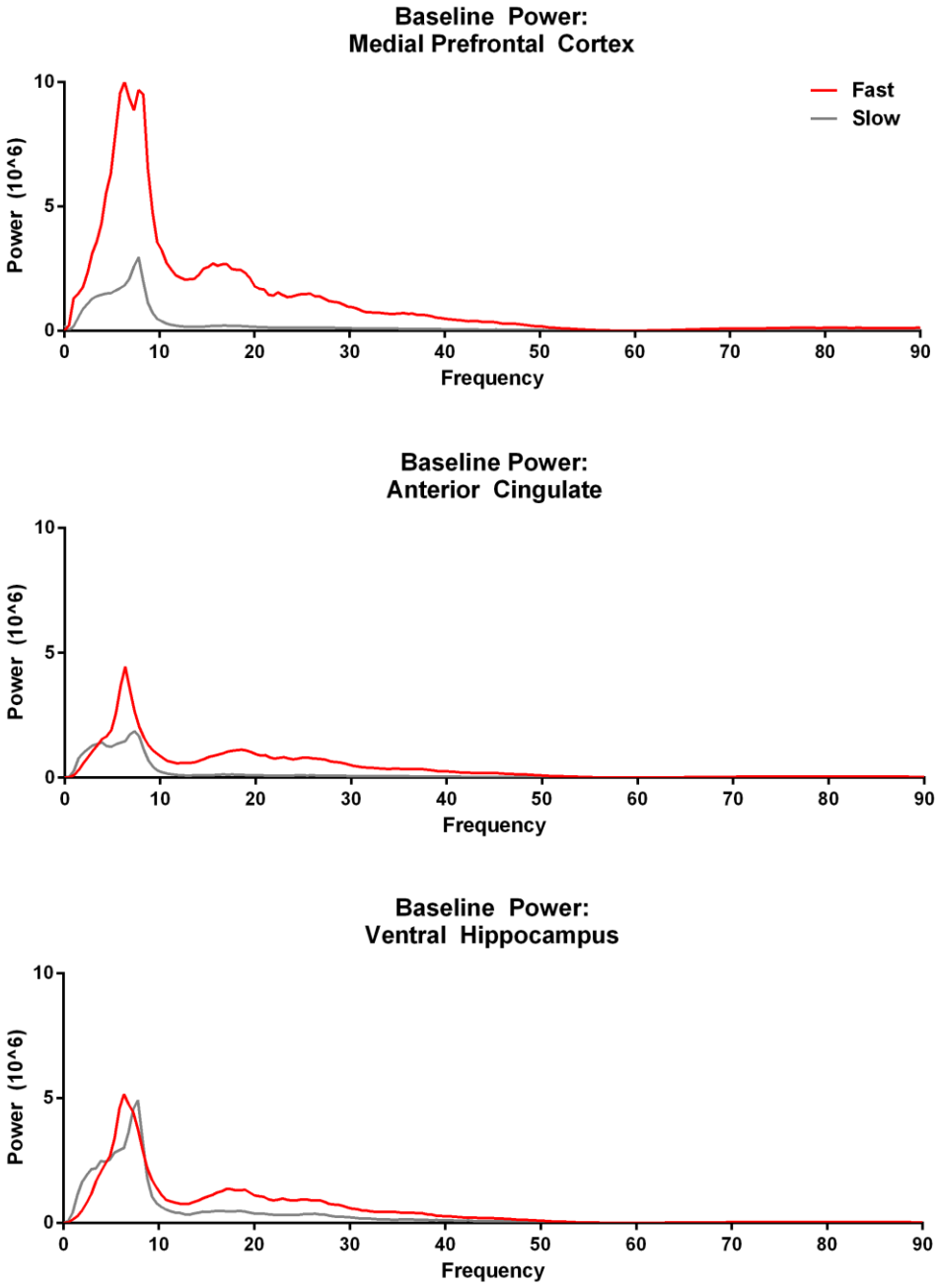

Figure 12 Baseline power spectrums comparing fast versus slow groups at each recording location.

Top is medial prefrontal cortex, middle is anterior cingulate, bottom is ventral hippocampus. Fast versus slow power spectrums were significantly different at all locations.

Activity in the theta frequency band (4-12 Hz) was clearly the dominant pattern within the signal, showing a significant peak in the power spectrum for all animals and across all recording locations. The strongest power is observed in the medial prefrontal cortex of the fast learning group. The amplitude of the power gradually decreased as frequency increased (See Figure 13). In both low gamma (30-50 Hz) and high gamma (70-90 Hz) the amplitude of power for the fast learning group was higher than the slow learning group. Dividing the broad power spectrum into sections for specific frequency bands and performing unpaired two-tailed t-tests confirmed a difference between fast and slow groups at each recording location (See Figure 13). Power in the theta frequency band was significantly different in the medial prefrontal cortex $t(30)=6.641$, $p<0.0001$, and the anterior cingulate cortex $t(30)=2.770$, $p=.0095$, but not in the ventral hippocampus $t(30)=.0867$, $p>0.05$. Power in the low gamma frequency band was significantly different in the medial prefrontal cortex $t(120)=9.010$, $p<0.0001$, in the anterior cingulate cortex $t(120)=8.685$, $p<0.001$, and in the ventral hippocampus $t(120)=5.723$, $p<0.0001$. Power in the high gamma frequency band was also significantly different across all three recording locations: medial prefrontal cortex $t(122)=17.85$, $p< 0.0001$, anterior cingulate cortex $t(122)=18.01$, $p<0.0001$ and ventral hippocampus $t(122)=7.573$, $p<0.0001$. Note that frequencies around 60 Hz were excluded due to a notch filter on the amplifier to reduce the influence of extraneous environmental noise from mains electricity hum.

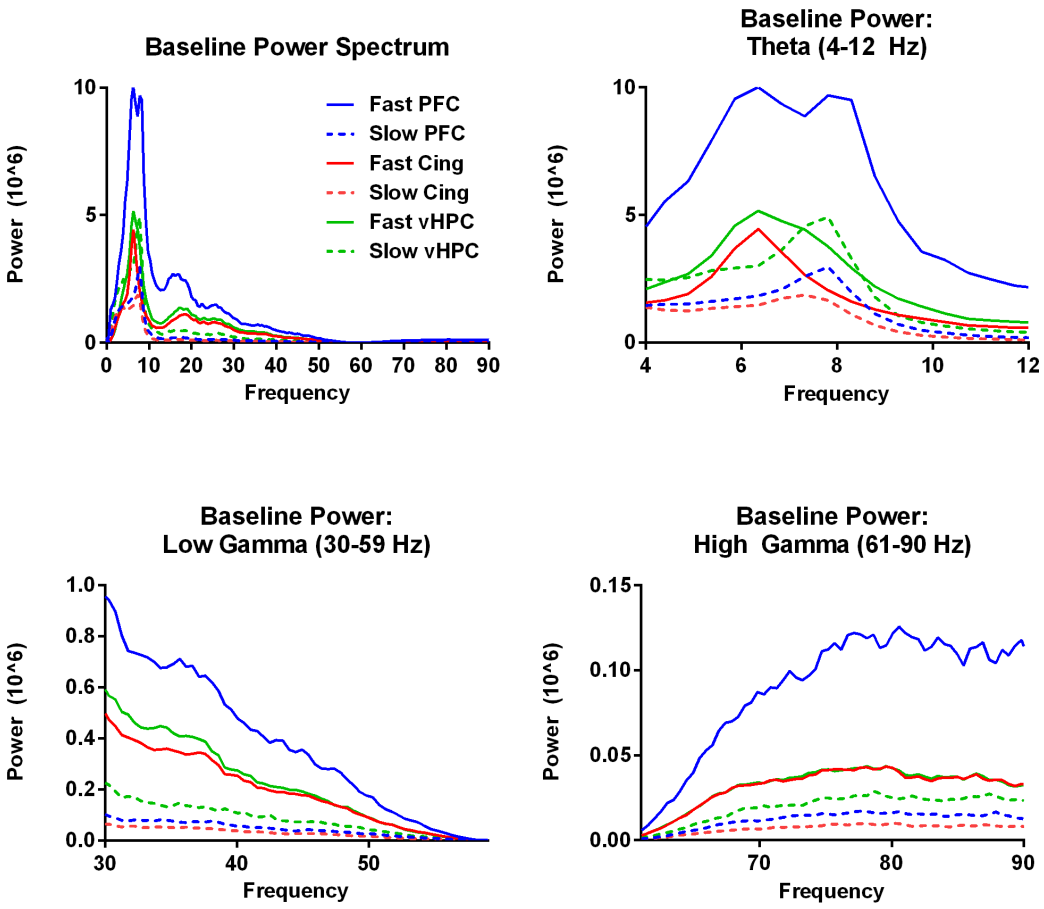

Figure 13 Baseline power spectrums by frequency bands

Top left is the full power spectrum from 0-90 Hz. Top right is the power spectrum in the theta frequency band (4-12 Hz). Bottom left is the power spectrum in the low gamma frequency band (30-59 Hz). Bottom right is the power spectrum in the high gamma frequency band (61-90 Hz).

4.5. Waveform Average Results

Waveform averages were calculated by analyzing a 1-second interval around stimulus triggering events. Time 0 represents stimulus light onset and the waveform average includes 0.5 second "Pre" stimulus onset and 0.5 second "Post" stimulus onset. The waveform averages represent the mean of all the sweeps over the span of the session. For example, a session with 100 trials would have 100 sweeps around events such as houselight, sample light, or choice light onsets. A flat waveform average indicates noise, or random activity; whereas discernible peaks in the waveform average indicate patterned activity.

One type of patterned activity that a waveform average can indicate is an evoked response. An evoked response, also known as an event-related potential, is an electrical signal that is distinct from spontaneous activity and is time-locked to onset of a sensory or motor event, such as a light illumination. Evoked potentials often appear as a coordinated peak or trough among relatively flat noise. Event-related oscillations are another type of time-locked patterned activity that can emerge from attention to onset of a stimulus and appear as rhythmic activity. In Figure 14, there is an example of an event-related oscillatory response to light illumination. In the one second prior to stimulus onset, the waveform averages are relatively flat. However, after stimulus onset at time 0 (represented by a red dashed line), the waveform averages all become synchronized into a resonant oscillatory pattern. Given that this oscillatory evoked response has a frequency of approximately 6-7 Hz, this demonstrates the stimulus-evoked event-related oscillatory phenomenon previously identified as theta rhythm reset.

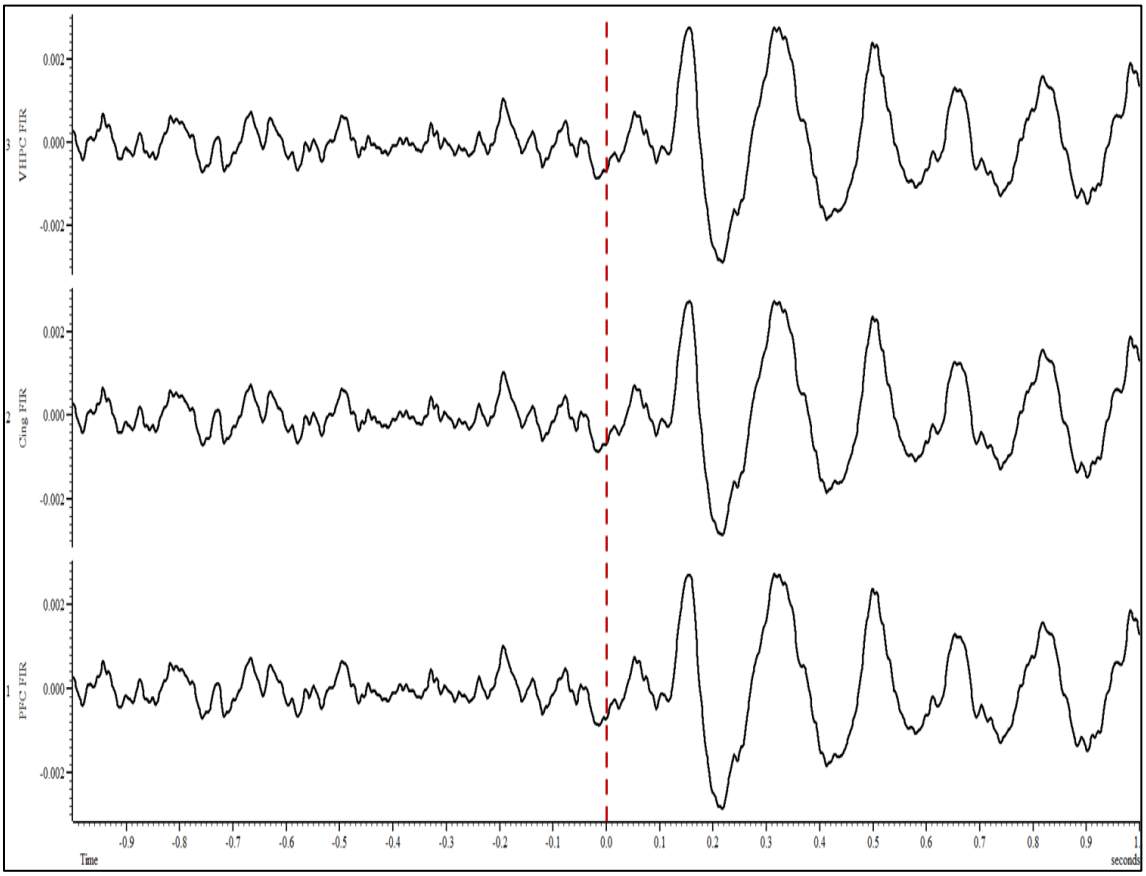

Figure 14 Theta Reset following light illumination.

Bottom trace represents waveform average in the medial prefrontal cortex, middle trace represents waveform average in the anterior cingulate cortex, top trace represents waveform average in the ventral hippocampus. Onset of light illumination is indicated by the red dashed line. This example is from an early recording in a member of the fast group.

Waveform averages for the medial prefrontal cortex, the anterior cingulate cortex, and the ventral hippocampus were performed on recordings from early and late recording sessions, and then sub-divided into fast and slow subject groups. Waveform averages were triggered to houselight onset as a non-mnemonic control, to the onset of the sample phase light, and to the onset of choice phase lights that eventually yielded either correct or incorrect responses. The purpose of these analyses was to determine whether or not there were any qualitative or quantitative differences in waveform averages or event-related potentials for the fast versus slow groups in response to stimulus onset and how these differences manifested across anatomical recording locations and as learning progressed from early to late sessions.

The amplitude of a waveform average can provide clues to the timing or processing of the signal. Across all recording locations and stimuli, the waveform averages with the lowest amplitude were the ones surrounding the houselight onset, indicating the decreased value of this stimulus compared to the other stimuli. In general, waveform averages showed varying levels of post-stimulus-evoked responses following onset of all stimuli except for the house light. Stimulus-evoked responses are demonstrated by large peaks in the waveform average that co-occur with stimulus onset. Most stimulus-evoked responses occur within the first 200 milliseconds after the stimulus onset. Waveform averages for fast versus slow groups in the prefrontal cortex are shown in figure 15, for the anterior cingulate cortex in figure 16, and for the ventral hippocampus in figure 17. Averages for early sessions are represented in the left column of each figure; averages for late sessions are represented in the right column. The top row represents averages around houselight onset, the 2nd from the top represents

waveform averages around sample phase hits, the 3rd from the top represents waveform averages around choice phase hits, and the bottom row represents waveform averages around choice phase misses. Unpaired, two-tailed t-tests for fast vs. slow group differences were performed on all waveform averages. All results from these t-tests are summarized in Table 2 with significant effects highlighted in gray and bolded text.

The medial prefrontal cortex showed the strongest stimulus-evoked responses, followed by the ventral hippocampus, and then the anterior cingulate cortex. In both early and late sessions, the prefrontal cortex response to the houselight is substantially blunted compared to the onset of other, more mnemonically relevant, stimuli. A significant difference between fast and slow group waveform averages around the houselight was observed in the late session. In the early sessions, averages for the slow group had a stronger evoked response to the onset of the sample light and the choice lights than the fast group, but this pattern reversed in the late sessions with the fast group showing a significantly stronger evoked response than the slow group.

The waveform averages for the cingulate cortex do not show evoked responses as clearly as the medial prefrontal cortex. The ventral hippocampal waveform averages show significant differences between fast and slow groups around the onset of sample hits during both the early and late recording sessions.

Area under the curve analyses were performed on the post-stimulus waveform averages to further quantify group differences. Area under the curve is an indirect integrated measurement related to the amplitude of the signal. A more organized or patterned signal will have higher amplitude and thus a larger total area under the curve. The total area under the curve data across all conditions was collapsed and then

reorganized into different comparisons including fast versus slow groups, early versus late sessions, comparison of different anatomical locations, comparison of different stimulus onsets. According to unpaired, two-tailed t-tests neither fast versus slow learning group nor early versus late sessions resulted in significantly different effects.

For the anatomical location comparison, the area under the curve was greatest for the medial prefrontal cortex, then the ventral hippocampus, then the anterior cingulate cortex (See Figure 21). A one-way ANOVA showed a statistically significant difference among the means ($F_{2,45}=3.528$, $p < 0.05$). Tukey's multiple comparisons test indicated that there was a significant difference between the mean area under the curve for the medial prefrontal cortex and the anterior cingulate cortex. This result is likely due to the substantially larger stimulus-evoked response in the medial prefrontal cortex.

The post-stimulus area under the curve for each stimulus light was smallest after the houselight onset, followed by onset of the light for sample hits, followed by light for choice misses (See Figure 22). Stimulus onset for choice hits produced the largest area under the curve. A one-way ANOVA showed a statistically significant difference among the means ($F_{3,44} = 8.720$, $p = .0001$). Tukey's multiple comparison test indicated that there was a significant difference between the mean area under the curve for the houselight versus both the choice hit and choice miss lights.

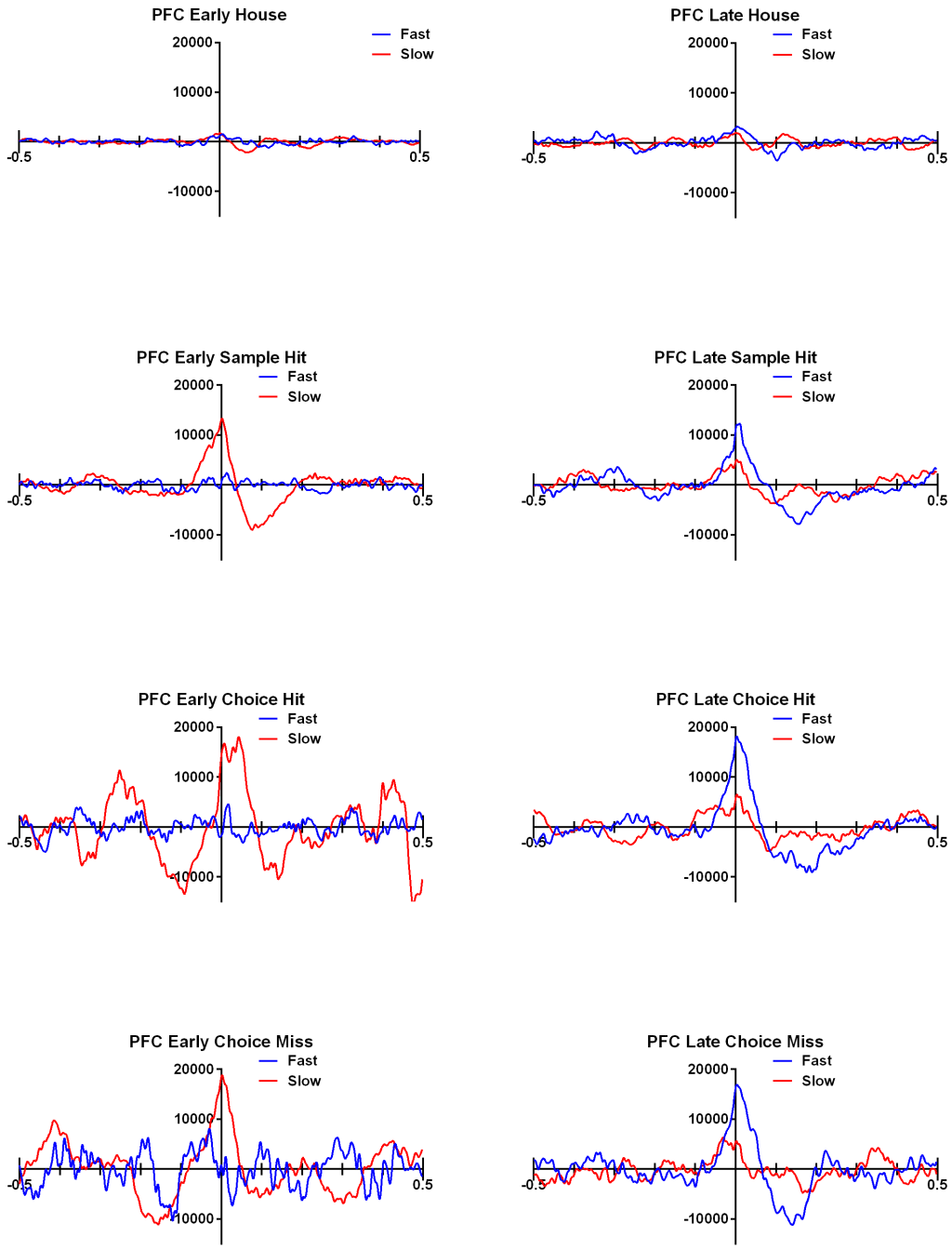

Figure 15 Waveform Averages of the Prefrontal Cortex.

X-Axis represents time from -0.5 seconds prior to stimulus onset to 0.5 seconds after stimulus onset. Onset marked by x=0. Y-axis is in microvolts.

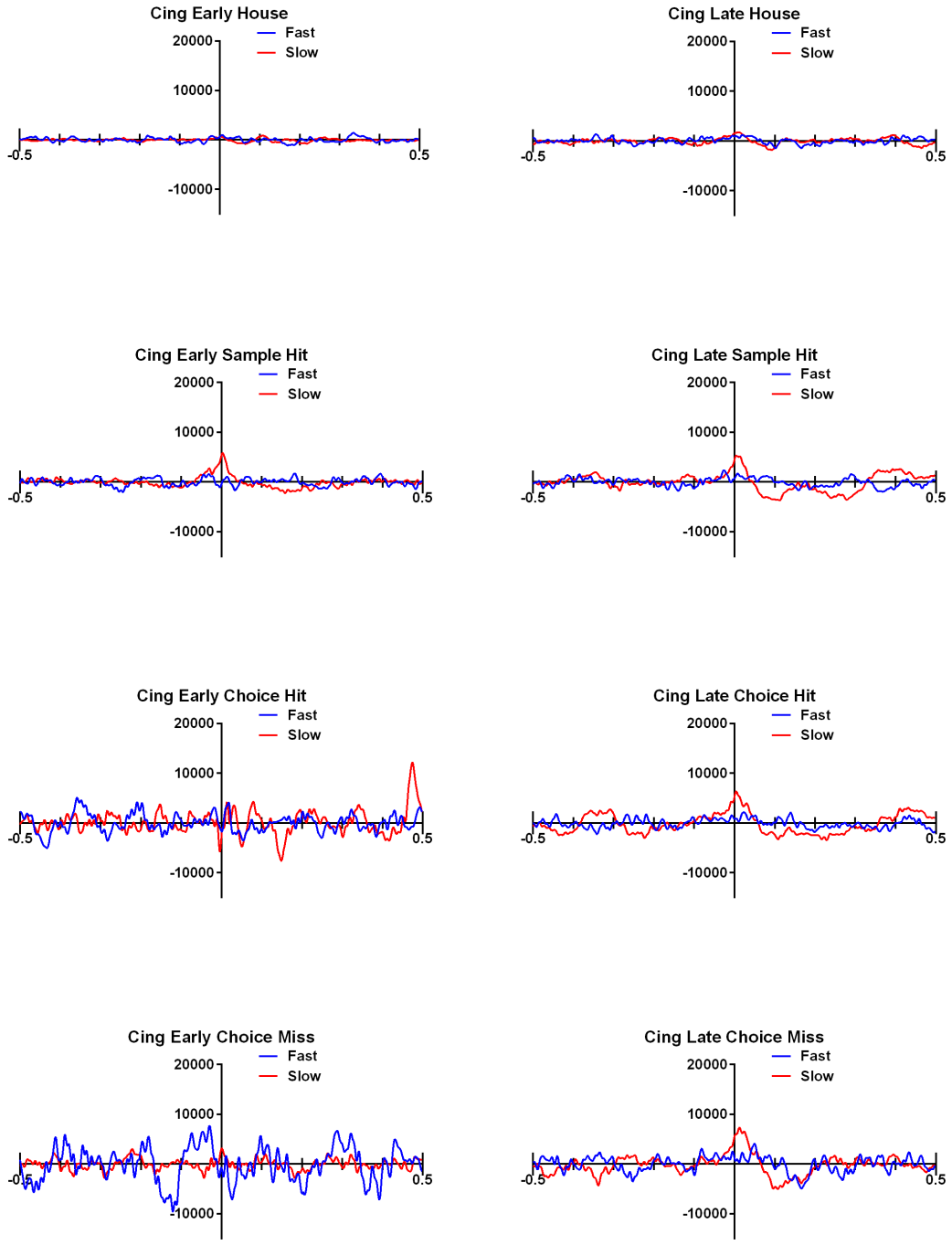

Figure 16 Waveform Averages of the Anterior Cingulate Cortex.

X-Axis represents time from -0.5 seconds prior to stimulus onset to 0.5 seconds after stimulus onset. Onset marked by x=0. Y-axis is in microvolts.

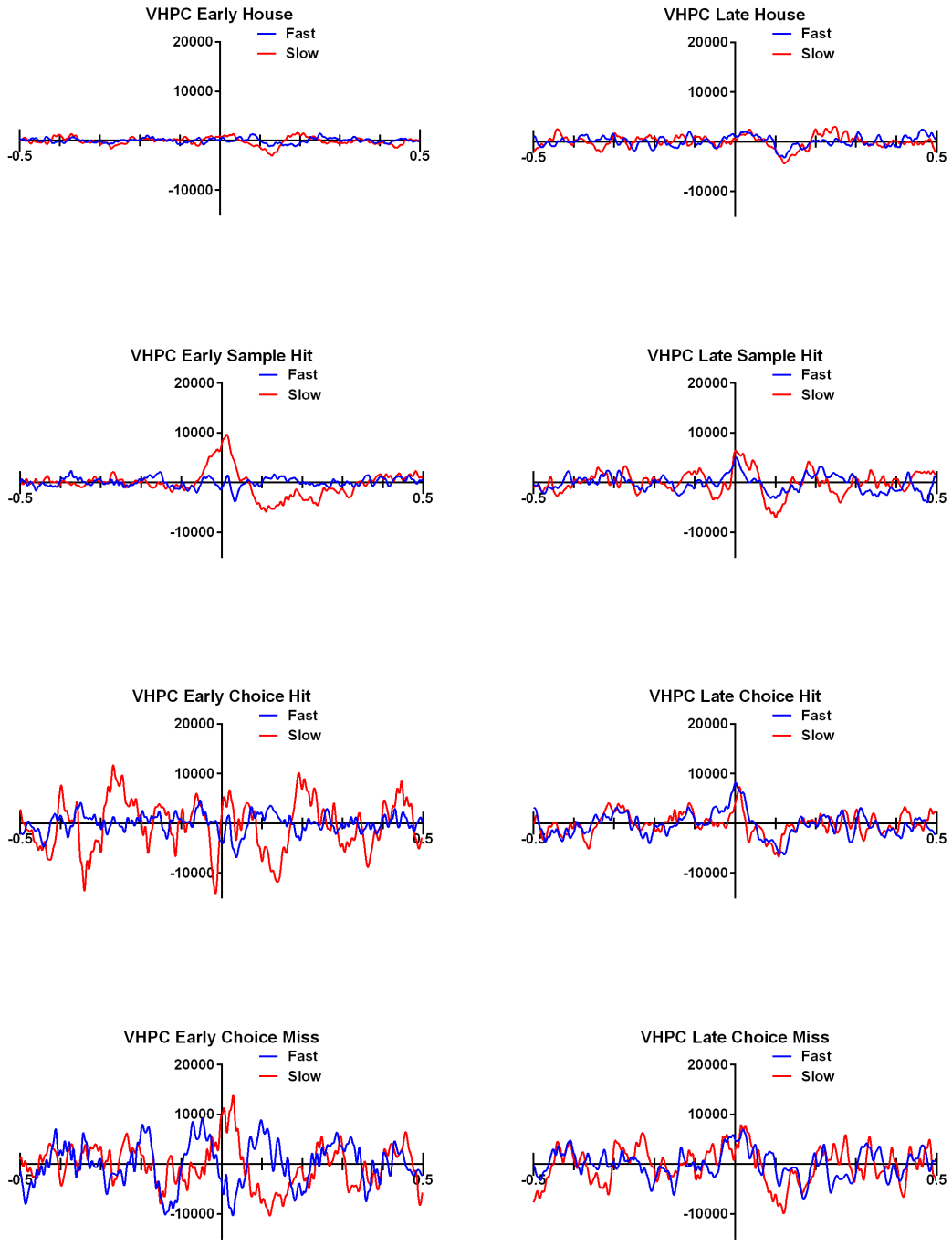

Figure 17 Waveform Averages of the Ventral Hippocampus.

X-Axis represents time from -0.5 seconds prior to stimulus onset to 0.5 seconds after stimulus onset. Onset marked by x=0. Y-axis is in microvolts.

			T-Test Value	Degrees of Freedom	P Value
PFC	Early	Sample Hit	0.29	1998	0.7686
		Choice Hit	0.63	1998	0.5257
		Choice Miss	2.26	1998	**0.0240 ***
	Late	**Sample Hit**	2.77	1998	**0.0056 ***
		Choice Hit	2.09	1998	**0.0372 ***
		Choice Miss	1.15	1998	0.2523
Cing	Early	Sample Hit	0.57	1998	0.5714
		Choice Hit	1.6	1998	0.1093
		Choice Miss	0.05	1998	0.9625
	Late	Sample Hit	0.46	1998	0.6451
		Choice Hit	0.96	1998	0.3357
		Choice Miss	2.09	1998	**0.0367 ***
VHPC	Early	**Sample Hit**	2.49	1998	**0.0129 ***
		Choice Hit	1.38	1998	0.1693
		Choice Miss	1.62	1998	0.1060
	Late	**Sample Hit**	2.22	1998	**0.0265 ***
		Choice Hit	1.42	1998	0.1563
		Choice Miss	1.22	1998	0.2233

Table 2. T-Test results for fast versus slow waveform averages.

Table represents results from series of non-overlapping unpaired, two-tailed t-tests comparing fast versus slow waveform averages around each stimulus onset, at each time point, and for each recording location. Significant effects are marked by an asterisk and gray highlighting.

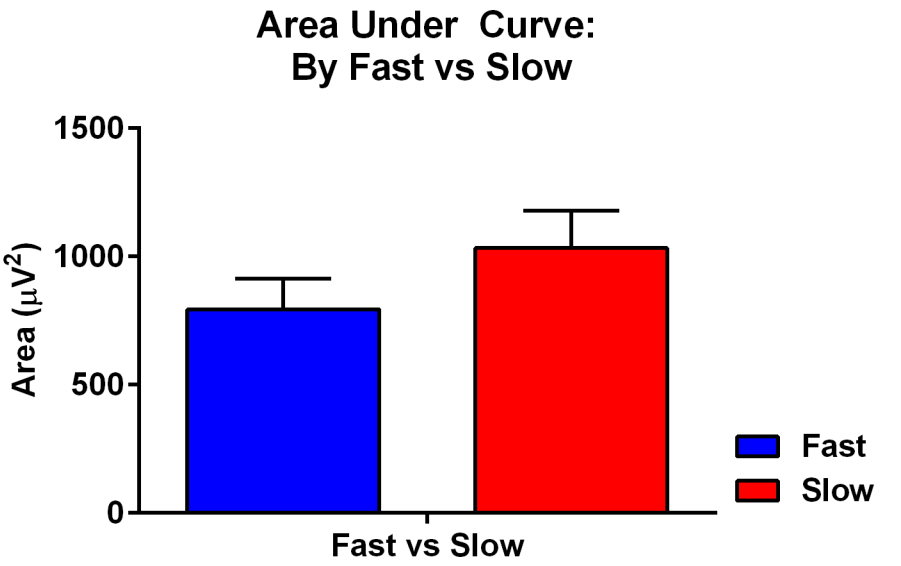

Figure 18 Post-stimulus area under the curve for fast versus slow groups. Error Bars indicate SEM.

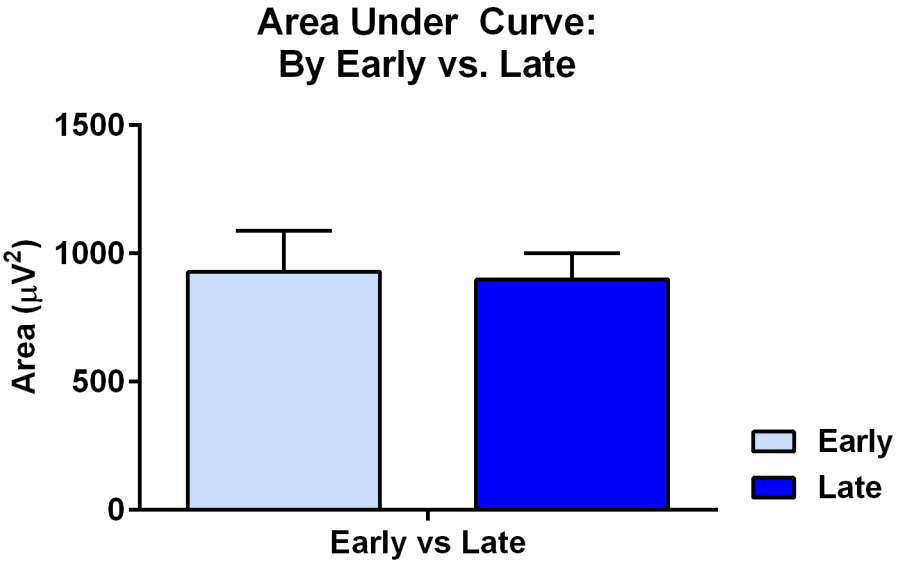

Figure 19 Post-stimulus area under the curve for early versus late sessions. Error Bars indicate SEM.

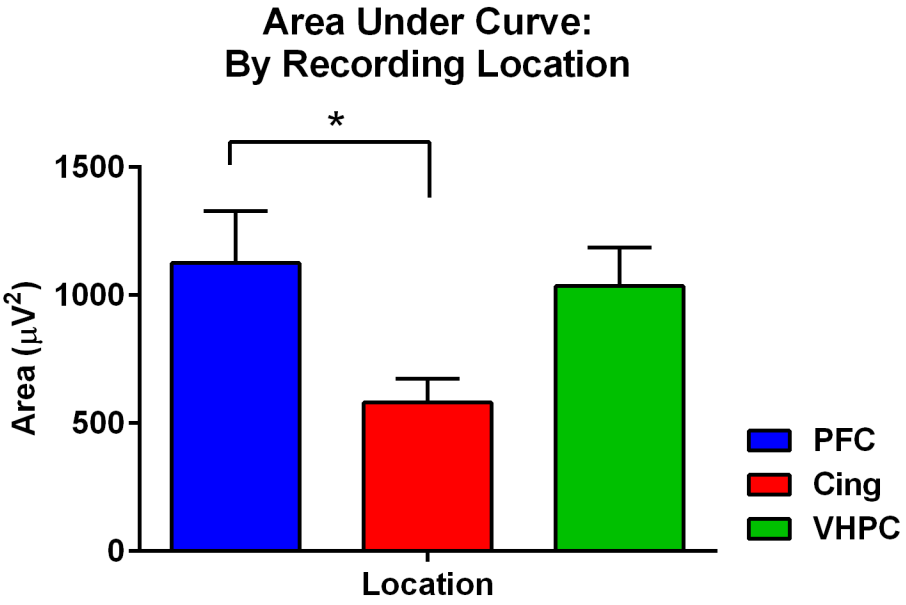

Figure 20 Post-stimulus area under the curve for all recording locations. Asterisk indicates significant p<0.05. Error Bars indicate SEM.

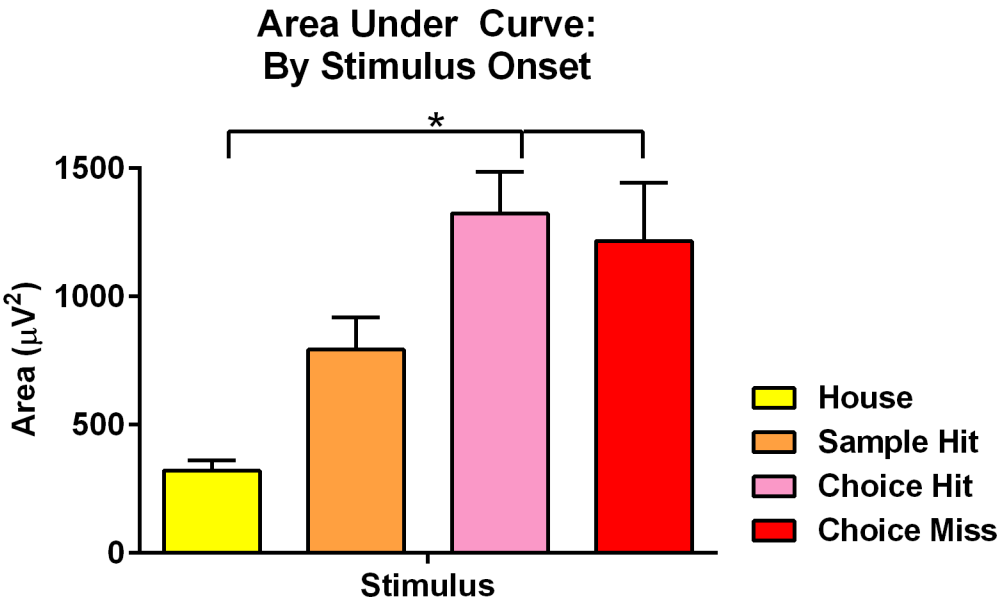

Figure 21 Post-stimulus area under the curve for all stimulus onsets. Asterisk indicates significant p<0.05. Error Bars indicate SEM.

4.6. Waveform Correlation Results

Waveform correlations are a way of quantifying the similarity between two waveforms or looking at their synchrony. It was hypothesized that when referenced to the waveform from the ventral hippocampus, the waveform correlation values would be higher in the medial prefrontal cortex than in the anterior cingulate cortex. Waveform correlations were performed on both early and late learning sessions and then subdivided into the post-hoc fast and slow groups. Correlations were performed gated to sample or choice phase onset respectively, or on the whole session. All correlations were referenced to the ventral hippocampus waveform.

When a waveform is correlated with itself, the result is an autocorrelation that shows a typical Ricker wavelet or "Mexican Hat function" appearance. This autocorrelation peaks at +1 (indicating a full correlation) at time point zero. The function is symmetrical around time point zero. There is a relatively narrow band of high positive correlation around time point zero and then the correlation decreases to around -0.25 (weak inversion) around time points $\pm$ 0.1 seconds. After approximately $\pm$0.15 to 0.20 seconds, the correlation is flat around the X axis indicating that the waveform is uncorrelated. The autocorrelation of the ventral hippocampus waveform (See Figure 22) is an example of this type of function demonstrating a perfect correlation.

When waveform correlations are performed and referenced to a non-self waveform, there are several ways that the resultant function can differ from the Mexican hat function observed in autocorrelations. First of all, the amplitude of peak correlation at time point zero is likely to be much lower than the autocorrelation. The function may take on a more asymmetrical appearance or have wider or narrower peak, indicating a

time lag. The function may also have more oscillatory resonance as the function extends away from time point zero in both directions, indicating other frequencies that may show synchrony. Across several conditions (fast/slow group, early/late session, sample/choice trigger), the waveform correlations for the medial prefrontal cortex and the anterior cingulate cortex respectively show a great deal of similarity with each other in terms of general shape and amplitude.

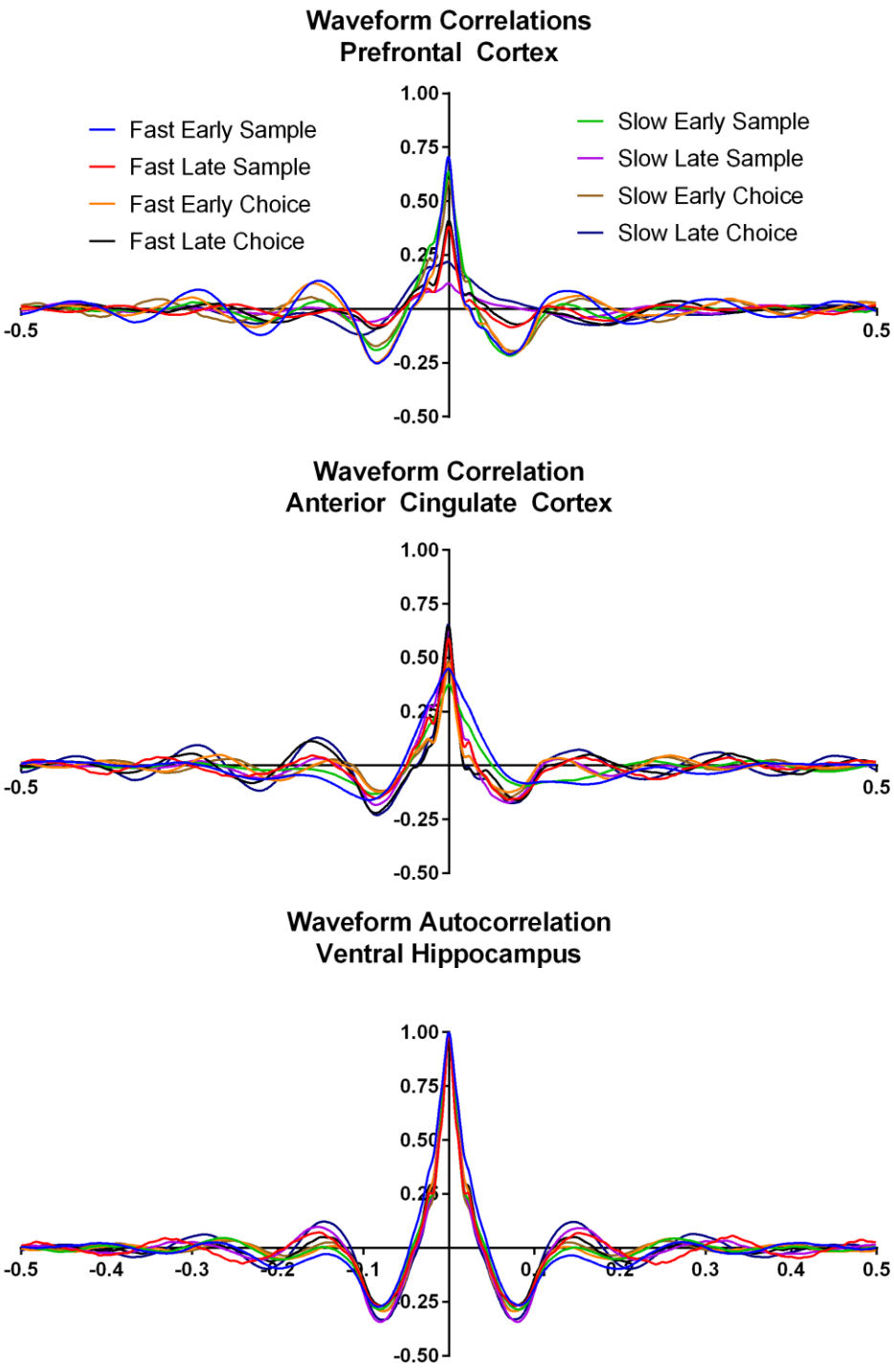

Figure 22 Learning Waveform Correlations by Anatomical Site

When the waveform correlations for the different time points are separated, it becomes clear that both the medial prefrontal cortex and the anterior cingulate are more highly correlated with the ventral hippocampus in the early sessions compared to the late recording sessions. In the early sessions the peak amplitude for both recording locations is approximately +0.75 indicating a moderately strong correlation, whereas this declines to approximately +0.50 in the later sessions. This pattern is observed when gated to either sample or choice phase onsets (See Figure 23).

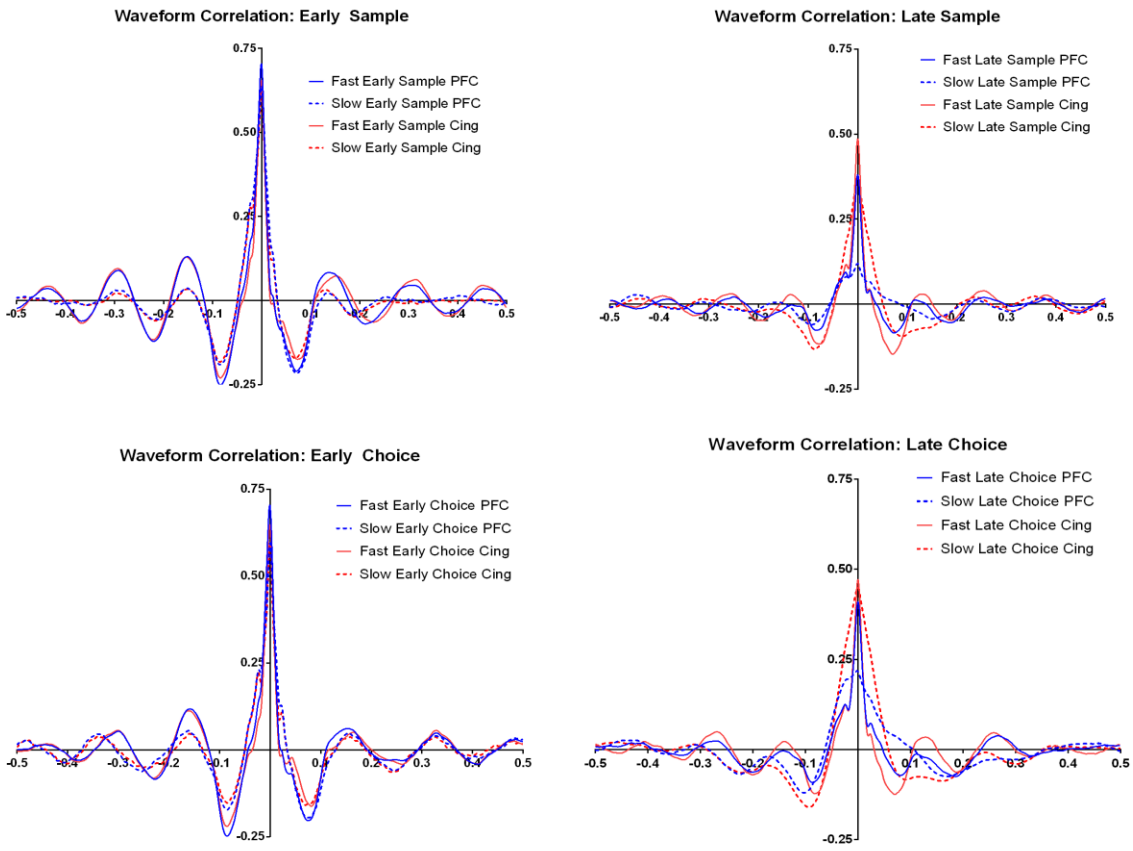

Figure 23 Mean Sample Phase and Choice Phase waveform correlations in early vs. late sessions .

The maximum correlation value was determined by the peak amplitude of the correlation at time point zero (See Figure 24). For the early sessions, both the medial prefrontal cortex and the anterior cingulate cortex showed comparably high correlations with the ventral hippocampus waveform. However, for both regions the maximum correlation value decreased in the late sessions. These decreases were most prominent in the medial prefrontal cortex correlations from the slow group and were evident when gated to either the sample phase or the choice phase of the task. A two-way ANOVA showed a significant main effect for the type of stimulus (Collectively fast or slow group, early or late session, sample or choice light) ($F_{7,64}=2.273$, $p<0.05$), but not a significant main effect for recording location nor an interaction.

To further characterize the change in amplitude of waveform correlations between the early and late recording sessions, values at all time points for the late session were subtracted from the early session. The resulting differences were averaged and plotted in Figure 25. At time point zero, all difference measures showed a negative value confirming that correlation amplitudes were higher in the early session than in the late session. Again, the difference was most prominent in the PFC recordings from the slow learners group. A two-way ANOVA on these difference measures indicated a significant main effect of time point ($F_{999,3996}=2.771$, $p<0.0001$), a significant main effect of condition ($F_{3,12}=3.639$, $p<0.05$), as well as a significant interaction ($F_{2997,11988}=1.376$, $p<0.0001$). Together, all of this supports the idea that both medial prefrontal cortex and anterior cingulate cortex waveforms decrease in similarity to the ventral hippocampus waveform as learning progresses.

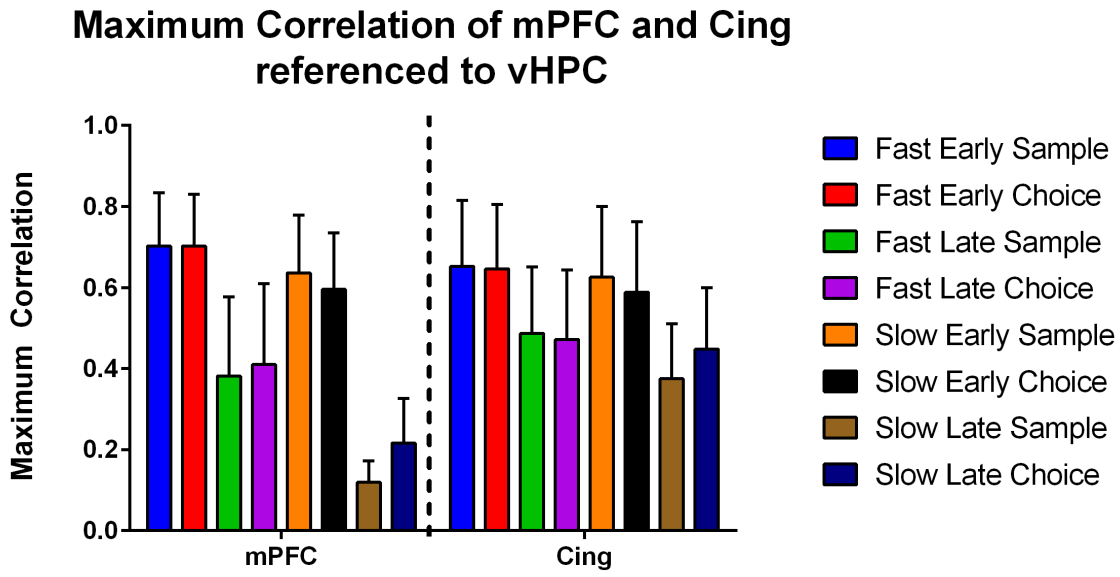

Figure 24 Maximum correlation of medial prefrontal cortex and anterior cingulate cortex waveforms referenced to the ventral hippocampus waveform.

Error bars represent SEM.

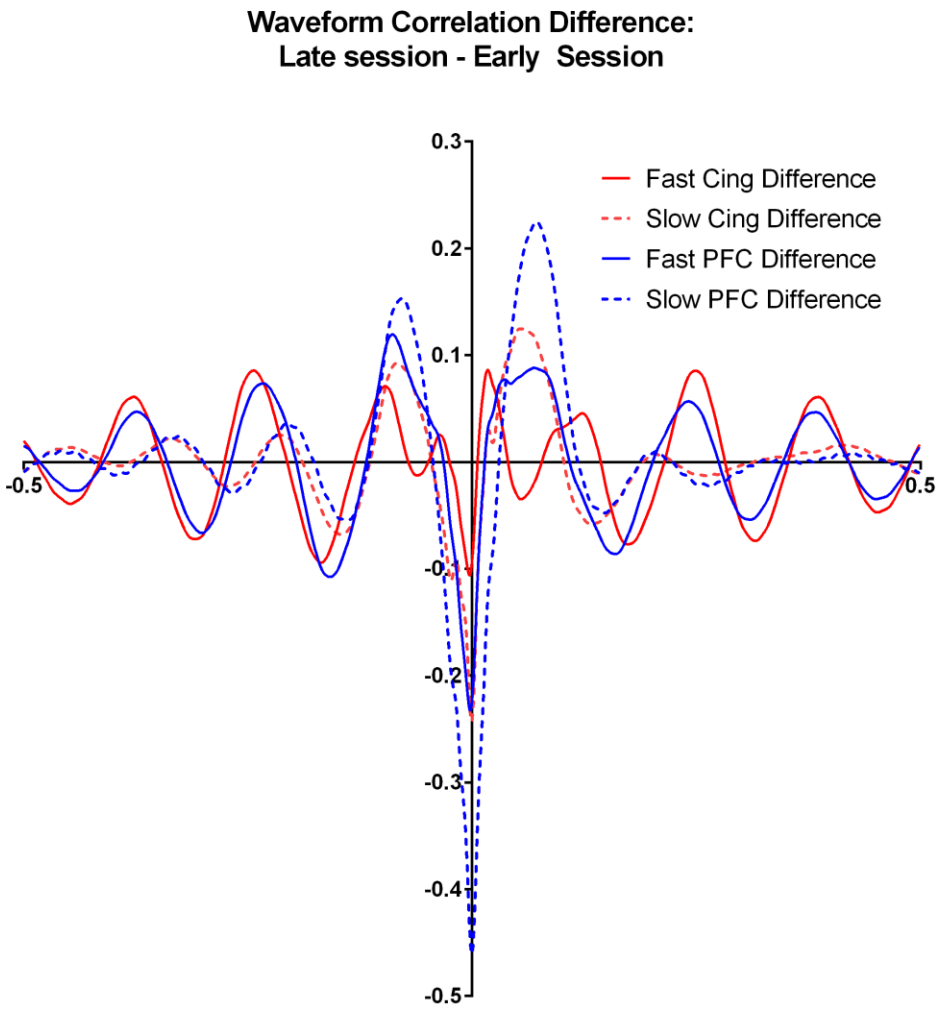

Figure 25 Mean waveform correlation difference: Late session –Early session.

4.7 Conclusions and Discussion

The power spectrum analyses of the 5 minute baseline recording session indicate that there are clear baseline physiological differences between the animals which would eventually become fast and slow learners of the delayed non-match to position task. Both the medial prefrontal cortex and the anterior cingulate cortex show fast versus slow group power spectrum differences in the theta, low gamma, and high gamma frequency ranges. Although the ventral hippocampus shows fast versus slow group power spectrum differences in low and high gamma, significant power differences were not observed in the theta frequency range. To the extent that there are physiological differences in baseline physiology between eventual fast and slow learning groups, these differences are not driven by the power of ventral hippocampal theta oscillations. This contradicts the findings in (Santos et al., 2008), but they focused their analyses on more dorsal regions of the hippocampus, which typically has much stronger power than the ventral hippocampus.

Santos and colleagues also observed a difference in speed of baseline frequency during periods of immobility and paradoxical sleep. In the current study, all animals showed theta-typical power spectrum peaks between 6.5 and 7.0 Hz, but there were not any significant differences in the peak frequency between the fast and slow learning groups. These differences may not have been observed for two reasons. First, our animals were freely moving around the operant box compared to having movement restrained. The analysis of frequency in the current experiments only had a resolution of 0.48 Hz which may have precluded seeing finer differences between groups in the theta range.

The baseline recordings were acquired immediately before the animals' first post-surgical training session on Working Memory C (DNMTP with a five second delay). All animals had previously experienced the context of the recording box during pre-surgical training on Working Memory A (bar press) and Working Memory B (sample phase) but had not been in the box for at least a week due to surgery and post-operative recovery. It is possible that the similarity of the power of ventral hippocampal oscillations between the fast and slow groups is due to contextual memory for the operant box and previous shaping steps. If baseline recordings were acquired on an animal's first exposure to the recording box environment, then it is likely that the power of ventral hippocampal theta oscillations would increase due to novelty and the formation of new contextual or episodic-like representations (Adey, 1967; Hasselmo et al., 1996; Wells et al., 2013).

Acetylcholinergic inputs to frontal cortex regions have frequently been associated with attention (Sarter et al., 2003). The fast learning group showed consistently stronger power than the slow learning group in these regions. This pattern supports the idea that animals that have more attentional capacity or are paying more attention on the initial day of training are likely to learn the task more efficiently than animals that have less attentional resources or are not paying as much attention for any other reason.

Waveform averages around the house light, sample hit, choice hit, and choice miss light onsets showed clear differences in the level of coordinated activity and stimulus-evoked responses. Event-related oscillatory behavior, such as theta reset, was observed in waveform averages for individual animals but not in mean waveform averages for groups, suggesting individual and trial by trial variability in this phenomenon. During the delay period, there was some evidence for coordinated

oscillatory patterning prior to the onset of the choice lights. This was particularly apparent in the ventral hippocampus recordings. Oscillatory patterning in the theta range during the delay period could potentially indicate the storage or maintenance of mnemonically relevant information until a response can be given.

When early versus late time point waveform averages were compared, the peak amplitude of the evoked responses around the sample hit, choice hit, and choice miss events was always slightly higher in the late session compared to the early session. This could indicate that these events acquire additional salience, attentional control, or memory processing as learning progresses. Further research would be needed to clarify the cognitive processes associated with these changes.

As hypothesized, there was significantly less coordinated activity or evoked responses surrounding the onset of the house light compared to the onset of other more mnemonically relevant light stimuli. Waveform averages around the onset of the house light had substantially lower amplitude than all other signal lights. The house light is located in the rear panel of the operant box and illuminates one second prior to sample light illumination. The houselight remains illuminated through the delay period until a choice response is given. The houselight is used as an attentional cue to focus and orient the animal towards the front panel for the sample light, and to help the animal differentiate the delay period (on) and the intertrial interval (off). Although the onset of the houselight is the most dramatic change in ambient brightness and it has obvious attentional associations, neither of these factors is sufficient to trigger strong stimulus-evoked responses similar to those observed after onset of the more mnemonically relevant lights.

Anatomically speaking, the medial prefrontal cortex showed the strongest stimulus-evoked responses, followed by the ventral hippocampus, and then the anterior cingulate cortex. Differences between the fast and slow groups were most interesting in the medial prefrontal cortex. In group averages around both the sample and choice light onsets, the fast group starts with a relatively flat waveform average in the early session that gains amplitude and shows more prominent stimulus-evoked responses over the course of learning. Conversely, the slow group starts with relatively strong stimulus-evoked responses in the early session that decrease by the late session. This result is counter to our hypothesis that the fast group would show stronger stimulus-evoked-responses than the slow group during both early and late sessions. While the fast group does show stronger stimulus-evoked responses in the late sessions, the stronger stimulus-evoked responses from the slow group during the early session are curious and worthy of further investigation in additional studies.

Results are generally similar to results seen by Paz and colleagues (2008). They showed that, in cats, the theta rhythm synchronizes activity of medial prefrontal cortex neurons during learning. During quiet waking activity of medial prefrontal cortex neurons was modulated by theta and as the conditioned stimulus in a trace fear paradigm gained predictive value for reward delivery, theta power in the medial prefrontal cortex increased. Conditioned stimulus presentation caused a larger increase in theta power at late versus early stages of training, especially in the prelimbic/infralimbic sub-regions of the medial prefrontal cortex. However, this study requires cautious interpretation because animals demonstrated substantial licking behavior after the conditioned stimulus but prior to reward delivery, a phenomenon that the authors referred to as anticipatory

licking. When rats engage in exploratory sniffing behavior, the vibrissae have been demonstrated to twitch rhythmically at about 7 beats per second, coordinating with the peak of limbic system theta rhythm activity (Komisaruk, 1970). Since licking involves very similar rhythmic behavior, this could be a potential confound in the interpretation of theta power increase.

Waveform correlations were used to assess the similarity or synchrony of medial prefrontal cortex and anterior cingulate cortex waveforms when referenced to the ventral hippocampal waveform. Based on peak amplitude of the correlations, the hypothesis that the ventral hippocampus correlates more with the medial prefrontal cortex than the anterior cingulate cortex was supported. However, both the medial prefrontal cortex and the anterior cingulate are more highly correlated with the ventral hippocampus in the early sessions compared to the late recording sessions. When correlation values from the late session were subtracted from the early session, all differences showed a negative value confirming that correlation amplitudes were higher in the early session than in the late session. This difference was most prominent in the medial prefrontal recordings from the slow learners group. Both the medial prefrontal cortex and anterior cingulate cortex waveforms decrease in similarity to the ventral hippocampus waveform as learning progress.

One potential interpretation of the decrease in similarity between waveforms in the frontal brain regions and the ventral hippocampus is that the working memory demands of the task may be more hippocampally dependent during early sessions and then more dependent on other regions, such as the medial prefrontal cortex or anterior cingulate cortex, as the task becomes more familiar. It is fairly well-established that the

role of hippocampus in memory recall decreases gradually (Squire et al., 2001; Maviel et al., 2004). Alternatively, hippocampal theta, gamma, and theta-gamma coupling have been shown to be affected by age, environmental change, and cholinergic activation (Jacobson et al., 2013), and decreased similarity could be due to testing in older animals who have been potentially over-trained on the task.

If the prefrontal cortex and the hippocampus process similar information on different time scales, then there should be time-specific deficits in working memory only. If the prefrontal cortex and the hippocampus process different information but on the same time scale, then damage to either structure should have similar effects on working memory performance. These hypotheses were tested by Yoon and colleagues (2008) by infusing muscimol, a potent GABA-A agonist, into both the medial prefrontal cortex or the dorsal hippocampus and tested spatial working memory with a delayed alternation maze task. When the medial prefrontal cortex was inactivated there was a working memory deficit, but short term and episodic-like memories were intact; when the hippocampus was inactivated there was a spatial working memory deficit as well as a short-term and episodic-like memory deficit. These authors found that muscimol infused into either structure reduced working memory accuracy at all delay periods, causing the authors to conclude that neither the medial prefrontal cortex nor the hippocampus alone was sufficient for working memory. However, interaction between the two structures is still viewed as necessary for working memory.

In the nearly three decades that operant DNMTP tasks have been available in the repertoire of behavioral neuroscientists, much has been learned about its specific neural substrates (see Dudchenko et al., 2012 for review). The traditional view of rodent

DNMTP is that the hippocampus is required for recall of the sample across the delay, and the prefrontal cortex is required for execution of the rule, however the literature shows a more complicated story. Delay-dependent impairments have been found in the hippocampus but not prefrontal cortex (Porter et al., 2000), lesions of the prefrontal cortex but not the hippocampus (Sloan et al., 2006), and lesions of the fornix and perforant path (Shaw and Aggleton, 1993; Chudasama and Muir, 1997; Winters and Dunnett, 2004). Ibotenate hippocampal and extrahippocampal lesions cause delay-dependent deficits, and selective lesions of the hippocampus that spare other structures and preserve fibers of passage severely disrupt performance on DNMTP (Hampson et al, 1999). Based on evidence from lesions and direct infusions to the hippocampal formation, the fornix, the perforant pathway, and the prefrontal cortex, the DNMTP task is at least partially dependent on both the hippocampus and prefrontal cortex (Dudchenko et al., 2012). The hippocampus appears to be necessary for DNMTP, but its specific involvement is still unclear. If the hippocampus is critical for performance in this task, then hippocampal activity must exhibit a representational code for task-relevant events and that when this representation is not present, is distorted, or is diminished, then there should be a corresponding decrement in task performance. These questions were explored by Deadwyler and colleagues by recording hippocampal ensemble activity during a two lever spatial delayed-non-match-to-sample performance in rats (Deadwyler et al., 1996). Results indicated that small numbers of hippocampal neurons, particularly within the CA1 and CA3 fields, could effectively represent "conjunctions" of task-relevant features. Procedures designed to reduce mediating strategies tend to recruit more hippocampal involvement than tasks with substantial mediation components

suggesting an important role for the hippocampus in mnemonic processing. Input to the hippocampus appears to be required for successful task completion. The prefrontal cortex appears to be necessary for successful task completion, but the delay-dependence of this region is still unresolved and may depend heavily on specific task parameters.

While the power spectrum, waveform average, and waveform correlation analyses all showed substantive differences between animals that would eventually become fast or slow task learners, a definitive indicator predictive of eventual behavioral success or efficiency was not identified. In the present study, electrode implantation and all recordings occurred after the animals had already experienced several exposures to the operant box and early shaping steps. Any physiological effects associated with first exposure to the environment or associations between stimuli and reward would have already been established. In future studies, it would be interesting to perform electrode implantations prior to any task training and see if physiological indicators predictive of eventual performance become clearer.

Chapter 5: Behavioral effects of Ethanol

5.1. Introduction

Consistently, in both human and animal studies, alcohol intoxication is associated with a variety of behavioral, cognitive, and general health impairments. According to the National Institute on Alcohol Abuse and Alcoholism, common consequences of alcohol intoxication include: reduced inhibitions, slurred speech, motor impairment, confusion, memory problems, concentration problems, breathing problems, coma, and possibly even death. The detrimental effects of ethanol on various aspects of cognitive functioning, particularly memory and attention, are the primary interest for the current study.

A large body of research indicates that ethanol has dissimilar effects on anterograde encoding and retrograde retrieval aspects of memory. In particular, the initial encoding of information appears to be especially vulnerable to alcohol-induced impairment. Ethanol preferentially blocks new memory formation without impairing previously formed memories (Wixted, 2005). Ethanol often causes anterograde amnesia in which individuals could "blackout" and experience total memory loss for events that occur while he or she is intoxicated, but ethanol is also associated with retrograde facilitation in which it is easier to remember material learned just before intoxication.

Alcohol produces state-dependent effects on recollective experience, familiarity, and awareness of memories (Duka et al., 2001). In humans, alcohol produces greater accuracy impairment during tasks that require the encoding and maintenance of stimulus

sequences than in tasks that require other working memory functions such as spatial array recognition or focused attention (Saults et al., 2007). Cognitive models such as alcohol myopia (Steele and Josephs, 1990) or the attention allocation theory (Steele and Josephs, 1988) say that alcohol selectively impairs one's ability to think or focus on information. The alcohol myopia theory suggests that alcohol reduces attentional capacity to focus on only the most salient information. This phenomenon is analogous to near-sighted vision: the individual clearly perceives close stimuli but has an increasingly difficult time focusing on stimuli far away. An intoxicated individual will selectively focus on helpful information but may not have the ability to focus on stressful or distracting information. Alcohol also has different effects on memory consolidation in social drinkers based on motivational factors (Bruce et al., 1999). Alcohol affects the speed and accuracy with which individuals process information (Schweizer & Vogel-Sprout, 2008). Alcohol slows the speed of information processing and decision-making, but does not slow the detection or response to stimuli (Tzambazis & Stough, 2000).

Ethanol acts on many different brain regions, but it produces similar cognitive and neurophysiological effects as lesions of the hippocampus (Matthews & Silvers, 2004). Hippocampal-dependent learning via an associative task and experience-dependent activation of the hippocampus as measured by immediate early genes are preferentially disrupted by ethanol (Melia et al., 1996). Low doses of ethanol produce selective dose-, delay- and time-dependent impairments in spatial working memory that are not indicative of general cognitive decrement (Givens, 1995; Givens and McMahon, 1997). Additionally, ethanol produces a loss of hippocampal responsivity to oscillating drive

from the medial septal area, and thus reduces the ability of the hippocampus to encode and retrieve memory information via theta activity (Givens et al., 2000).

All of the above research suggests that different aspects of cognitive functioning are susceptible to alcohol-induced impairment. If alcohol affects some aspects of memory but not others, it is likely that different pharmacological and neurobiological mechanisms trigger different mnemonic and attentional functions. The connection between alcohol consumption and memory impairments is important to develop a comprehensive understanding of the behavioral and biomedical effects of alcohol consumption.

The purpose of the experiments within this chapter is to characterize the dose-dependent cognitive and behavioral effects of acute ethanol in the operant delayed non-match to position task. Dependent measures assessing working memory will include overall session accuracy and accuracy broken down by short, medium, or long delay intervals. It is hypothesized that as dosage of ethanol increases then the overall accuracy will decrease. Due to enhanced working memory load at longer delays, we expect that ethanol will preferentially disrupt performance at longer delays. Performance on the sample phase of the task is often reported as a measure of vigilance. It is hypothesized that vigilance will be unaffected by ethanol and there will not be any dose-dependent effects on the rate of incorrect responses during the sample phase.

The number of lever presses during the intertrial interval and delay period could be mediated by several different cognitive mechanisms. If acute ethanol dose-dependently causes an increase in extraneous lever presses, then effects may be due to reduced behavioral inhibition or increased impulsivity. If acute ethanol dose-dependently

decreases the rate of extraneous lever presses, then effects may be due to changes in attention, motivation, or motor impairments. It is hypothesized that there will be a combination of effects depending on dosage. It is expected that low doses of ethanol will cause an increase in the number of intertrial interval and delay lever presses, but high doses will cause a decrease in extraneous lever presses.

The number of omissions to sample and choice phase stimuli and reaction time for responses will provide clues as to acute ethanol's effects on attention, motivation, and motor impairments. Similar to above, we expect an inverted-U shaped relationship for the different doses. We hypothesize that when compared to controls, low doses of ethanol will decrease the number of omissions and decrease the reaction time for responses. Conversely, we expect that high doses of ethanol will cause an increase in the number of omissions and will increase the number of omissions and the reaction time for responses.

5.2. Subject Information and Specific Methods

There were 23 animals that underwent behavioral training and electrode implantation surgery. Seven animals died or were removed from the study before completion and three additional animals failed to reach behavioral criterion (> 70% overall accuracy) necessary for undergoing ethanol injections. A total of 13 animals reached criterion necessary to undergo DNMTP testing with acute ethanol injections. One animal was excluded from further analysis due to exceptionally low trial completion rates across multiple doses. One cohort of remaining animals (n = 4) was tested under the "Working Memory E" program with 5, 10, and 15 second delay periods randomly

interspersed throughout the session. A separate cohort of animals (n = 8) was tested under the "Working Memory D" program with 5 and 10 second delay periods randomly interspersed throughout the session. Working Memory D and E versions of the task were analyzed for accuracy at each delay interval separately, but combined for all other analyses (n=12). All animals received all doses including a saline vehicle control, 0.25 g/kg ethanol, 0.50 g/kg ethanol, 0.75 g/kg ethanol, and 1.00 g/kg ethanol. Dose order was determined via a Latin Square design. All intraperitoneal injections occurred 10 minutes prior to the beginning of behavioral testing and neurophysiological recording if applicable.

5.3. Effects of Ethanol and Delay on Accuracy

It was hypothesized that animals would have the highest accuracy at the shortest delay intervals and that accuracy would decrease as the length of delay intervals increased. It was also hypothesized that acute ethanol would impair accuracy in a dose-dependent and delay-dependent manner. The experimental design was completely within-subjects and any effects were determined by looking at dose-dependent and delay-dependent changes in overall accuracy and within-session performance.

The effects of ethanol on accuracy in the working memory task were first assessed by looking at the session overall performance for each dosage group (See Figure 26). The overall session accuracy is reflective of an average of performance across all delay intervals. Overall session accuracy was analyzed via one-way repeated measure ANOVA. A significant effect was observed ($F_{3.899, 42.89} = 12.39$, $p < 0.0001$) Dunnett's multiple comparison test was used to compare the effect of the saline control vs. all other

doses. Overall session accuracy was significantly lower for the 0.50 g/kg ethanol, 0.75 g/kg ethanol, and 1.00 g/kg ethanol conditions. The no injection control group did not differ from saline and is therefore not included in subsequent analyses.

Next, the mean percent correct for each dosage group at each specific delay interval was calculated (See Figures 27 and 28). Accuracy data for each delay interval were analyzed with a two-way repeated measures ANOVA with dose (6 levels: no injection control, a saline vehicle control, 0.25 g/kg ethanol, 0.50 g/kg ethanol, 0.75 g/kg ethanol, and 1.00 g/kg ethanol) and delay (up to 4 levels: Session Overall, 5 seconds, 10 seconds, and when applicable 15 seconds). Analysis of the Working Memory E accuracy yielded a significant main effect of Dose ($F_{5,15} = 5.938$, $p < 0.01$), but not for main effect of Delay ($F_{3,9} = 2.457$, $p = 0.1296$). There was not a significant interaction between dose and delay ($F_{15,45} = 0.2639$, $p = 0.9965$). Dunnett's multiple comparison test was used to compare the effect of the saline control vs. all other doses at each delay category. Significant ($p < 0.05$) results were found in the saline vs. 1.00 g/kg ethanol conditions in the overall session accuracy, accuracy at the 10 second delay interval, and accuracy at the 15 second delay interval. No other significant post-hoc results were found.

Analysis of the Working Memory D task yielded a similar pattern of results to those above (See Figures 29 and 30). After a two-way repeated measures ANOVA, there was a significant main effect of dose ($F_{5,35} = 6.207$, $p < 0.001$). There was not a significant main effect of delay ($F_{2,14} = 1.221$, $p = 0.3244$) nor a significant interaction between dose and delay ($F_{2,14} = 1.058$, $p = 0.4059$). Dunnett's multiple comparison test was used to compare the effect of the saline control vs. all other doses at each delay

category. Significant ($p < 0.05$) results were found in the saline vs. 1.00 g/kg ethanol conditions in the overall session accuracy, accuracy at the 10 second delay interval. No other significant post-hoc results were found. Saline vs. 1.00 g/kg ethanol was significant at the overall session accuracy ($p < 0.001$), at the 5 second delay ($p < 0.0001$), and at the 10 second delay ($p < 0.05$). Saline vs 0.75 g/kg ethanol was significant at the 5 second delay ($p < 0.05$) and saline vs 0.50 g/kg ethanol was significant at the 10 second delay interval ($p < 0.050$).

In addition to overall accuracy, within session performance was also evaluated by separating each 100 trial session into 10 blocks containing 10 trials each (See Figure 31). Since delay is no longer a factor, Working Memory E (n = 4) and Working Memory D (n = 8) are collapsed into a single group (n = 12) for subsequent behavioral analyses. Average number of correct responses out of 10 for each block was calculated. A two-way repeated measures ANOVA with dose (6 levels) by block (10 levels) yielded significant main effects of both dose ($F_{5,55} = 10.71$, $p < 0.0001$) and block ($F_{9,99} = 2.651$, $p < 0.01$). The interaction between dose and block was not significant ($F_{45,495} = 0.8619$, $p = 0.7253$). Dunnett's multiple comparison test was used to compare the effect of the saline control vs. all other doses at each block of 10 trials. Proportion of correct responses was significantly lower for the 1.00 g/kg ethanol dose compared to the saline control at all blocks except for the 2nd sequential block of trials (trials 11-20). The proportion of correct responses for the 0.75 g/kg dose of ethanol was significantly worse than the saline control during the 5th block in the middle of the session.

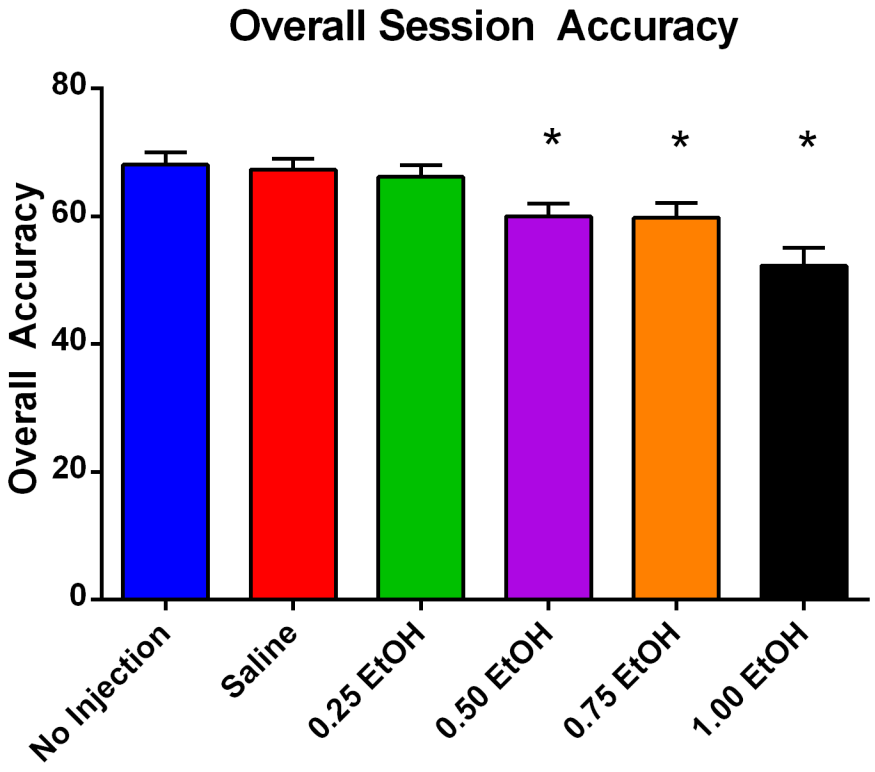

Figure 26 Mean overall session accuracy decreases as dosage of ethanol increases.

Rats had significantly worse mean session accuracy performance at the 0.50 g/kg, 0.75, and 1.00 g/kg ethanol dose compared to saline controls. (= $p < 0.05$ difference from saline control) Error bars indicate SEM.*

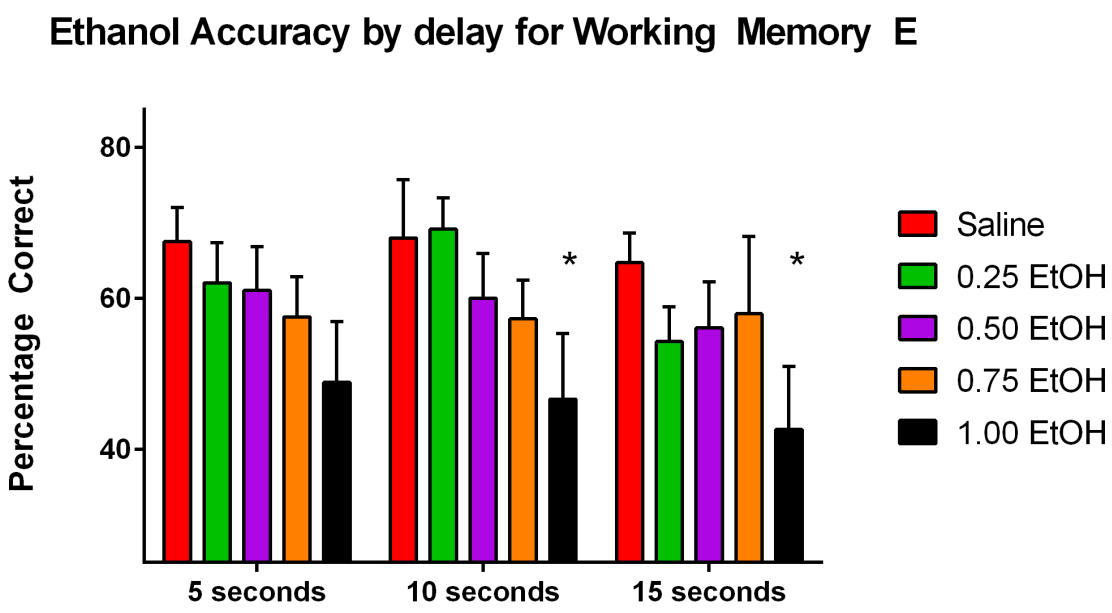

Figure 27 Mean percentage of correct responses on Working Memory E for each delay interval at all ethanol doses tested.

Rats had significantly worse performance at the 1.00 g/kg ethanol dose than saline controls for the overall session, at the 10 second delay interval, and at the 15 second delay interval. (= $p < 0.05$ difference from saline control) Error bars indicate SEM*

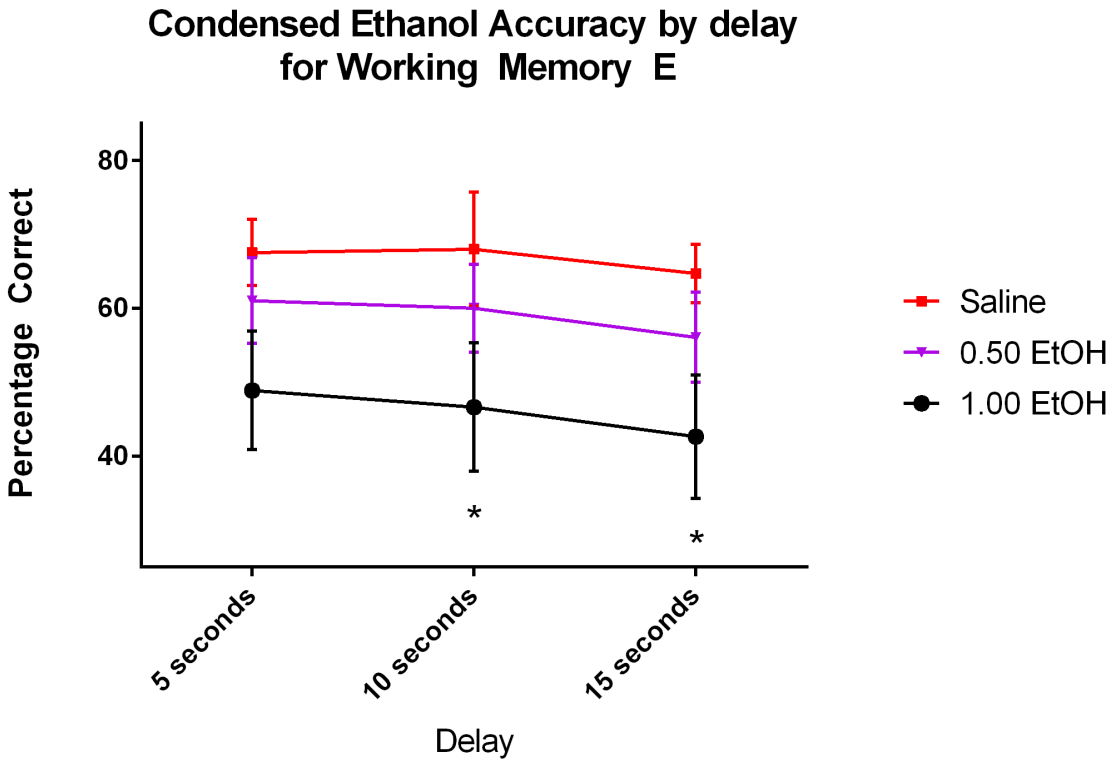

Figure 28 Mean percentage of correct responses on Working Memory E for each delay interval at a subset of ethanol doses tested.

Rats had significantly worse performance at the 1.00 g/kg ethanol dose than saline controls for the overall session, at the 10 second delay interval, and at the 15 second delay interval. (= $p < 0.05$ difference from saline control) Error bars indicate SEM.*

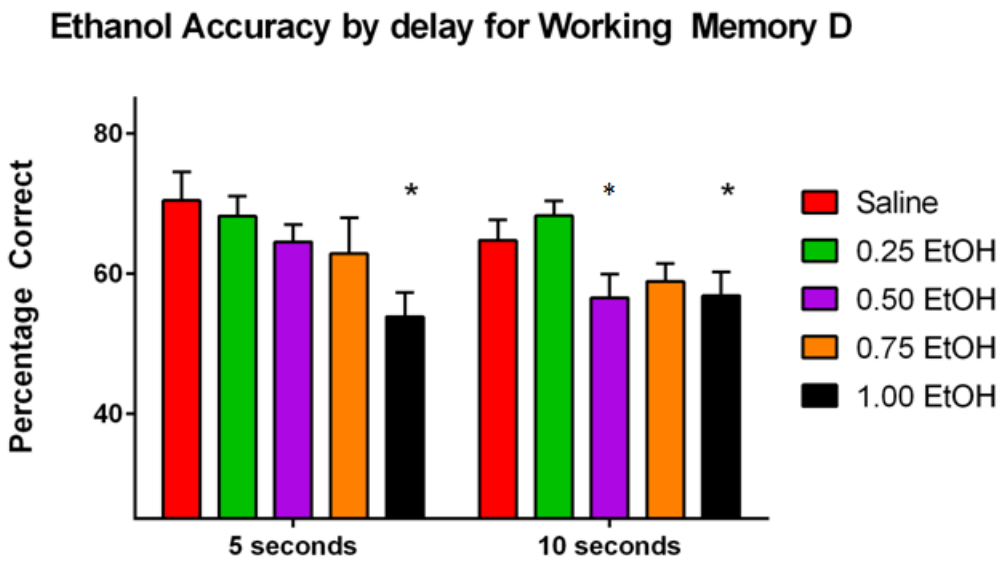

Figure 29 Mean percentage of correct responses on Working Memory D for each delay interval at all ethanol doses tested.

Rats had significantly worse performance at the 1.00 g/kg ethanol dose than saline controls for the overall session, at the 5 second delay, and at the 10 second delay interval. Rats also had significantly worse performance than the saline control at 0.75 g/kg ethanol dose on the 5 second delay interval and at the 0.50 g/kg ethanol dose on the 10 second delay interval. (= $p < 0.05$ difference from saline control) Error bars indicate SEM.*

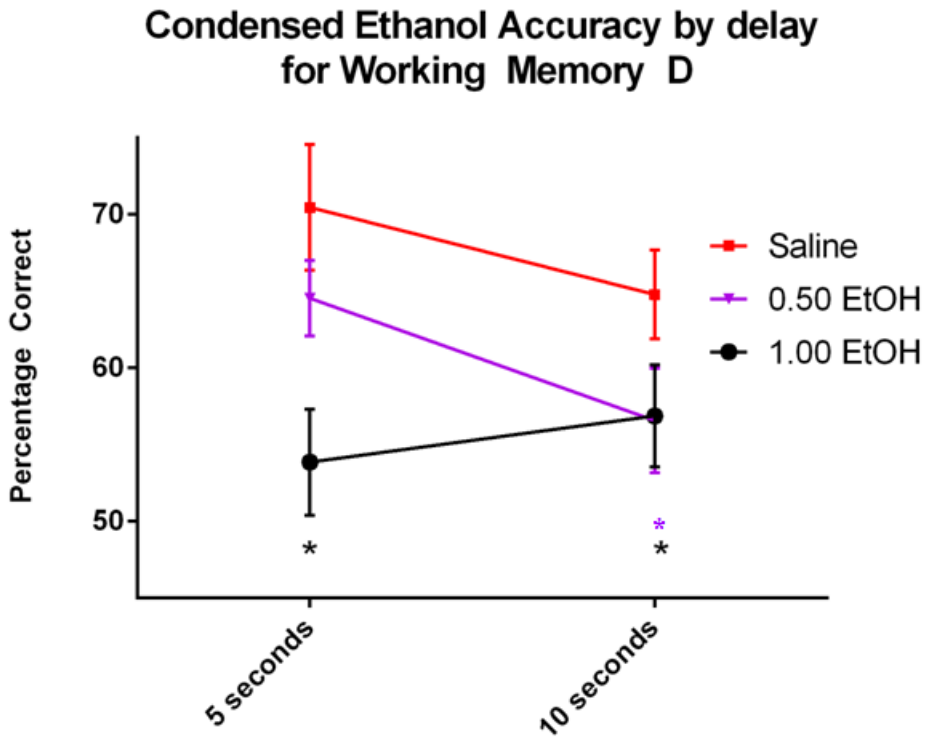

Figure 30 Mean percentage of correct responses on Working Memory D for each delay interval at a subset of ethanol doses tested.

Rats had significantly worse performance at the 1.00 g/kg ethanol dose than saline controls for the overall session, at the 5 second delay, and at the 10 second delay interval. Rats also had significantly worse performance than the saline control at the 0.50 g/kg ethanol dose on the 10 second delay interval. (= $p < 0.05$ difference from saline control) Error bars indicate SEM.*

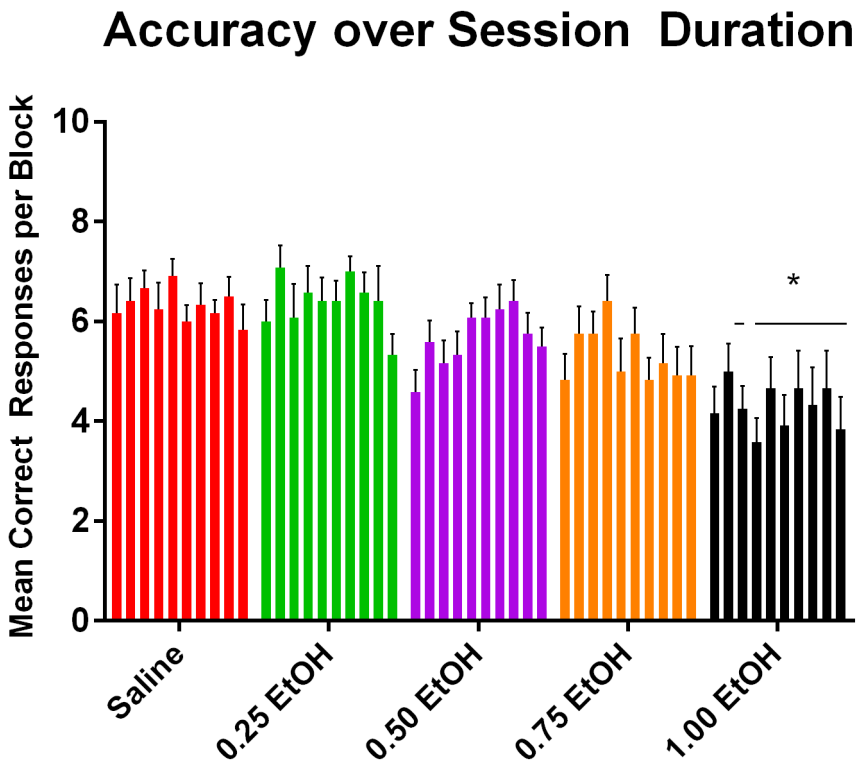

Figure 31 Within-Session Accuracy. Mean proportion of correct responses per 10 trials. Data presented as sequential blocks of 10 trials over the 100 trial session.

Rats had significantly worse proportion of correct responses at the 1.00 g/kg ethanol dose than saline controls for all blocks except for the 2nd block of 10 trials. (= $p < 0.05$ difference from saline control) Error bars indicate SEM.*

5.4. Effects of Ethanol on Sample Phase Misses

All cohorts were combined for subsequent analyses. It was hypothesized that ethanol would have no effect on accuracy for responses in the sample phase of the task. As shown in Figure 32, although as dosage of ethanol increased the number of sample misses slightly decreased, a one-way repeated-measures ANOVA did not find a significant effect of dose on number of sample misses ($F_{3.359, 36.95} = 1.565$, $p = 0.2106$).

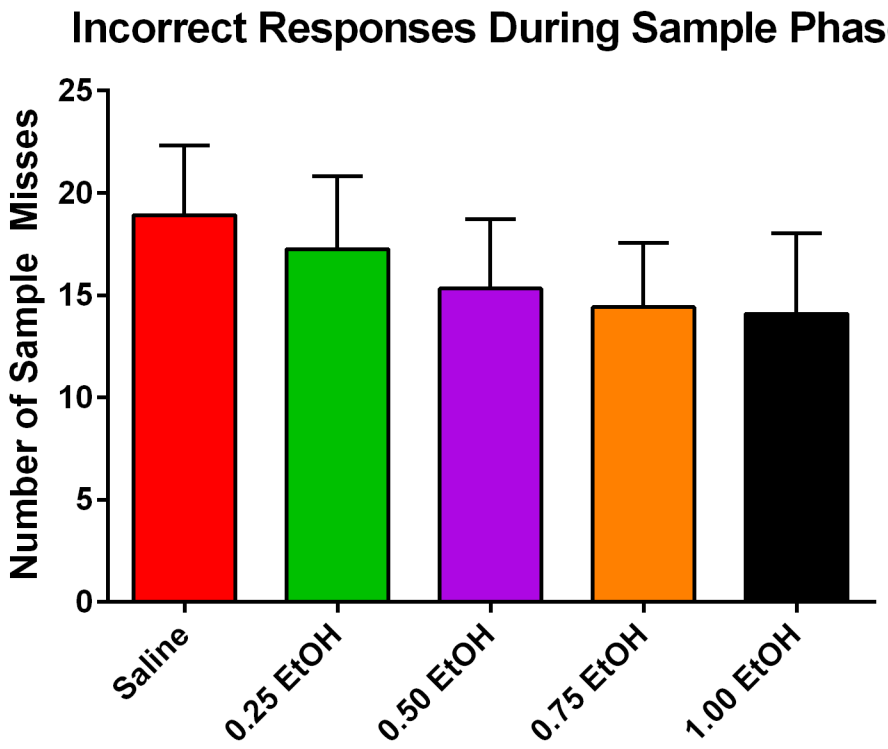

Figure 32 Number of Incorrect Responses during the Sample Phase.

Mean number of sample misses per each dose. No statistically significant differences were found. Error bars indicate SEM.

5.5. Effects of Ethanol on Number of Lever Presses during the Intertrial Intervals and Delay Periods

It was hypothesized that the lowest doses of ethanol (0.25 and 0.50 g/kg) would increase lever presses in the intertrial interval and delay period whereas the highest doses of ethanol (0.75 and 1.00 g/kg) would decrease extraneous locomotion and decrease the number of lever presses during both of these time periods.

The mean number of lever presses during the 10 second intertrial interval was calculated respectively for each dosage condition (See Figure 33). A one-way repeated-measures ANOVA found that there was a significant effect of dose on the number of lever presses during the Intertrial Interval ($F_{2.846,31.31} = 5.401$, $p < 0.01$). Dunnett's multiple comparison test was used to compare the effect of the saline control vs. all other doses and found that there were significantly fewer lever presses at the 0.75 g/kg ethanol dose compared to saline control ($p < 0.01$).

The mean number of lever presses during the delay periods was also calculated respectively for each dosage condition (See Figure 34). A one-way repeated-measures ANOVA found that there was a significant effect of dose on the number of lever presses during the delay periods ($F_{2.773,30.50} = 6.591$, $p < 0.01$). Dunnett's multiple comparison test was used to compare the effect of the saline control vs. all other doses and found that there were significantly fewer lever presses at the 0.75 g/kg ethanol dose ($p < 0.01$) and at the 1.00 g/kg ethanol dose ($p < 0.05$).

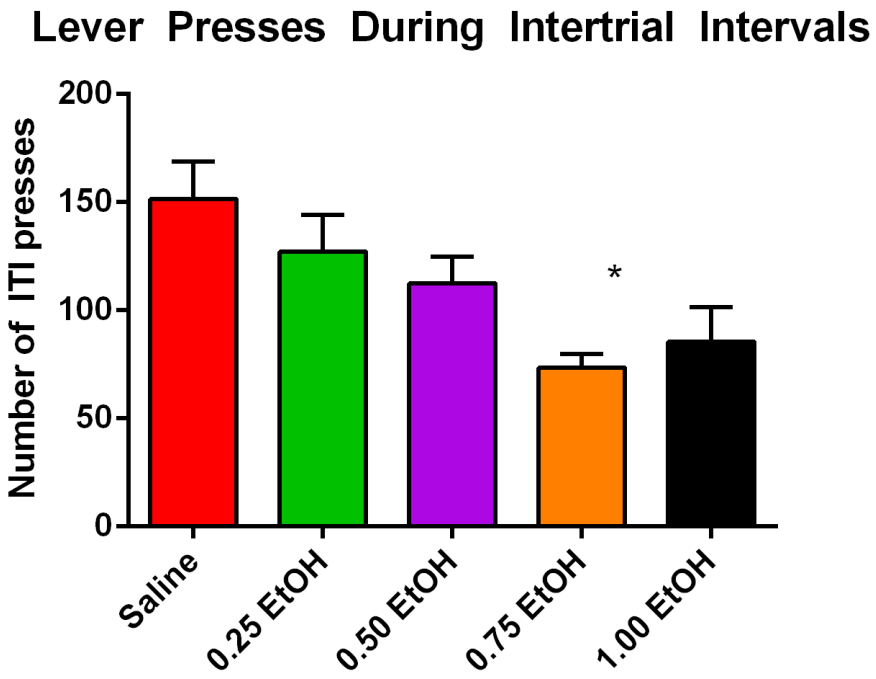

Figure 33 Lever Presses during the Intertrial Interval.

Mean number of lever presses for each dose. 0.75 g/kg ethanol had significantly fewer lever presses than the saline control (= $p < 0.01$ difference from saline control) Error bars indicate SEM.*

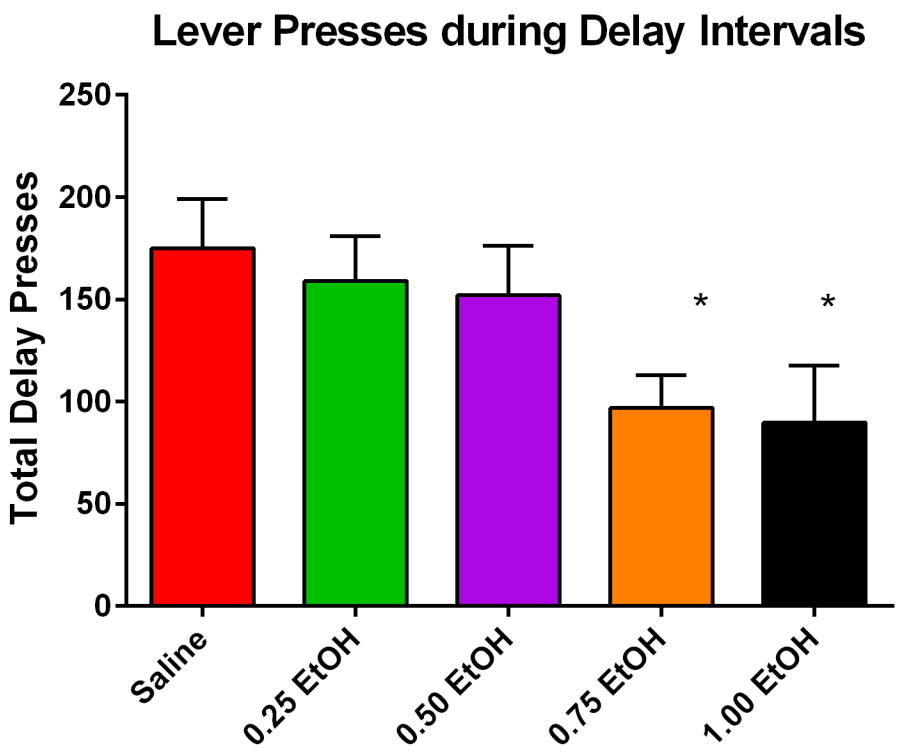

Figure 34 Lever Presses during the Delay Periods.

Mean number of lever presses for each dose. Significantly fewer lever presses were observed for the 0.75 g/kg and 1.00 g/kg doses of ethanol compared to saline controls. (= $p < 0.05$ difference from saline control) Error bars indicate SEM.*

5.6. Effects of Ethanol on Omissions

It was hypothesized that the lowest doses of ethanol (0.25 and 0.50 g/kg) would decrease omissions whereas the highest doses of ethanol (0.75 and 1.00 g/kg) ethanol increase omissions when compared to controls. Animals had up to 3 seconds to respond to signals in both the sample phase and the choice phase of the task or else the trial was counted as an omission. An omission in the sample phase restarted an intertrial interval and created a new randomized sample phase signal. An omission in the choice phase ended the trial and started an intertrial interval. Omission data is presented in Figure 35. In a two-way repeated measures ANOVA (phase by dose), there was a significant main effect for dose ($F_{5,55} = 3.308$, $p < 0.05$). There was a trend towards a statistically significant main effect for sample vs choice phase ($F_{1,11} = 3.880$, $p = 0.0746$). There was a significant interaction between phase and dose ($F_{5,55} = 2.451$, $p < 0.05$). Dunnett's multiple comparisons test was used to perform post-hoc analyses of each dose compared to saline controls. For the sample phase, there was a significant difference between the 0.75 g/kg dose of ethanol ($p < 0.05$) and for the 1.00 g/kg dose of ethanol ($p < .001$). There were not any significant post-hoc differences found for total number of omissions during the choice phase of the task.

Although there were very few omissions during the choice phase of the task regardless of dosage, the timing of the omissions that did occur was investigated next (See Figure 36). Choice omissions were separated into three blocks comprising the beginning (trials 1-33), middle (trials 34-66), and end (trials 67-100) of the session. In a two-way repeated measures ANOVA (dose by session time), There was a significant main effect of dose ($F_{5,55} = 3.015$, $p < 0.05$) but not a significant main effect of session

time ($F_{2,22} = 0.5627$, $p = 0.5777$). There was a significant interaction between the factors ($F_{10,110} = 2.105$, $p < 0.05$), but this was likely driven by the dosage effect. In a follow-up post-hoc analysis using Dunnett's multiple comparison test, There were significant differences in the number of omissions between saline and 1.00 g/kg ethanol at the beginning and middle of the session, but not at the end of the session. This suggests that satiety was not a factor in contributing to choice phase omissions.

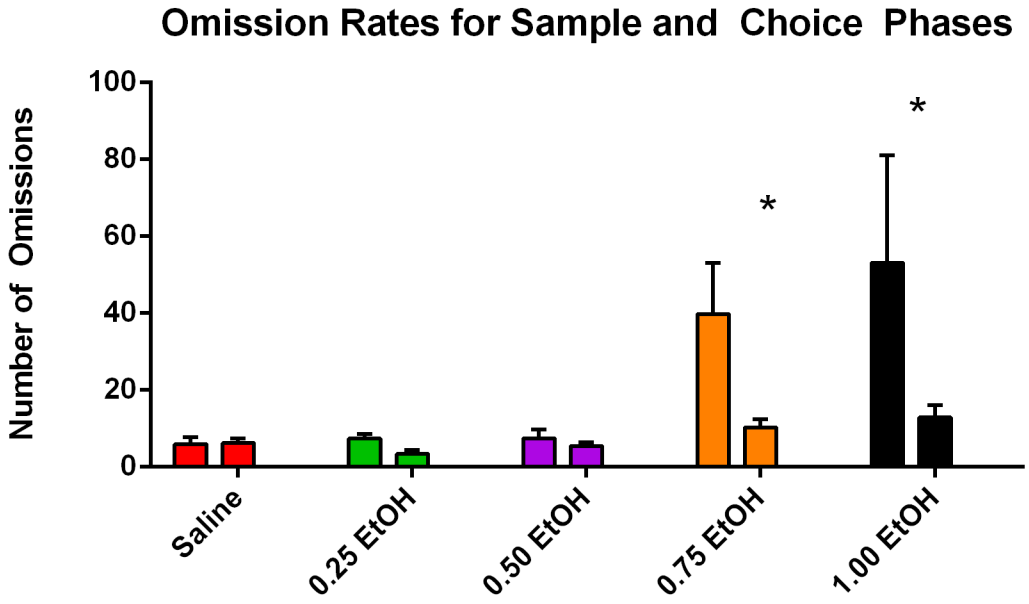

Figure 35 Average Number of Omissions during Sample and Choice Phases Respectively.

Mean number of omissions for each dose. The left column in each dosage group represents the sample phase, the right column represents the choice phase. Significantly more omissions were observed for the 0.75 g/kg and 1.00 g/kg doses of ethanol in the sample phase compared to saline, but this difference was not observed for the choice phase of the task. (= $p < 0.05$ difference from saline control) Error bars indicate SEM.*

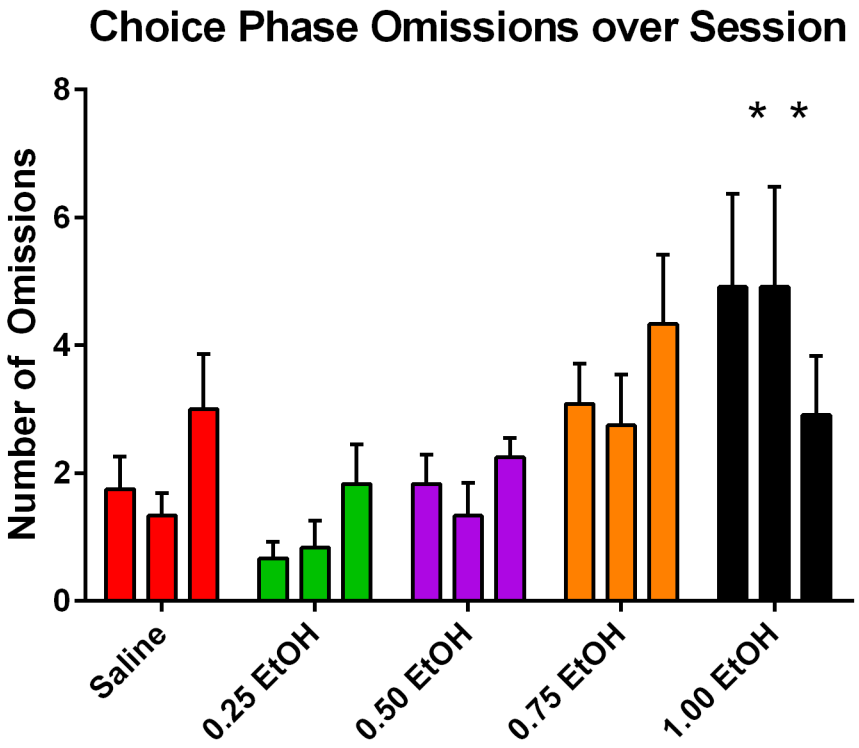

Figure 36 Timing of when choice phase omissions occur.

The left- most column in each dosage group represents the mean number of omissions during the beginning of the session, the middle column represents the middle of the session, and the right-most column represents the end of the session. When compared to saline controls, the 1.00 g/kg ethanol dose had significantly more omission during the beginning and middle of the session but not the end of the session. (= $p < 0.05$ difference from saline control) Error bars indicate SEM.*

5.7. Effects of Ethanol on Reaction Times

It was hypothesized that the lowest doses of ethanol (0.25 and 0.50 g/kg) would speed up reaction times whereas the highest doses of ethanol (0.75 and 1.00 g/kg) ethanol would slow down reaction times in both the sample phase and the choice phase compared to controls. Reaction time data is presented in Figure 37. A two-way repeated measures ANOVA was calculated for phase (sample and choice) and dose. A significant main effect of dose was found ($F_{5,55} = 7.804$, $P < 0.0001$). There was not a significant main effect for phase ($F_{1,11} = 3.313$, $p = .0960$) nor an interaction between phase and dose ($F_{5,55} = 0.4707$, $p = 0.7965$). Dunnett's multiple comparisons test was used to compare the effects of each dose vs. saline controls for both sample phase reaction times and choice phase reaction times. During the sample phase, animals had significantly slower reaction times at both the 0.75 g/kg and 1.00 g/kg ethanol doses ($p < 0.01$). During the choice phase, animals had significantly slower reaction times following the 1.00 g/kg ethanol dose ($p < 0.0001$).

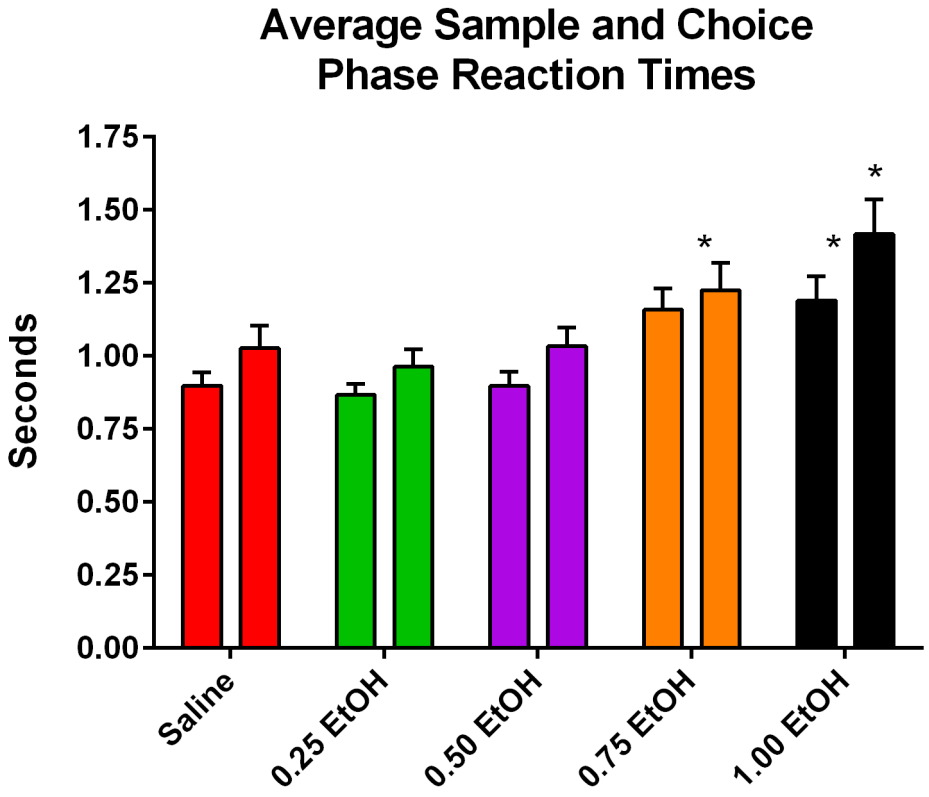

Figure 37 Average Sample and Choice Phase Reaction Times.

Mean reaction time for each dose. The left bar in each dosage group represents mean reaction time for the sample phase, the right bar in each group represents mean reaction time for the choice phase. Significantly slower reaction times were observed for the 0.75 g/kg and 1.00 g/kg doses of ethanol compared to saline controls in the sample phase, and significantly slower reaction times were observed for the 1.00 g/kg ethanol dose compared to saline controls in the choice phase. (= $p < 0.05$ difference from saline control) Error bars indicate SEM.*

5.8. Conclusions and Discussion

The operant delayed non-match to position task used in the current experiments allowed investigation of the effects of acute ethanol on several cognitive and behavioral constructs including working memory, attention, inhibition control, impulsivity, motivation, and motor function. Dependent measures included accuracy, sample phase misses, number of lever presses during the intertrial interval or delay period, omissions, and reaction time. Although all of the dosages were in the low to moderate range, there were several significant dose-dependent effects observed.

Accuracy is the most explicit measure of working memory effects. As hypothesized, ethanol dose-dependently impaired accuracy for the overall session. As dosage increased accuracy decreased. As shown in Chapter 3, performance generally declines as delay interval increases indicating a more demanding working memory load. In Working Memory E versions of the task, the highest dose of ethanol was significantly different from saline controls at the medium and long delay but not at the short delay. In Working Memory E versions of the task, the highest dose of ethanol was significantly different from saline controls at both the 5 second and 10 second delay.

It is possible that the decline in accuracy observed after higher doses of ethanol could be due to impairments in factors other than working memory. To rule out motivational effects such as satiety or fatigue, and to assess time dependent effects of ethanol, accuracy was divided into 10 sequential blocks of 10 trials each. All sessions began 10 minutes after ethanol injections and were completed within 45 minute to 1 hour, thus each animal would progress through the ascending and descending limbs of the blood alcohol concentration curve while in the task. Even in control conditions, there is a

slight decrease in accuracy for the last block of trials, likely indicating that the animals are satiated from water rewards already received or are exhausted. This decline of performance at the end of the session was not different by dosage. Generally speaking, all dosage conditions showed relatively stable accuracy performance across the whole session, including the highest dose of ethanol. Therefore, motivational effects are unlikely to explain the dose-dependent effects of ethanol on accuracy.

Responses to the sample phase of the task do not require the retrieval of any mnemonic information but simply require the animal to press the lever underneath the illuminated signal light. Correct responses are usually attributed to attention, whereas incorrect responses are usually attributed to hyperlocomotion or impulsivity. As dosage increased, the number of sample misses decreased slightly but not significantly. This confirms the expected hypothesis that vigilance to the sample phase will be unaffected by ethanol and there will not be any dose-dependent effects on the rate of incorrect responses during the sample phase.

As dosage increased, the number of lever presses during both the intertrial intervals and delay periods decreased significantly. We hypothesized an inverted-U shaped relationship where low doses would have activational effects thus increasing the number of lever presses, but high doses would decrease the number of lever presses. The hypothesis for low doses was not supported by the present data, but the hypothesis for high doses was supported for both intertrial interval and delay periods. When this information is combined with the decrease in incorrect sample phase responses after high doses of ethanol, it is likely that the 0.75 and 1.00 g/kg exhibit less non-essential locomotor activity.

The highest does of ethanol were associated with a substantial increase in number of omissions. However, almost all omissions that occurred were in the sample phase. Once an animal initiated a trial, they mostly remained engaged through the completion of the choice phase. Although there were few omissions to the choice phase of the task, the timing of when these omissions occurred was subsequently analyzed. After the 1.00 g/kg dose of ethanol, the number of omissions in the beginning third and middle third of the task was significantly higher than saline controls, but this difference disappeared by the final third of the task. The decrease of choice omissions at the end of the task challenges the assumption that satiety or exhaustion is responsible for the increase in omissions.

We hypothesized that low doses of ethanol would decrease reaction time whereas high doses would increase reaction time. We observed significantly slower reaction times for the 0.75 g/kg dose during the sample phase and for the 1.00 g/kg dose during both the sample and choice phases. Although there was a significant dose-dependent decrease in reaction times it is important to consider the practical significance of these findings. All mean reaction times were between 1 and 1.5 seconds which is well within the 3 second window of opportunity to the sample and choice phase lights. Observed effects on accuracy are thus unlikely to be due to motoric or attentional components and are thus likely specific to working memory.

DNMTP has a long history as a tool for pharmacological research. One of the most prevalent models used is cholinergic blockade induced by the muscarinic M1 antagonist scopolamine. Scopolamine has a thin line between specific effects on cognition and non-specific side-effects and behavioral changes (for review see Klinkenberg and Blokland, 2011). Scopolamine infused directly into the PFC causes

delay-independent decreases accuracy without specific side effects (Dunnet et al., 1990; Herremans et al., 1996). Scopolamine appears to enhance response switching behaviors indicating a potential advantage in non-match versions and a potential disadvantage in matching versions, but this behavior did not translate to improved accuracy in either version of the task (Chudasama and Muir, 1997). Further analysis has revealed that scopolamine causes delay-dependent effects in animals using more mediating strategies, but delay-independent effects in animals using fewer mediating strategies (Dudchenko et al., 2012), perhaps supporting a role for acetylcholine in mediating some attentional components of the task. Physostigmine, a reversible cholinesterase inhibitor that interferes with the metabolism of acetylcholine, yields a mild but significant enhancement of performance in the DMTP task (Dunnett, 1985). When the operant DNMTP paradigm was used to assess the effect of cannabinoid agonists, another commonly used psychoactive drug, delay dependent effects were observed (Heyser et al., 2003).

Antagonists of the ionotropic NMDA glutamate receptor have also been well-tested in DNMTP paradigms. The NMDA receptor has many potential sites for modulatory control, including the glutamate transmitter recognition site, the co-agonist (Glycine) recognition site, a site within the ion channel that binds PCP, sites modulated by endogenous polyamines, a zinc modulation site, and a protein sensitive redox site. Delay-dependent impairment of a matching-to-place task with chronic and intrahippocampal infusion of the NMDA-antagonist D-AP5 has been observed by Steele and Morris (1999). Willmore and colleagues (2001) tested PCP site antagonists, competitive NMDA antagonists, glycine site antagonists, and NR2B antagonists and

found that DNMTP accuracy was only impaired with PCP site antagonists such as PCP, MK-801, and Memantine. Other studies have found similar selective delay-dependent deficits with PCP and MK-801 but non-selective impairments with Memantine and other competitive and non-competitive NMDA antagonists (Cole et al., 1993; Smith et al., 2001; Ballard and McAllister, 2000). Combined, these results indicate that there is a glutamatergic component to successful task completion, and this is most likely mediated by activity at the MK-801 and PCP sites within the ion channel of the NMDA glutamate receptor.

Some studies have used a similar delayed non-match to position task to study the behavioral effects of GABA-ergic or Glutamatergic drug infusion to either dorsal or ventral sub-regions of the hippocampus (Robinson and Mao, 1997; Mao and Robinson 1998). When scopolamine was infused into the dorsal hippocampus, there were more omissions. When scopolamine was infused into the ventral hippocampus, there were also more omissions, but the sample phase response accuracy decreased. An infusion of MK-801 into the dorsal hippocampus caused delay-independent deficits, decreased the sample phase response accuracy, and increased response bias. An infusion of MK-801 into the ventral hippocampus did not find significant disruption of DNMTP delayed choice. When muscimol, a GABA-A agonist was infused into the dorsal hippocampus, there was a decrease in the number of trials and a disruption in discrimination patterns. When muscimol was infused into the ventral hippocampus, there were no significant effects observed. Only MK-801 produced effects on choice accuracy, but these effects were delay independent. All other significant impairments were on measures of vigilance or attention. It is worth noting that these studies used very short sample stimulus duration

compared to many other comparable studies, therefore impairments in attention may have overruled any potential effects on memory.

In the present study, both the delay-dependent effects on accuracy and the delay-independent results, including decreased number of extraneous lever presses, increased omissions, and decreased reaction time are similar to the GABA-ergic and Glutamatergic effects observed by others. Additional research is needed to determine the specific pharmacological effects of acute ethanol on the delayed non-match to position working memory task.

Chapter 6: Neurophysiological effects of ethanol

6.1. Introduction

It has been well-established that ethanol affects both GABAergic and glutamatergic systems within the brain. Considering the integral role that these neurotransmitters play in establishing and maintaining neurophysiological patterns, it is logical that ethanol would affect many aspects of neurophysiology. The neurophysiological effects of ethanol are likely to be observed at the cellular level by altering firing rates of pyramidal neurons and inhibitory interneurons and also at the population level by altering stimulus-evoked responses and local field potential oscillatory patterns such as theta and gamma rhythms.

For quite a while, it has been known that the theta rhythm activity is highly susceptible to ethanol-induced modulation (Whishaw, 1976). Previous research in this lab demonstrating the ethanol-induced vulnerability of hippocampal neurons ranges from single neuron activity (Givens et al., 1998) to multi-unit activity (Givens et al., 2000). Ethanol suppresses hippocampal theta activity in the same doses that caused impairments in working memory as indicated by a change in choice accuracy in a delayed alternation task (Givens, 1995). Additionally, ethanol produces a loss of hippocampal response to oscillating drive from the medial septal area, and thus reduces the ability of the hippocampus to encode and retrieve memory information via theta activity (Givens et al., 2000). Adult rats that received very high doses of prenatal ethanol had a higher theta

score while moving than control animals (Cortese et al., 1997), showing that ethanol can have long-term consequences for the development and maintenance of neuronal oscillations.

Brain oscillations have been proposed as potential endophenotypes of cognition (Porjesz et al., 2005), and as potential biomarkers for alcoholism (Rangaswamy & Porjesz, 2008). Brain oscillations are valuable as endophenotypes because they are highly heritable, are modulated by genes controlling neurotransmitters in the brain, and they provide links to associative and integrative brain functions (Rangaswamy & Porjesz, 2008). Some electrophysiological characteristics of alcoholics may be under genetic control and precede the development of alcoholism and thus may be markers of predisposition towards alcoholism and related disorders (For review see Porjesz et al., 2005; Başar and Güntekin, 2008). The resting EEG in humans shows increased theta power among alcoholics, which may be an electrophysiological index of imbalance in the excitation-inhibition homeostatic mechanisms in the cortex. When an EEG is performed under the influence of alcohol, low doses increase slow alpha activity; moderate doses increase slow alpha and theta activity but decrease beta activity. The P300 response is an event-related potential that is commonly elicited by unusual stimuli in the oddball paradigm. The amplitude of the P300 is lower in abstinent alcoholics and at-risk offspring of alcoholics than in non-drinkers, suggesting a genetic component to the coordinated physiological response to unusual stimuli. In alcoholic subjects, event-related oscillations show reduced energy in delta, theta, and gamma frequency bands.

Although the field of ethanol research understands a great deal about the pharmacology of ethanol in the brain, it is difficult to translate these synaptic mechanisms

into the psychological phenomena observed in impaired cognition. Therefore, to understand the neural mechanisms of ethanol modulation of encoding and retrieval mechanisms for working memory, it is necessary to incorporate physiological mechanisms that are relevant to *in vivo* neural circuits. The theta and gamma rhythms are some of the most promising neurophysiological findings associated with working memory. Through investigation of ethanol modulation of theta and gamma activity in the neural circuit including the ventral hippocampus and the Prelimbic/infralimbic region of the medial prefrontal cortex, and to a slightly lesser extent the anterior cingulate cortex, we expect to find dose-dependent effects of ethanol on whole session, stimulus-evoked power, and regional coherence in the theta and gamma frequency ranges.

If overall activity in the theta and gamma frequency band is vulnerable to ethanol, then power spectrum amplitude for all anatomical recording sites should decrease as dosage increases. If there is synchronization between anatomical sites in response to encoding (sample phase) or retrieval (choice phase) relevant stimulus onsets, then there should be a high correlation and a predictable relationship across the stimulus triggered power analyses. We hypothesize that the amplitude of evoked responses and thus power around stimulus onset will decrease after high doses of ethanol relative to the saline control. We hypothesize that coherence between the ventral hippocampus and the frontal regions will be more synchronous in control and low-dosage conditions and will decline in synchrony as dosage increases. We expect to see higher coherence between the ventral hippocampus and the medial prefrontal cortex than between the ventral hippocampus and the anterior cingulate cortex.

The proposed experiments will enhance our understanding of the neurophysiological ramifications of acute ethanol intoxication. This information could be useful in explaining deficits in learning and working memory, and may eventually contribute to effective treatments to reduce cognitive deficits associated with alcohol consumption, alcoholism, or other conditions.

6.2. Subject Info and Specific Methods

All subjects had to achieve behavioral criterion (>70% overall accuracy) in order to be eligible for ethanol injections. Intraperitoneal injections of ethanol were performed 10 minutes prior to initiation of behavioral testing and neurophysiological recordings. The order of doses was pseudo-randomized via a Latin Square design. All subjects (N=8) received all doses of ethanol. To improve clarity in some subsequent analyses and discussions, "Low" doses include 0.25 and 0.50 g/kg ethanol, and "High" doses include 0.75 and 1.00 g/kg ethanol. "Broad spectrum" refers to all frequencies from 0-90 Hz. "Theta band" refers to frequencies between 4 and 12 Hz, "low gamma band" refers to frequencies between 50 and 70 Hz, and "high gamma band" refers to frequencies between 70 and 90 Hz.

6.3. Effects of ethanol on power spectrum analyses

Power spectrum analyses are used to determine the general strength of the signal at each frequency. In the following analyses, power is presented as microvolts squared (μV^2). We hypothesized that the medial prefrontal cortex, the anterior cingulate cortex, and the ventral hippocampus would all show dominant power within the theta (4-12 Hz)

band of frequencies. Across theta, low gamma (50-70 Hz), and high gamma (70-90) Hz, we expected that the saline control would show the highest power, and that acute ethanol would progressively and dose-dependently attenuate the power of the signal.

As expected, the largest peak of activity for all recording locations was observed in the theta frequency band. Power over the broad spectrum and frequency bands of interest for the medial prefrontal cortex are presented in Figure 38, for the anterior cingulate cortex in Figure 39, and for the ventral hippocampus in Figure 40. The peaks with highest amplitude were observed in the ventral hippocampus followed closely by the medial prefrontal cortex. The peak amplitude for the anterior cingulate cortex was 4-5 times lower than the peaks observed in the other regions. In the theta frequency band, all recording sites showed peaks of activity specifically in the rat-typical 6-8 Hz range. When the power at the low gamma frequencies was focused on, all recordings showed a similar linear decrease in power as frequency increased. The power at low gamma was strongest in the ventral hippocampus. The power in the medial prefrontal cortex and the anterior cingulate cortex was comparable. In the high gamma frequency range, all recordings showed a relatively stable and consistent level of power as frequency increased. Again, power was highest in the ventral hippocampus but comparable in the medial prefrontal cortex and the anterior cingulate cortex.

Dose-dependent attenuation of power for the whole session was observed in the theta band, low gamma band, and high gamma band of the medial prefrontal cortex. The strongest power was observed in the saline condition, the next strongest power at low doses, and finally the weakest power was observed following the high doses of ethanol. One-way ANOVAs on mean power values for each dose was significant for the medial

prefrontal cortex broad spectrum ($F_{4,920}$ =4.023, $p<0.001$), theta band ($F_{4,75z}$ =5.939, $p<0.01$), low gamma band ($F_{4,200}$ =4.47, $p< 0.01$), and high gamma band ($F_{4,200}$ =284.9, $p<0.0001$). Dunnett's post-hoc multiple comparison test was used to compare the mean power for each dose of ethanol with the saline control. For the broad spectrum and theta frequencies, significant differences were found between saline and the 0.50, 0.75, and 1.00 g/kg doses. For low gamma frequencies, significant differences were found between saline and the high doses of ethanol. For high gamma frequencies, significant differences were found between saline and all doses of ethanol.

Although the overall power of the anterior cingulate cortex was much lower than in the medial prefrontal cortex, there was still dose-dependent attenuation of power across the whole recording session. In the broad spectrum, theta, low gamma, and high gamma frequency bands the strongest power was observed in the saline control group, followed by the low doses of ethanol and then the high doses of ethanol. A one-way ANOVA on mean power values for each dose only showed significance for the high gamma frequencies ($F_{4,200}$ = 130.7, $p<0.0001$). According to Dunnett's multiple comparison test, all doses of ethanol were highly significantly different from saline.

The ventral hippocampus showed the strongest power of all recording sites, but the dose-dependent effects of ethanol were less clear than the above regions. The 0.75 g/kg dose of ethanol generally resulted in the highest power whereas the 0.50 g/kg dose of ethanol generally resulted in the weakest power with all other doses falling somewhere in between. The one-way ANOVAs on mean power values for each dose were significant for the ventral hippocampus broad spectrum ($F_{4,920}$ =2.798, $p<0.05$), theta band ($F_{4,75}$ =4.025, $p<0.01$), low gamma band ($F_{4,200}$ =7.244, $p< 0.0001$), and high

gamma band ($F_{4,200}$ =242.3, $p<0.0001$). Dunnett's post hoc multiple comparison test was used to compare saline to each ethanol dose group. Significant post-hoc differences were found between saline and the 0.50 g/kg dose of ethanol at all frequency bands, and additionally between saline and the 0.75 and 1.00 g/kg doses of ethanol in the high gamma band.

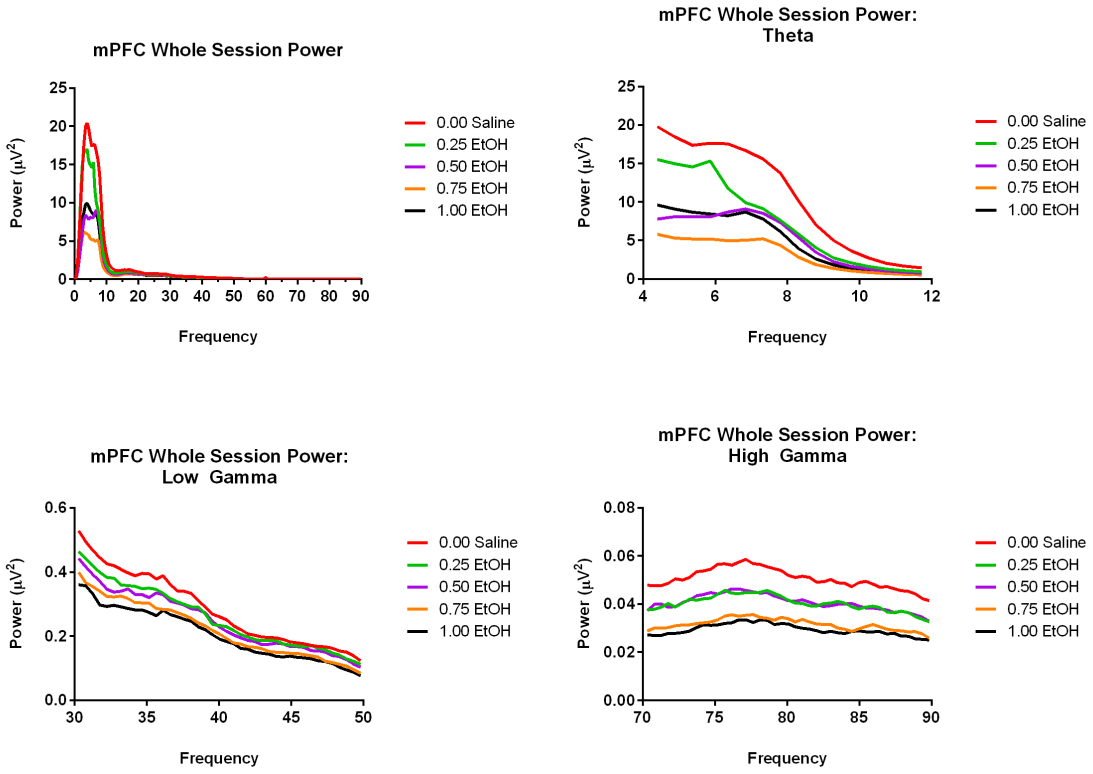

Figure 38 Power of whole session in medial prefrontal cortex

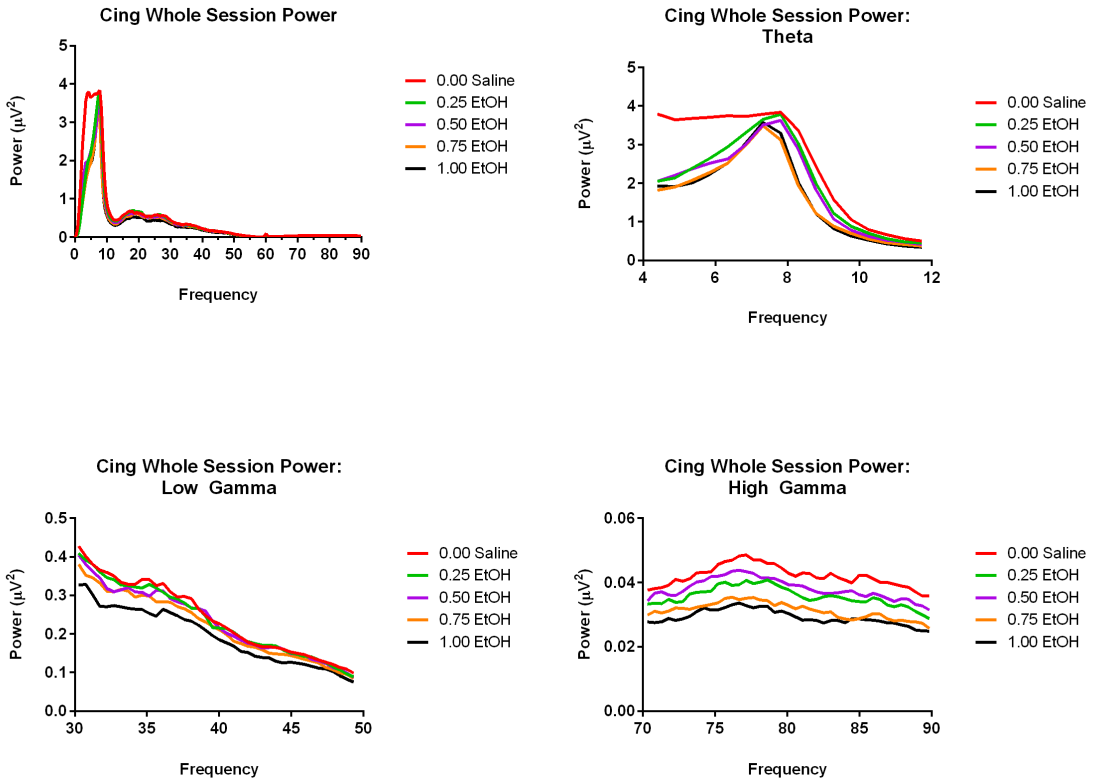

Figure 39 Power of whole session in anterior cingulate cortex

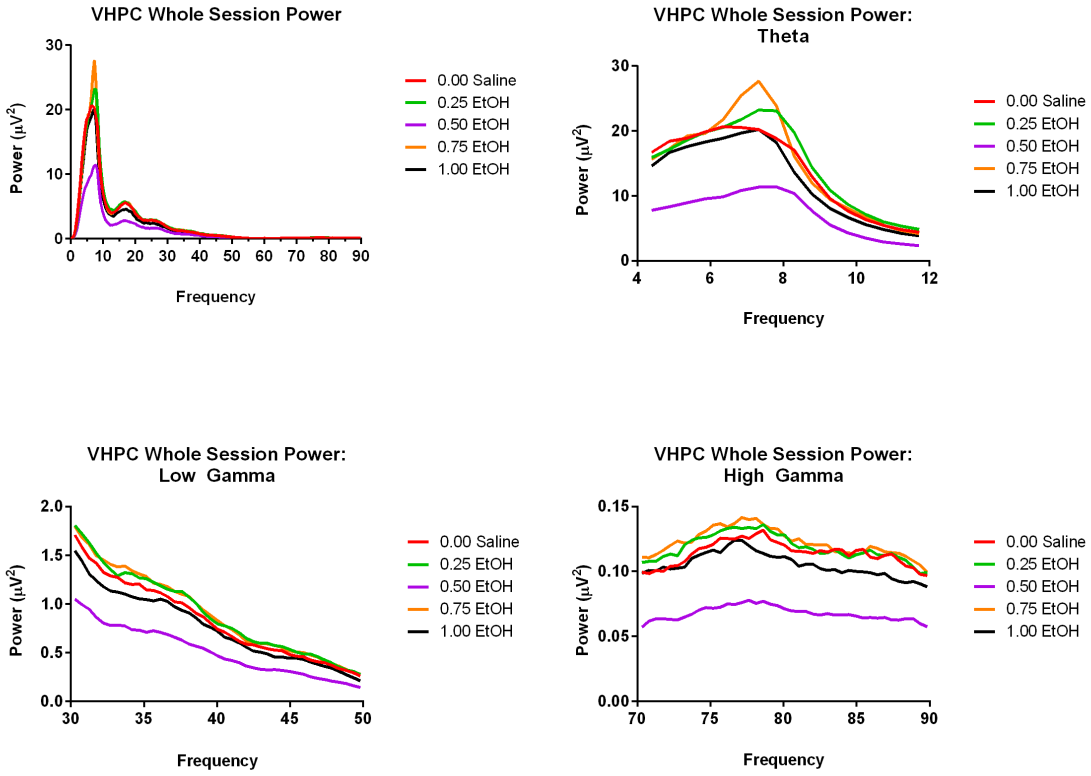

Figure 40 Power of whole session in ventral hippocampus

Additional power spectrum analyses were performed on around the onset of sample and choice lights to determine if there were more subtle dose-dependent effects on processing task-relevant stimuli. Separate Power spectrums were performed on the two seconds prior to stimulus onset ("Pre") and two seconds after stimulus onset ("Post"). Power analyses comparing the pre and post conditions around sample and choice lights for each recording location are presented in Figure 41. The area under the pre and post power spectrum curves for all frequencies 0-90 Hz was computed and used as a single measure to quantify the amount of power around each stimulus and for each dosage (See Figure 42). A consistent change in area under the curve from pre to post power would indicate stimulus-evoked potentials. In the medial prefrontal cortex, there was no clear pattern of increased or decreased power before or after the sample or choice stimuli. In the anterior cingulate cortex, there was a suppression of theta power following both sample and choice lights. A two-way ANOVA showed significant main effects for both timing ($F_{1,9} = 16.29$, $p<0.01$) and dosage ($F_{9,9} = 6.739$, $p<0.01$). In the ventral hippocampus, changes in theta power were not observed as the power was generally similar both before and after sample and choice light onset. A two-way ANOVA showed a significant effect for dosage ($F_{9,9}=28.25$, $p<.0001$), likely driven by the decreased power observed in the 0.50 g/kg dosage around both sample and choice lights.

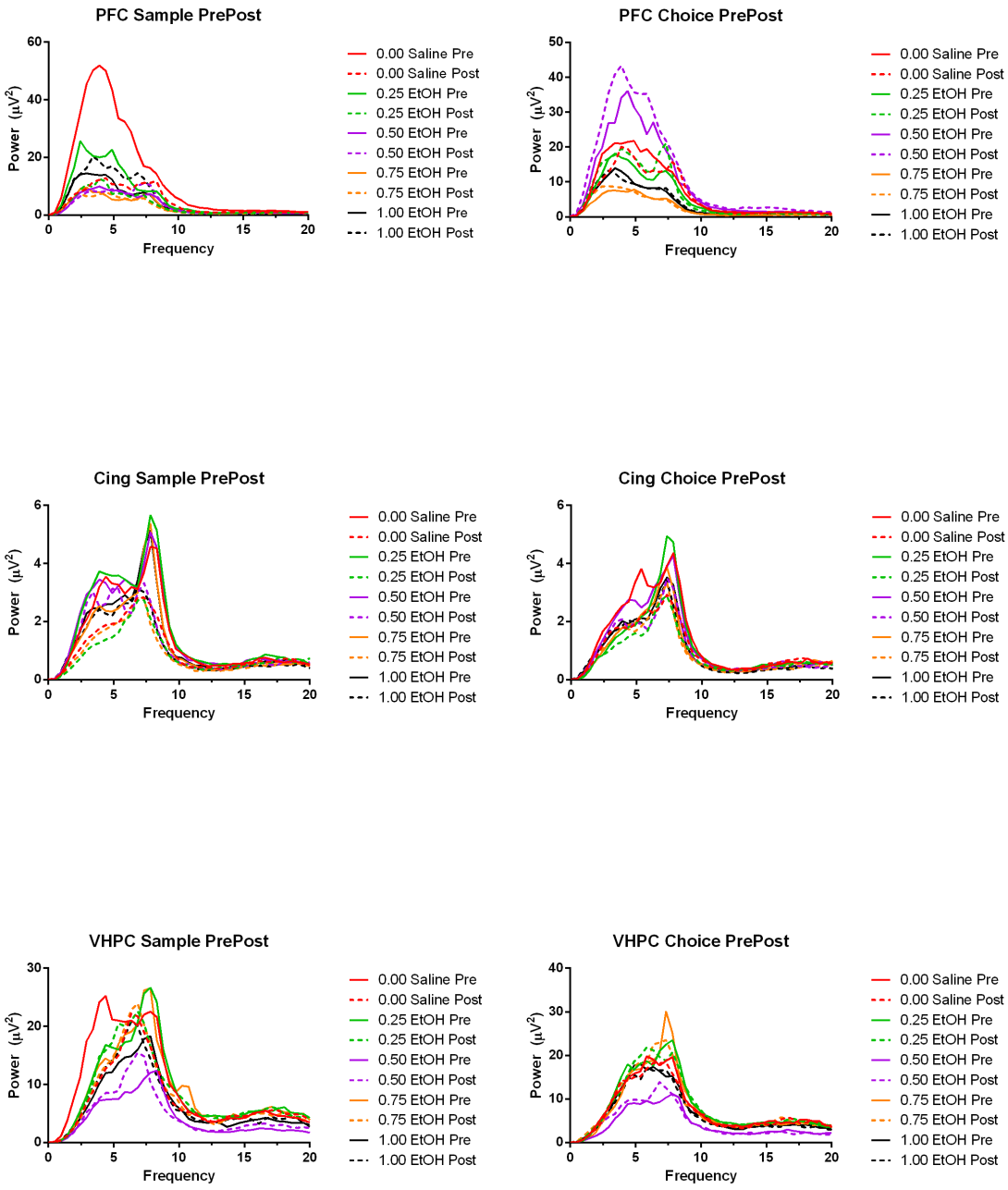

Figure 41 Power before and after sample and choice onset

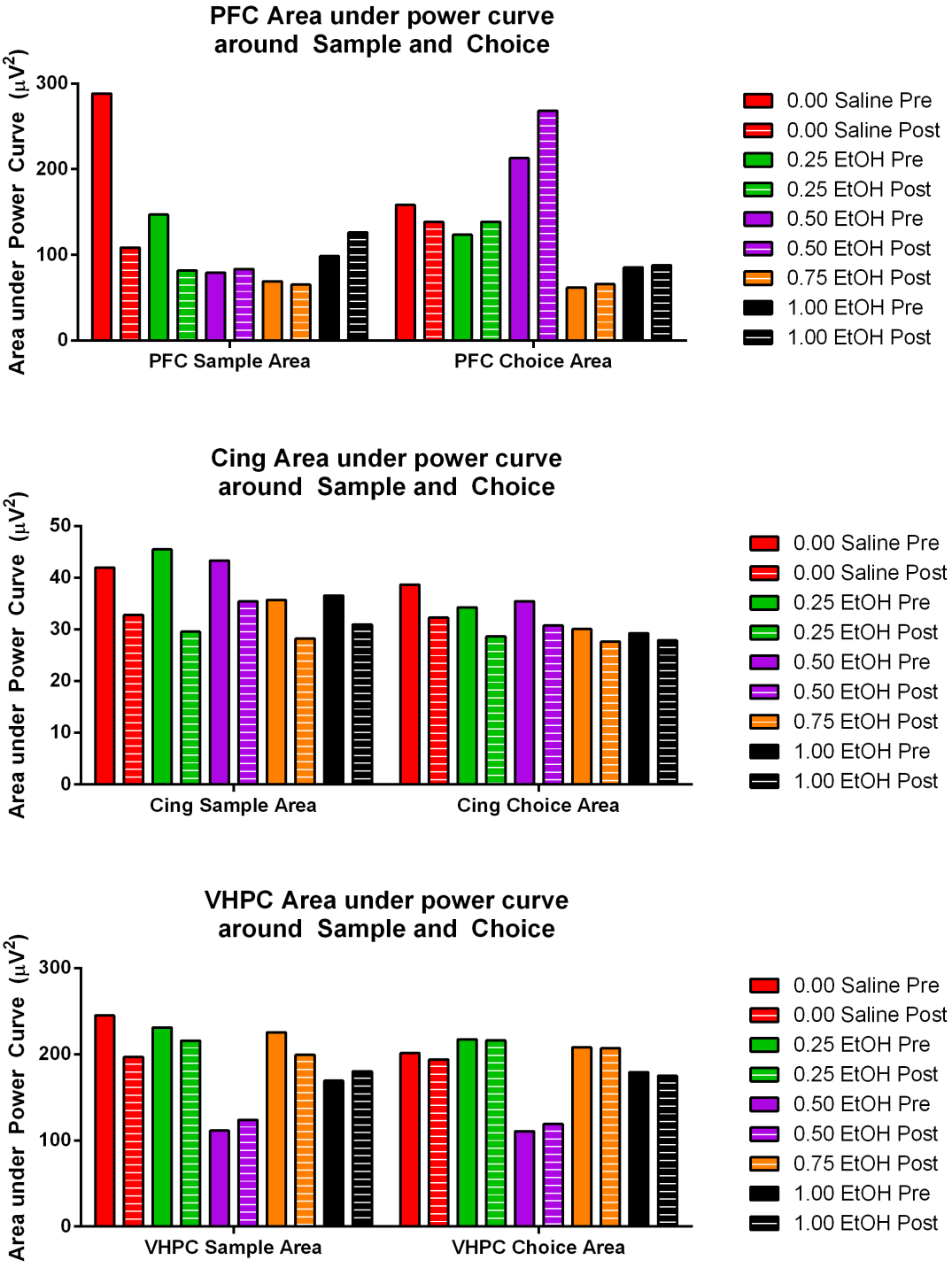

Figure 42 Area under Power Spectrum Curves Before and After Stimulus Lights

6.4. Effects of ethanol on Coherence

Coherence is a frequency-specific measure of synchrony between two signals that reflects the consistency of their temporal relationship. To investigate questions of cross-region synchrony, coherence analyses were performed on both the medial prefrontal cortex and the anterior cingulate cortex relative to the ventral hippocampus. Since the ventral hippocampus projects more directly to the medial prefrontal cortex than the anterior cingulate cortex, we hypothesized that coherence at theta, low gamma, and high gamma frequencies would be higher in the medial prefrontal cortex than in the anterior cingulate cortex. Furthermore, we hypothesized that acute ethanol would progressively disrupt coherence in a dose-dependent manner.

Mean coherence values for medial prefrontal cortex and anterior cingulate cortex across frequencies in the theta, low gamma, and high gamma frequency bands are displayed in Figure 43. The left panel represents the prefrontal cortex; the right panel represents the anterior cingulate cortex. Contrary to our initial hypothesis, the coherence between the anterior cingulate cortex and the ventral hippocampus is actually higher than the coherence between the medial prefrontal cortex and the ventral hippocampus at all frequency bands of interest. In the theta frequency band, both sites show a peak of higher coherence between 6 and 10 Hz. In both the low and high gamma frequency bands, both sites show remarkably stable and consistent coherence values as frequencies increase. However, the coherence is generally higher in low gamma than high gamma.

The effects of ethanol on coherence follow a different pattern than those observed for power in the previous section. In most cases, the saline control appears in the middle with low doses of ethanol showing an elevated level of coherence with the ventral

hippocampus and high doses of ethanol showing diminished coherence. This relationship is clearer when mean coherence values for each group are collapsed across frequencies into a single value, as shown in Figure 44. Separate one-way ANOVAs on coherence for broad spectrum, theta band, low gamma band, and high gamma band frequencies at both the medial prefrontal cortex and the anterior cingulate cortex all showed highly significant effects of dosage. Dunnett's post-hoc multiple comparison test was used to compare the coherence value for each dose of ethanol relative to saline controls (See Table 3 for a summary of statistical results).

The medial prefrontal cortex generally showed an inverted-U shaped relationship between dose of ethanol and coherence. Low doses of ethanol generally increased coherence relative to controls, whereas high doses of ethanol decreased coherence. Over the broad spectrum, all doses were significantly different from the saline control. In the theta band, 1.00 g/kg ethanol was significantly different from the saline control. In the low gamma band significant differences were found for all doses, and in the high gamma band significant differences were found for all doses except 0.50 g/kg.

Coherence between the anterior cingulate cortex and the ventral hippocampus was also affected by ethanol, with the highest doses showing a decrease in coherence relative to the saline control. Over the broad spectrum, all doses except the lowest one (0.25 g/kg) were significantly different from the saline control. In the theta, low gamma, and high gamma frequency bands the 0.50, 0.75, and 1.0 g/kg doses of ethanol were significantly different from the saline control.

The gamma frequency bands show clear separation of coherence based on dose of ethanol in both the medial prefrontal cortex and the anterior cingulate cortex. However,

the low gamma frequency range was the only band in which the lowest dose of ethanol was significantly different from the saline control in both recording locations. Therefore, coherence in the low gamma frequency range may be the most sensitive measure of effects of acute ethanol upon coherence between the ventral hippocampus and frontal brain regions.

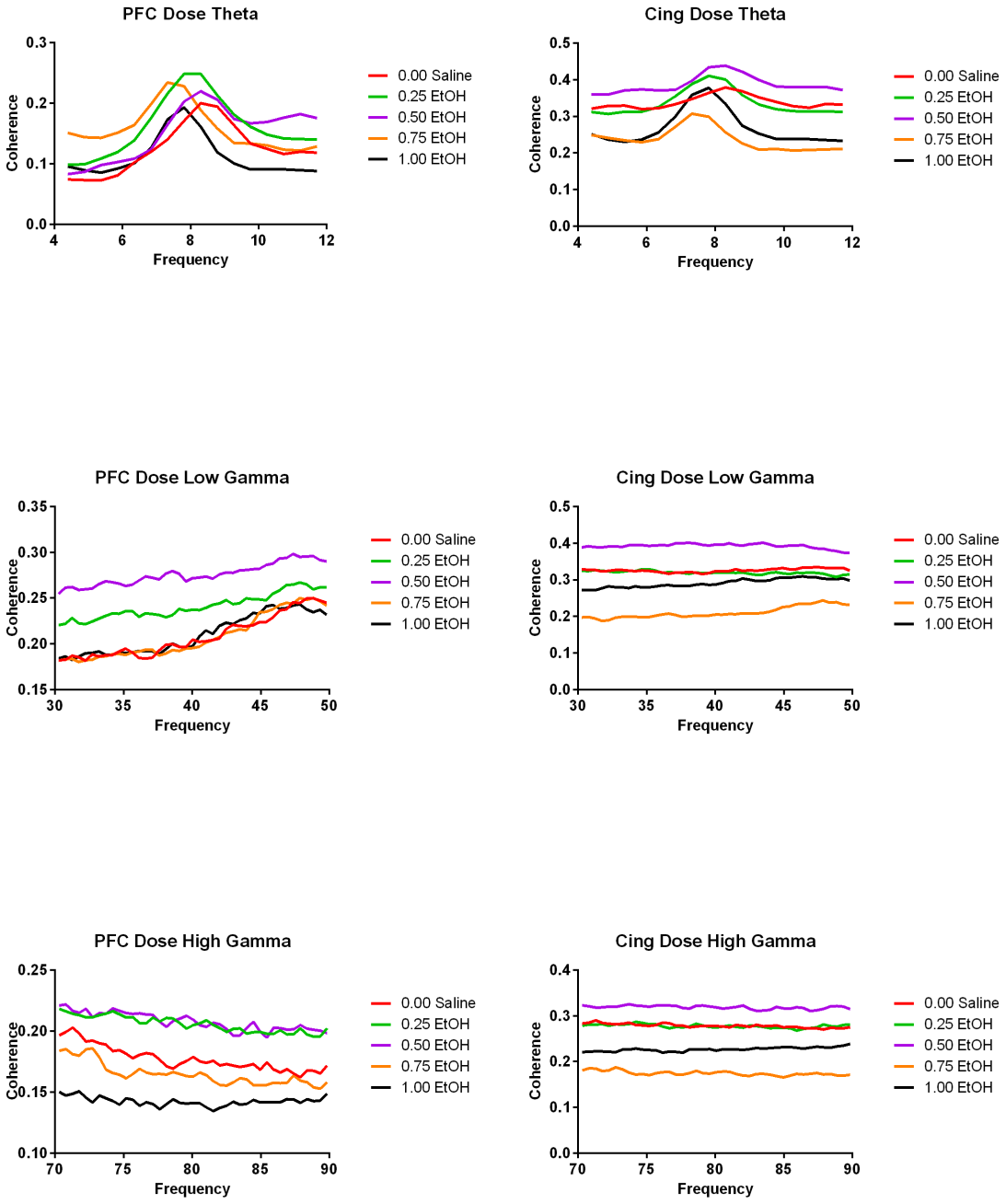

Figure 43 Coherence across frequencies for medial prefrontal cortex and anterior cingulate cortex relative to ventral hippocampus.

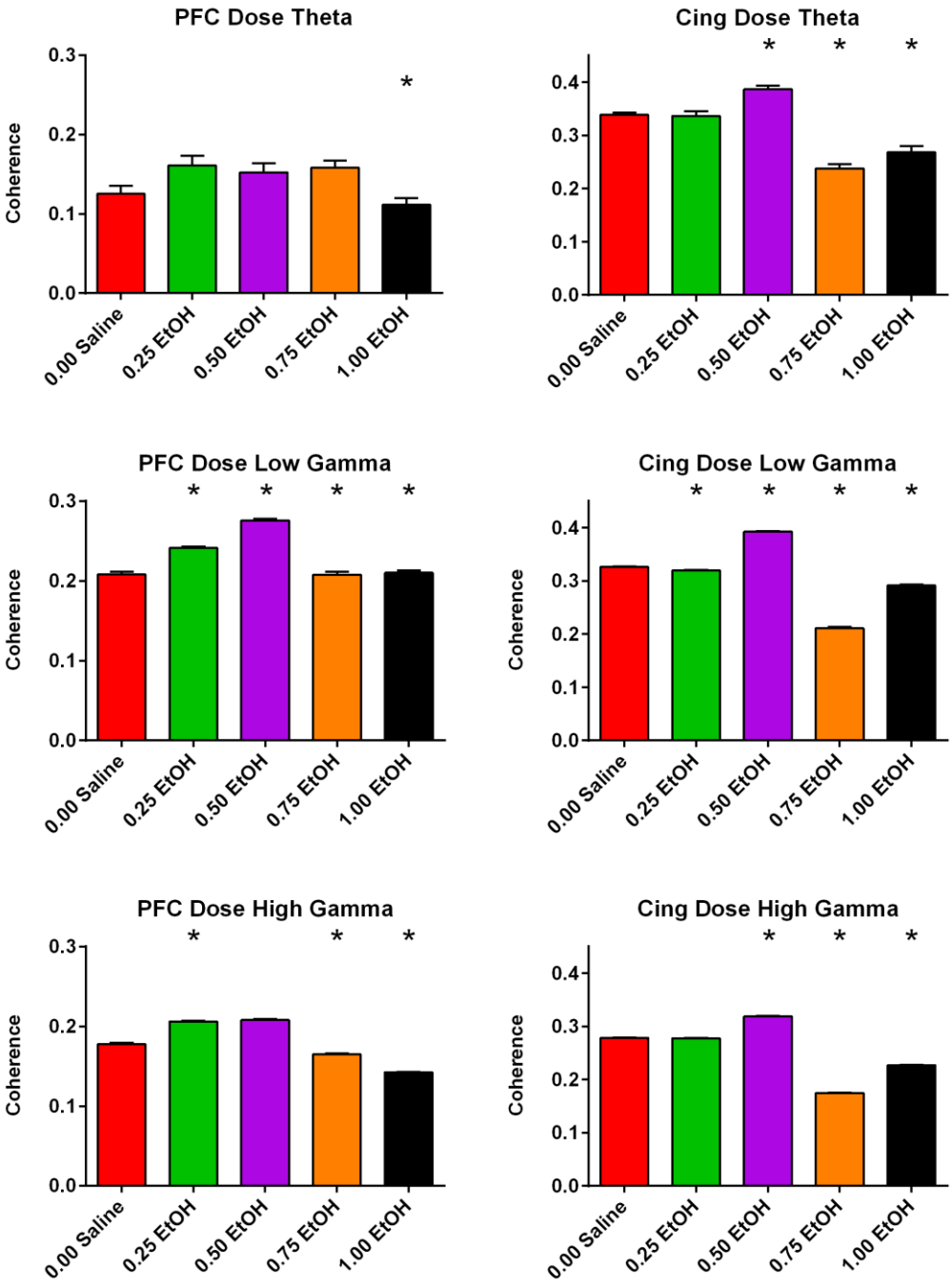

Figure 44 Group mean coherence for medial prefrontal cortex and anterior cingulate cortex relative to ventral hippocampus.

Asterisks indicate significant difference from saline control ($p<0.05$). Error Bars indicate SEM.

	One-Way ANOVA			Dunnett's post-hoc multiple comparison test			
	F	df	P	Saline vs. 0.25 EtOH	Saline vs. 0.50 EtOH	Saline vs. 0.75 EtOH	Saline vs. 1.00 EtOH
PFC Broad Spectrum	47.92	4, 920	<0.0001	****	**	****	****
PFC Theta	4.566	4, 75	<0.01	ns	ns	ns	**
PFC Low Gamma	98.15	4, 200	<0.0001	****	****	****	****
PFC High Gamma	525.9	4, 200	<0.0001	****	ns	****	****
Cing Broad Spectrum	263.8	4, 920	<0.0001	ns	****	****	****
Cing Theta	52.13	4, 75	<0.0001	ns	***	****	****
Cing Low Gamma	1905	4, 200	<0.0001	*	****	****	****
Cing High Gamma	6871	4, 200	<0.0001	ns	****	****	****

Table 3. T-tests on coherence

Ns indicates non significance. Significant post-hoc comparisons are indicated by a series of asterisks demonstrating strength of significance. One asterisk $p<0.05$, two asterisks $p<0.01$, three asterisks, $p<0.001$, four asterisks, $p<0.0001$.

6.5. Conclusions and Discussion

We hypothesized that the medial prefrontal cortex, the anterior cingulate cortex, and the ventral hippocampus would all show dominant power within the theta band of frequencies. Across theta, low gamma, and high gamma frequency bands, we expected that the saline control would show the highest power, and that acute ethanol injections would progressively and dose-dependently attenuate the power of the signal obtained over the whole recording session. In general, this hypothesis was supported by the data of the present study and corresponds to previous work in rats (Givens, 1995) and humans (Ehlers et al., 1989). We also expected to observe this dose-dependent attenuation in short windows around task-relevant stimulus onsets. In general, present support for this hypothesis was inconclusive. The medial prefrontal cortex and the ventral hippocampus did not show a consistent difference in the power before or after stimulus onset. The anterior cingulate cortex generally showed theta suppression after a stimulus. This was an unexpected result given that the literature generally shows increased theta power following stimulus onset (See general discussion).

This loss of energy could be indicative of the sedative hypnotic effect associated with reduced lever presses described in the previous chapter, or this loss of energy could be associated with specific cognitive impairments. In humans performing a Stroop-induced conflict task, ethanol reduces theta power overall, but conflict related theta power is reduced selectively by alcohol in the anterior cingulate cortex and lateral fronto-parietal regions (Kovacevic et al., 2012). In humans, it has been found that intracranial recordings during a memory task showed that increased power during encoding predicted subsequent successful recall (Sederberg et al., 2003). Conversely, if power is suppressed

by ethanol, then that reduction may correlate with subsequent failures to encode or retrieve information, which are observed under the influence of ethanol. Transient decline in power could be due to a decrease in septal cholinergic activity or an increase in septal GABAergic activity (Sakimoto et al., 2013).

Both hippocampal-dependent learning and experience-dependent activation of the hippocampus are disrupted by ethanol (Melia et al., 1996). Ethanol also modulates synaptic plasticity in both *in vitro* and *in vivo* contexts (McCool, 2011). For example, Fujii and colleagues (2008) used hippocampal slices from rats to show that induction of long-term potentiation was blocked if the tetanus was delivered in the presence of ethanol, muscimol (a GABA-A agonist) or AP5 (an NMDA receptor antagonist). When the slices were from rats that had been chronically fed a liquid diet containing ethanol, there was less impairment in LTP induction when the tetanus was delivered in the presence of ethanol, muscimol, or AP5. This tolerance effect in animals exposed to chronic ethanol consumption is likely mediated by a reduction in GABAergic inhibition or an increase in NMDA receptor activity in hippocampal CA1 neurons (Fujii et al., 2008).

The other main investigation for this chapter was to determine the effects of ethanol on coherence between the ventral hippocampus and the frontal brain regions of interest. We hypothesized that coherence at theta, low gamma, and high gamma frequencies would be higher in the medial prefrontal cortex than in the anterior cingulate cortex. This hypothesis was not supported by the present data. Surprisingly, stronger coherence with the ventral hippocampal signal was consistently observed in the anterior cingulate cortex. We also hypothesized that acute ethanol would progressively disrupt

coherence in a dose-dependent manner. This hypothesis was supported by the data with low doses showing little change or a slight increase in coherence, whereas high doses generally suppressed ventral hippocampal-frontal brain region coherence in the theta, low gamma, and high gamma frequency bands.

Although the anterior cingulate cortex had substantially less power at all frequencies compared to the medial prefrontal cortex and the ventral hippocampus, it demonstrated stronger coherence with the ventral hippocampal signal than the medial prefrontal cortex did. This was not expected due to the direct, monosynaptic, glutamatergic projection from the CA1/Subiculum sub-region of the ventral hippocampus to the pre-limbic/infralimbic sub-region of the medial prefrontal cortex that was covered extensively in Chapter 1. Other anatomical connections or functional implications must explain the higher coherence between the ventral hippocampus and the anterior cingulate cortex during the performance of the delayed non-match to position operant working memory task.

The observed physiological effects of acute ethanol are likely due to its effects on GABA, Glutamate, or some combination of the two neurotransmitter systems. Previous studies have used a similar delayed non-match to position task to study the behavioral effects of GABA-ergic or Glutamatergic drug infusion to either dorsal or ventral sub-regions of the hippocampus and found both delay-dependent and independent effects(Robinson and Mao, 1997; Mao and Robinson 1998). Given the behavioral and physiological effects of ethanol observed in this dissertation, it is surprising that the aforementioned researchers found that neither NMDA antagonists nor GABA-A agonists had any significant effect on behavior when infused into the ventral hippocampus.

Similar to the coherence results of the present study, ethanol has been shown to reduce the phase locking of neural activity in both the human and rodent brain (Ehlers et al., 2012). The authors conclude that these findings are consistent with the hypothesis that ethanol reduces synchrony within and between neuronal networks, perhaps by increasing the level of noise in key neuromolecular interactions.

The electrophysiological effects of ethanol on central neurons have been relatively well-characterized. Ethanol actions on neuronal excitability generally fall into one of three categories (Siggins et al., 1987). The first category is alterations in the voltage-dependent ionic conductances underlying action potentials. The second category is changes in passive membrane conductances and therefore resting membrane potentials. The third category is pre- or post-synaptic changes in synaptic transmission, including alterations in transmitter release or sensitivity of receptors or transmitter activated conductances. These effects likely vary based upon timing and dosage of ethanol.

Ethanol suppresses activity of hippocampal pyramidal cells and it can do so through a variety of mechanisms including altering activity in afferent regions, enhancing perisomatic inhibitory currents on the pyramidal cell, increasing the excitability of inhibitory interneurons, or activating regions such as the ventral tegmental area or the raphe nucleus that inhibit pyramidal cells and potently excite inhibitory interneurons (Reviewed in White et al., 2000). In experiments recording from hippocampal neurons while rats traversed a symmetric Y-maze, ethanol potently suppressed the firing of hippocampal place cells without altering place-field location (White and Best, 2000). These authors did not observe any effect on interneuron firing activity at the highest dose used in the present study (1.0 g/kg), but did find interneuron was occasionally suppressed

by 1.5 g/kg ethanol. This suggests that the decrease in power and coherence observed after injections of 1.0 g/kg ethanol in the present study are likely driven by mechanisms other than increasing the excitability of the local inhibitory interneuron network.

Additional research is needed to determine the pharmacological and physiological mechanisms underlying acute ethanol's dose-dependent effects on power and coherence presented in this chapter. It would be interesting to compare the effects of ethanol, selective NMDA antagonists, and GABA-A agonists and see if the pattern of results is replicated. It would also be interesting to use higher doses of ethanol and see how this affects power and coherence between frontal brain regions and the ventral hippocampus.

Chapter 7: General Discussion

7.1. Conclusions

The behavioral results indicate that the variable delayed non-match to position operant conditioning protocol is an effective methodology to study goal-maintenance working memory in rodents. The task showed delay-dependence with performance generally decreasing as delays increased. With very few exceptions, animals were able to acquire the rules of the task and gradually improve from near chance levels to achieve the pre-defined behavioral criterion for overall accuracy at each of the training stages.

As learning progressed, some notable physiological changes were observed. Waveform averages around mnemonically-relevant stimuli showed higher amplitude after learning of the task rules was well established. These stimulus-triggered waveform averages showed the highest amplitude in the medial prefrontal cortex and the weakest amplitude in the anterior cingulate cortex. Both the medial prefrontal cortex and the anterior cingulate cortex were more highly correlated with the ventral hippocampus in the early sessions and decreased in similarity to the ventral hippocampus waveform as learning progressed. This suggests that the ventral hippocampus may play different roles in early task acquisition and after the task is acquired.

In retrospective analyses of animals that were eventually classified as fast or slow learners, there were differences in the power spectrum at baseline and waveform averages around task-relevant stimuli. In the medial prefrontal cortex and the anterior cingulate

cortex, the fast learning group had higher baseline power in theta and gamma frequency bands. In the ventral hippocampus, the fast learning group had higher baseline power in the gamma frequency band but not the theta frequency band. The stimulus-triggered waveform averages in the fast group appear to increase in amplitude over time whereas the slow group starts with strong amplitude that decreases over time. Combined, this data suggests that the fast learning group may have greater initial attentional capacity or focusing capability than the slow learning group.

The delayed non-match to position task was sensitive to the effects of acute ethanol on several cognitive and behavioral constructs including working memory, attention, inhibition control, impulsivity, motivation, and motor function. In general, low doses of ethanol (0.25 or 0.50 g/kg) had either neutral or slight activational effects whereas high doses (0.75 or 1.00 g/kg) had more detrimental effects. Specifically, the high doses of ethanol decreased accuracy, decreased number of extraneous lever presses during the intertrial interval or delay period, increased the number of omissions, and slowed down reaction time. It is unlikely that these effects were due to changes in motivation or locomotor impairment, but it is possible that they reflect changes in attention or conservation of effort.

Acute ethanol dose-dependently affected power and coherence measures. Alcohol progressively and dose-dependently attenuated the power of the signals obtained over entire recording sessions. This was generally true for broadband, theta, and gamma power. The medial prefrontal cortex and the ventral hippocampus did not show a consistent difference in power before or after a stimulus, but the anterior cingulate cortex generally showed theta power suppression after a stimulus. Counter to the original

hypothesis, the anterior cingulate cortex consistently showed stronger coherence with the ventral hippocampal signal than did the medial prefrontal cortex. Low doses of ethanol generally showed little change or a slight increase in coherence between signals from the frontal regions and the hippocampus, but high doses generally suppressed ventral hippocampal-frontal brain region coherence in the theta, low gamma, and high gamma frequency bands.

In conclusion, neural oscillations—particularly theta and gamma rhythms—play a meaningful role in the acquisition of rules for the variable delayed non-match to position operant conditioning working memory task. The medial prefrontal cortex, the anterior cingulate cortex, and the ventral hippocampus are all part of a circuit involved in working memory processing. Furthermore, acute ethanol causes dose-dependent behavioral and neurophysiological effects. Continued investigation of neural oscillations in the hippocampal-frontal brain circuit will likely yield important information about the anatomical regions, cognitive processes, and neurophysiological mechanisms underlying successful or disrupted working memory performance.

7.2. Discussion

The role of theta in prefrontal-hippocampal interactions during working memory

Lesion studies suggest that hippocampal-prefrontal cortex interactions are critical for spatial working memory (Floresco et al., 1997; Wang and Cai, 2006). The theta rhythm has been proposed as a mediator for interactions between these regions during working memory performance (Benchenane, 2011; Gordon, 2011; Colgin, 2013). A

decrease in theta coherence between hippocampal CA1 and the medial prefrontal cortex is associated with poor performance in a working memory task (Sigurdsson et al., 2010).

Neuronal firing coherence in theta band between hippocampus in medial prefrontal cortex increases during spatial working memory (Siapas et al., 2005; Jones & Wilson, 2005; Hymen et al., 2010). Although there is not a direct anatomical connection between the dorsal hippocampus and the medial prefrontal cortex, most hippocampal recordings from these studies took place in the dorsal sub-region and required the animal to actively traverse through various mazes. The additional locomotion and spatial navigation that is particularly well-suited to the dorsal hippocampus may help explain the strength of coherence observed despite lack of a direct anatomical projection.

Siapas and colleagues (2005) demonstrated that prefrontal neurons demonstrate phase locking to hippocampal theta oscillations at a lag of approximately 50 milliseconds. 80% of hippocampal cells and 40% of prefrontal cortex cells showed phase locking to the hippocampal theta rhythm. The authors suggest that phase locking between these regions likely occurs from both excitatory input to pyramidal cells and inhibitory control over local networks of interneurons. Rather than hyperpolarizing pyramidal cells, the hippocampal-prefrontal cortex pathway feed-forward inhibition can act to rhythmically decrease pyramidal cell input impedance thus modulating their excitability (Siapas et al., 2005). Other potential explanations for phase locking include both regions being co-modulated at theta frequency by subcortical structures, resonant properties of individual cells modulating phase locking, influence by external neurotransmitters and modulators, or a combination of permissive/modulating actions and active pacemaker rhythmic interactions form other regions.

Jones & Wilson (2005) demonstrated that correlated firing between CA1 and the prefrontal cortex is selectively enhanced during behavior that recruits spatial working memory. This may allow the integration of spatial information from the dorsal hippocampus into the broader decision-making network. According to the authors, CA1-medial prefrontal cortex synchrony may be enhanced during specific behavioral epcohs by two potential mechanisms. The first potential mechanism is that there are simultaneous increases in theta modulated activity. This mechanism is unlikely given that the observed enhanced correlations were independent of changes in theta power. The second potential mechanism is that firing rates and local field potentials are modulated at similar frequencies and require precise temporal control of spiking relative to the theta rhythm.

Hymen and colleagues (2010) found that working memory performance in a delay non-match to sample operant task correlates with prefrontal-dorsal hippocampal theta interactions but not with prefrontal neuron firing rates. Medial prefrontal cortex cells fired at similar rates during both error and correct trials, but 46% of cells were theta entrained on correct trials compared to only 17% cells that were theta-entrained on error trials. While Jones and Wilson (2005) found that there was a decrease of prefrontal entrainment to hippocampal theta only in the choice phase of a spatial working memory task, Hymen and colleagues found evidence of selective reduction in medial prefrontal cortex unit entrainment to dorsal hippocampal theta in both sample and choice phases of error trials. The additional finding of selective reduction also occurring in the sample phase of error trials suggests that not only is hippocampal-prefrontal theta entrainment important for retrieval in the test stage, but it may also be involved in stimulus encoding

processes. In results presented in Chapter 4, physiological differences between the fast and slow learning groups parallel findings by Hymen and colleagues. Group differences in the waveform average around sample hit responses were more pronounced in the ventral hippocampus, and group differences on choice responses were more pronounced in the medial prefrontal cortex (See Table 2). This finding supports a more dominant role for the ventral hippocampus in encoding stimulus processes and a more dominant role for the medial prefrontal cortex in retrieving information.

Most of the previously mentioned studies on hippocampal entrainment of prefrontal neurons relied upon recordings from the dorsal sub-region of the hippocampus. Although the power and amplitude of theta oscillations are much stronger in this sub-region compared to the ventral sub-region, only ventral portions of the hippocampus project directly to the medial prefrontal cortex. In a more recent study of mice performing a T-maze delayed non-match to position spatial working memory task, synchrony was found between the medial prefrontal cortex and both the dorsal and ventral sub-regions of the hippocampus but this synchrony was dependent specifically upon the ventral sub-region of the hippocampus (O'Neill et al., 2013). Infusion of GABA-A agonist muscimol into the ipsilateral ventral hippocampus significantly reduced coherence with the medial prefrontal cortex to a much higher degree than infusion to the contralateral ventral hippocampus or either type of infusion to the dorsal hippocampus. This study helps contextualize the results from previously cited studies by showing that hippocampal-prefrontal synchrony is due to specific anatomical and functional projections and is not due to artifacts from passive spread of signal by volume conduction. If the previously observed medial prefrontal cortex theta signal was volume

conducted from the hippocampus, then it should show more similarity with the dorsal region than the ventral region because the amplitude and power of the oscillations are much stronger and the dorsal region is physically closer to the medial prefrontal cortex. The pivotal role of the ventral hippocampal sub-region in affecting the physiology of the medial prefrontal cortex, and the fact that the coherence between these structures is decreased with a GABA-A agonist similar to ethanol, are both important findings parallels to the experimental results within this dissertation.

Similar to the findings in Jones and Wilson (2005), and by Hymen and colleagues (2010), O'Neill and colleagues (2013) also found that medial prefrontal cortex theta power and phase locking were higher during the choice phase of the task that required working memory compared to the sample phase where overt behavior was the same but spatial working memory was not required. O'Neill and colleagues conclude that the ventral hippocampus acts as a conduit for spatial working memory by relaying spatial information from the dorsal hippocampus to the decision-making circuitry within the medial prefrontal cortex. Although the dorsal hippocampus was not investigated in the current studies, we did observe similar physiological signals between the ventral hippocampus and the medial prefrontal cortex and anterior cingulate cortex further supporting that these structures comprise a spatial working memory circuit.

Other regions that could have contributions to synchrony.

The ventral hippocampal to medial prefrontal cortex pathway that has been a point of emphasis throughout this dissertation starts in the CA1/subiculum of the ventral hippocampus, proceeds through the alveus, then the fimbria/fornix, then the septum,

nucleus accumbens, infralimbic region of the medial prefrontal cortex, and then finally terminates in the prelimbic and medial orbital sub regions of the medial prefrontal cortex (Jay and Witter, 1991; Thierry 2000). Afferent projections or neuromodulatory input to any of those regions could conceivably affect synchrony between the hippocampus and frontal cortex. The ventral hippocampus CA1/subiculum region also sends inhibitory projections to the ventral pallidum of the basal ganglia and thus may activate prefrontal cortex neurons through an indirect disinhibitory process (Thierry et al., 2000).

Double-labeled cells that project to both hippocampus and the medial prefrontal cortex were found in the nucleus reuniens of the thalamus and to a slightly lesser degree in the entorhinal cortex, but not the septum (Varela et al., 2013). The nucleus reuniens, a midline thalamic nuclei, receives afferents from areas involved in generation of theta rhythm (Vertes, 2004), and visual and motor regions (McKenna and Vertes, 2004). Thus the nucleus reuniens could be a contributor to theta synchronization between these two areas. Specifically, nucleus reuniens cells with collaterals in both the medial prefrontal cortex and the hippocampus could be important during exploratory activity to synchronize both structures (Varela et al., 2013).

Anatomy and functions of the anterior cingulate cortex

The anterior cingulate cortex has reciprocal connections with a number of thalamic nuclei, including intralaminar, lateral, midline, ventrolateral, ventromedial, ventral posterior, and especially the mediodorsal nuclei (Shibata, 1993) and receives projections from several neurotransmitter specific brainstem areas including serotonergic projections from the raphe nucleus, noradrenergic projections from the locus coeruleus,

and dopaminergic projections from the ventral tegmental area (Buchanan et al., 1994). It is possible that any of these thalamic or brainstem regions are projecting to both the ventral hippocampus and the anterior cingulate cortex, providing the appearance of enhanced coherence.

The basal forebrain cholinergic system and various subregions of the prefrontal cortex are characterized by numerous reciprocal projections (Gaykema et al., 1990). The septal area is another likely candidate for mediating coherence between the hippocampus and the anterior cingulate cortex. The lateral septal nucleus projects prominently to the medial septal diagonal band complex (Swanson and Cowan, 1979), which has previously been hypothesized as a pacemaker for hippocampal and frontal theta rhythms (Givens et al, 2000). The medial-septohippocampal pathway has been proposed as a site for the memory-impairing effects of ethanol by enhancing GABAergic transmission in, thereby reducing the regularity and vigor with which rhythmically bursting neurons drive theta rhythms. In a study involving a delayed non-match to sample eight arm radial maze task, rats with selective lesions suggested that the septo-cingulate cholinergic pathway is critically involved in working/episodic-like memory, but that the septo-hippocampal cholinergic pathway is either not contributing to the working/episodic memory used in this task or it is involved at short (1hour) but not long (4 or 8 hour) delays (Dougherty et al., 1998).

Functional dissociations have been observed between the rat pre-limbic and anterior cingulate cortex. In a study investigating the effects of reversible lidocaine lesions on performance in a radial-arm spatial working memory task, the prelimbic region is involved in process through which recently acquired information is used to organize

and modify foraging behavior, whereas the anterior cingulate cortex may play an important role in response flexibility (Seamans et al., 1995). The anterior cingulate cortex is often activated during scenarios of response conflict and plays important roles in error detection, positive feedback, and providing an error signal for adjusting behavior (Bisonette et al., 2013). Activity in the anterior cingulate cortex also signals need for increased attention on subsequent trials so that learning can occur, reflecting past reward history. As discussed in Chapter 4, the anterior cingulate waveform average showed significant differences between fast and slow learning groups around the onset of choice lights that eventually yielded incorrect responses (See table in Table 2). The anterior cingulate waveform averages did not show significant group differences to either sample hit or choice hit responses; further supporting a role in error detection. If ethanol causes more errors of commission, as was observed in Chapter 5, then higher activity in the anterior cingulate cortex could make sense from the perspective of error detection and additional feedback on incorrect responses.

In experiments with macaque monkeys, theta activity in the anterior cingulate cortex emerged particularly during trials that required adjustment of stimulus-response rules following an erroneous representation in the previous trial (Womelsdorf et al., 2010), suggesting a role for anterior cingulate cortex theta activity in cognitive control processes. Cingulate-hippocampal coherence has been observed in rats while trajectory coding in a sequential choice task (Remondes & Wilson, 2013). In human experiments, the anterior cingulate cortex has been shown to have increased theta power to Stroop-induced conflict scenarios that is reduced selectively by alcohol (Kovacevic et al., 2012). Ethanol attenuates theta power to conflict across successive processing stages, suggesting

that ethanol induced deficits in cognitive control may result from theta suppression in executive networks. Selective vulnerability of the top-down executive functions to ethanol may result in reduced self-restraint and propensity of engaging in continued or heavy drinking.

Neurophysiological and neuroanatomical studies also suggest that the anterior cingulate is involved in motor responding. The anterior cingulate projects to both the primary and supplementary motor areas (Sesack et al., 1989). Functional magnetic resonance imaging in humans has shown that motor-related changes in anterior cingulate cortex activity occur in relation to motor responses in working, but not reference memory tasks (Petit et al., 1998), suggesting that just the physical act of movement is not sufficient to induce changes in activity in this region. Activity in the anterior cingulate cortex may reflect a "state of readiness" to make a behavioral response based on information being held in working memory during a delay period (Jung et al., 1998). Slower reaction times associated with attenuated theta power to conflict scenarios was observed in the human anterior cingulate cortex, suggesting that ethanol also impairs motor preparation and execution strategies (Kovacevic et al., 2012). This aligns with the decreased number of intertrial interval and delay period lever presses as well as the increase in number of omissions and reaction times observed at high doses of ethanol in Chapter 5.

7.3. Future Directions

Behavior

The operant delayed non-match to position protocol has numerous advantages for investigating behavioral and neurophysiological phenomena associated with working memory. While the task still assesses spatial working memory, it does so with far less locomotive interference and navigational processing confounds than comparable maze tasks. The precise timing of stimuli and responses is ideally suited for physiological analyses. However, the major disadvantage to this task is the amount of time that it takes for animals to reach criterion at each shaping step and advance through the training. One potential way to speed-up the learning time may be to vary the delays for each animal so as to optimize performance (Robinson et al., 2000; Han et al., 2000). Instead of each animal receiving 5, 10, and 15 second delays as in the current protocol, delays could be titrated in order to keep a cohort's performance at comparable levels. Rats who are lagging behind could be given shorter delays (e.g. 4, 8, 12 seconds) while rats who are moving ahead could be given longer delays (e.g. 7, 14, 21 seconds). This approach may be advantageous for reducing variability in time to achieve performance criterion, but it should be used cautiously as delay differences within a cohort may induce subtle and unexpected behavioral effects. For example, it has previously been shown that varying signal length or intensity or intertrial interval length decreases accuracy in operant signal detection paradigms (Echevarria et al., 2005).

Pharmacology

All of the doses of ethanol used in the present experiment are considered in the low to moderate range. One potential future direction would be to expand the dosing regimen to include higher doses (e.g. 2.0 g/kg and 3.0 g/kg) that are more analogous to what is observed following excessive binge drinking behavior. These high dosages may help illuminate general understanding of mechanisms underlying blackout episodes. Another potential future direction would be to isolate which receptors are responsible for specific behavioral and neurophysiological effects associated with ethanol. Since ethanol acts as a GABA-A agonist and an NMDA antagonist, then other compounds with similar pharmacological profiles could be used to identify receptors associated with delay-dependent or delay-independent effects. Since GABA-A agonist muscimol has already been shown to disrupt coherence in the hippocampal-prefrontal spatial working memory circuit (O'Neill et al., 2013), it would be hypothesized that GABA-A agonists would have more pronounced delay-dependent effects than NMDA antagonists or other compounds related to ethanol.

Another important future direction would be to block the impairing effects of ethanol or identify compounds that increase baseline performance in the operant delayed non-match to position working memory task. One compound that is immediately interesting in this regard is caffeine because these two compounds are commonly consumed simultaneously. It would be interesting to explore whether or not caffeine attenuates the memory deficits and decrements in power and coherence that we have found to be sensitive to low-moderate doses of ethanol. Caffeine's primary pharmacological function is to block inhibitory adenosine receptors, which may have

excitatory effects on a variety of neurotransmitter systems that are likely inhibited by ethanol. In a rodent study involving a novel-odor habituation task, caffeine was shown to have preventative properties against ethanol-induced retrograde amnesia (Spinetta et al., 2008). It would be interesting to explore the behavioral and neurophysiological differences between control conditions, ethanol only conditions, caffeine only conditions, and ethanol plus caffeine conditions. It would be hypothesized that the greatest working memory deficits would be observed in the highest dosage of the ethanol only condition, caffeine with ethanol would attenuate these deficits, and caffeine alone would have minimal detrimental effect and may slightly enhance working memory performance.

Physiology

In the experiments within this dissertation, local field potentials were recorded from a stereotrode in the frontal cortex to record from the pre-limbic/infra-limbic sub-region of the medial frontal cortex and the anterior cingulate cortex, and from the CA1/subiculum region of the ventral hippocampus optimized for electrical connection with the frontal regions based on a stimulation protocol. These areas remain key focal points for the understanding of neurophysiological mechanisms underlying working memory, but the addition of other recording sites would clarify the role that afferent projections play in modulating this circuit. Based on literature reviewed previously, two main regions have emerged as possible indirect modulators of theta activity in the hippocampal-prefrontal spatial working memory circuit: the medial septal region and the nucleus reunions of the thalamus. Future studies should investigate the role of these

potential modulatory regions on theta and/or gamma rhythms in the hippocampus—medial prefrontal cortex—anterior cingulate cortex working memory circuit.

Previous research has also indicated that distracters interact with ethanol on performance measures. In a human study involving a modified oddball task, ethanol attenuated early sensory event-related potentials as well as the P300 "oddball" response following distracter but not target items (Campbell & Lowick, 1987). The amplitude of the P300 is lower in abstinent alcoholics and at-risk offspring of alcoholics than in non-drinkers, suggesting that there may be a genetic component to the ethanol-induced attenuation of coordinated physiological response to unusual stimuli (Porjesz et al., 2005). Therefore, another potential future direction for physiological analyses would be to add distracting items to the task (e.g. tone or other non-visual stimulus that is irrelevant to successful task performance) and compare the resultant event-related potentials under the influence of ethanol. It would be expected that high doses of ethanol would attenuate the event-related potentials following onset of distracting stimuli.

The physiological analyses within this dissertation focused on ways to determine the amount of energy at a given frequency within a signal (power), stimulus-evoked responses (waveform averages), and synchrony between waveforms across distal brain regions (waveform correlations and coherence). Theta and Gamma activity were analyzed as separate but highly-related entities. In future studies, phase-phase synchrony between theta and gamma rhythms in the regions of interest will be specifically addressed.

7.4. Summary

The effects of acute ethanol intoxication on neurophysiological correlates of working memory remain important and interesting questions for further analysis. Information gained from this line of research could be useful in explaining deficits in learning and memory, and may eventually contribute to effective pro-cognitive treatments. Information about the acute effects of ethanol on memory could contribute to an understanding and possible prevention of injuries and fatalities associated with situations such as driving under the influence of alcohol. Furthermore, studying the acute effects of alcohol on encoding and retrieval may lead to a better understanding of the neural structures vulnerable to chronic effects and possible treatment benefits or prevention strategies for alcohol abuse and alcoholism.

References

Adey, W.R. (1967). Intrinsic organization of cerebral tissue in alerting, orienting, and discriminative responses. In: G.C. Quarton, T. Melnechuk and F.O. Schmitt, Editors, *The Neurosciences*, The Rockefeller University Press, New York (1967), pp. 615–633.

Adhikari, A., Topiwala, M. A., & Gordon, J. A. (2010). Synchronized Activity between the Ventral Hippocampus and the Medial Prefrontal Cortex during Anxiety. *Neuron*, 65(2): 257-269.

Atkinson, R.C., & Shiffrin R.M. (1968). Human memory: A proposed system and its control process. In K.W. Spence & J.T. Spence (Eds.), The Psychology of learning and motivation: *Advances in research and theory,* Vol 2. New York: Academic Press, 1968. Pp 89-195.

Axmacher, N., Mormann, F., Fernández, G., Elger, C. E., & Fell, J. (2006). Memory formation by neuronal synchronization. *Brain Research Reviews*, 52(1): 170-182.

Baddeley, A. (2000). The episodic buffer: a new component of working memory. *Trends In Cognitive Sciences*, 4(11):417-423.

Baddeley, A. (2010). Working memory. *Current Biology*, 20(4): 136-140.

Baddeley, A.D. & Hitch, G.J. (1974). Working Memory. *In The Psychology of Learning and Motivation*, (Bower, G.A., Ed.), pp 47-89, Academic Press.

Ballard, T., & Mcallister, K. H. (2000). The NMDA antagonist EAA 494 does not impair working memory in an operant DNMTP task in rats. *Pharmacology Biochemistry And Behavior*, 65(4):725-30.

Barch, D.M., Ceasar, A. (2012). Cognition in schizophrenia: core psychological and neural mechanisms. *Trends in Cognitive Sciences*, 16, 1: 27-34.

Barch, D.M., Smith, E. (2008). The Cognitive Neuroscience of Working Memory: Relevance to CNTRICS and Schizophrenia. *Biol Psychiatry*, 64: 11-17.

Başar, E., & Güntekin, B. (2008). A review of brain oscillations in cognitive disorders and the role of neurotransmitters. *Brain Research*, 1235: 172-193.

Başar, E., Başar-Eroglu, C., Karakaş, S., & Schürmann, M. (2001). Gamma, alpha, delta, and theta oscillations govern cognitive processes. *Official Journal Of The International Organization Of Psychophysiology*, 39(2-3): 241-8.

Belluscio, M. A., Mizuseki, K., Schmidt, R., Kempter, R., & Buzsáki, G. (2012). Cross-frequency phase-phase coupling between θ and γ oscillations in the hippocampus. *The Official Journal Of The Society For Neuroscience*, 32(2): 423-35.

Benchenane, K., Peyrache, A., Khamassi, M., Tierney, P. L., Gioanni, Y., Battaglia, F. P., & Wiener, S. I. (2010). Coherent Theta Oscillations and Reorganization of Spike Timing in the Hippocampal- Prefrontal Network upon Learning. *Neuron*, 66(6): 921-936.

Berry, S.D., Thompson, R.F. (1978). Prediction of learning rate from the hippocampal electroencephalogram. *Science*, 200(4347): 1298-1300.

Bisonette, G.B., Powell, E.M., Roesch, M.R. (2013) Neural structures underlying set-shifting: roles of medial prefrontal cortex and anterior cingulate cortex. Behavioral Brain Research, 250: 91-101.

Bland, B.H. & Oddie, S.D. (2001). Theta band oscillation and synchrony in the hippocampal formation and associated structures: the case for its role in sensorimotor integration. *Behavioral Brain Research*, 127: 119-136.

Bland, B.H., Oddie, S.D., & Colom, L.V. (1999). Mechanisms of neural synchrony in the septohippocampal pathways underlying hippocampal theta generation. *The Journal of Neuroscience*, 19(8): 3223-3237.

Bruce, K.R., Shestowsky, J.S., Mayerovitch, J.I., &Pihl, R.O. (1999). Motivational effects of alcohol on memory consolidation and heart rate in social drinkers. *Alcoholism: Clinical and Experimental Research*, 23(4): 693-701.

Buchanan, S.L., Thompson, R.H., Maxwell, B.L., & Powell, D.A. (1994). Efferent connections of the medial prefrontal cortex in the rabbit. *Experimental Brain Research*, 100: 469-483.

Burette, F., Jay, T. M., & Laroche, S. (1997). Reversal of LTP in the hippocampal afferent fiber system to the prefrontal cortex in vivo with low-frequency patterns of stimulation that do not produce LTD. *Journal of Neurophysiology,* 78: 1155-1160.

Burgess, N., & Hitch, G. (2005). Computational models of working memory: putting long-term memory into context. *Trends In Cognitive Sciences*, 9(11): 535-541.

Burke, J. F., Zaghloul, K. A., Jacobs, J., Williams, R. B., Sperling, M. R., Sharan, A. D., & Kahana, M. J. (2013). Synchronous and Asynchronous Theta and Gamma Activity during Episodic Memory Formation. *Journal Of Neuroscience*, 33(1): 292-304.

Buzsáki, G. (2002). Theta oscillations in the hippocampus. *Neuron*, 33(3), 325–340.

Buzsáki, G. (2006). *Rhythms of the Brain*. Oxford University Press. Oxford, England.

Buzsáki, G., & Wang, X. (2012). Mechanisms of Gamma Oscillations. *Annual Review of Neuroscience*, 35: 203-225.

Buzsáki, G., Anastassiou, C. A., & Koch, C. (2012). The origin of extracellular fields and currents — EEG, ECoG, LFP and spikes. *Nature Reviews Neuroscience*, 13(6): 407-420.

Buzsáki, G., Logothetis, N., & Singer, W. (2013). Scaling Brain Size, Keeping Timing: Evolutionary Preservation of Brain Rhythms. *Neuron*, 80(3): 751-764.

Buzsáki, G.,& Draguhn, A. (2004). Neuronal Oscillations in Cortical Networks. *Science*, 304(5679): 1926-1929.

Campbell, K.B., Lowick, B. M. (1987). Ethanol and event-related potentials: the influence of distractor stimuli. *Alcohol*, 4(4): 257-263.

Canolty, R., Edwards, E., Dalal, S., & Soltani, M. (2006). High gamma power is phase-locked to theta oscillations in human neocortex. *Science,* 313(5793): 1626–1628.

Cenquizca, L. A., & Swanson, L. W. (2007). Spatial organization of direct hippocampal field CA1 axonal projections to the rest of the cerebral cortex. *Brain Research Reviews*, 56(1): 1-26.

Chrobak, J.J. & Buzsáki, G. (1998). Operational dynamics in the hippocampal-entorhinal axis. *Neuroscience and Biobehavioral Reviews*, 22(2): 303-310.

Chudasama, Y., & Muir, J. (1997). A behavioural analysis of the delayed non-matching to position task: the effects of scopolamine, lesions of the fornix and of the prelimbic region on mediating behaviours. *Psychopharmacology,* 134 (1): 73-82.

Cole, B., Klewer, M., Jones, G., & Stephens, D. (1993). Contrasting effects of the competitive NMDA antagonist CPP and the non-competitive NMDA antagonist MK 801 on performance of an operant delayed matching to position task. *Psychopharmacology,* 111(4): 465-71.

Colgin, L. L. (2013). Mechanisms and Functions of Theta Rhythms. *Annual Review Of Neuroscience*, 36(1): 295-312.

Cortese, B., Krahl, S., Berman, R., & Hannigan, J. (1997). Effects of prenatal ethanol exposure on hippocampal theta activity in the rat. *Alcohol*, 14(3): 231-235.

Cowan, N. (2001). The magical number 4 in short-term memory: A reconsideration of mental storage capacity. *Behavioral And Brain Sciences*, 1: 87-114.

Cowan, N. (2005). Working-memory capacity limits in a theoretical context. In C. Izawa & N. Ohta (Eds.), *Human learning and memory: Advances In theory and applications* (pp. 155-175). The 4th Tsukuba international conference on memory. Erlbaum.

Criswell H.E., Breese G.R. (2005). A conceptualization of integrated actions of ethanol contributing to its GABAmimetic profile: a commentary. *Neuropsychopharmacology*, 2005, 30: 1407–1405.

Csicsvari, J., Jamieson, B., Wise, K., & Buzsáki, G. (2003). Mechanisms of gamma oscillations in the hippocampus of the behaving rat. *Neuron,* 37(2): 311-322.

Deadwyler, S. A., Bunn, T., & Hampson, R. E. (1996). Hippocampal ensemble activity during spatial delayed-nonmatch-to-sample performance in rats. *The Official Journal Of The Society For Neuroscience*, 16(1): 354-72.

Dougherty, K.D., Turchin, P.I., Walsh, T.J. (1998). Septocingulate and septohippocampal cholinergic pathways: involvmenet in working/episodic memory. *Brain Research*, 810: 59-71.

Dudchenko, P. A. (2004). An overview of the tasks used to test working memory in rodents. *Neuroscience & Biobehavioral Reviews*, 28(7): 699-709.

Dudchenko, P., Talpos, J., & Young, J. (2013). Animal models of working memory: a review of tasks that might be used in screening drug treatments for the memory impairments found in schizophrenia. *Neuroscience & Biobehavioral Reviews,* 37(9 Pt B): 2111-24.

Duka, T., Weissenborn, ., Dienes, Z. (2001). State-dependent effects of alcohol on recollective experience, familiarity, and awareness of memories. *Psychopharmacology*, 153: 295-306.

Dunnett, S.B. (1985). Comparative effects of cholinergic drugs and lesions of nucleus basalis or fimbria-fornix on delayed matching in rats. *Psychopharmacology*, 87: 357-363.

Dunnett, S.B., Evenden, J.L, Iversen, S.D. (1988). Delay-dependent short-term memory deficits in aged rats. *Psychopharmacology*, (Berl.) 96: 174-180.

Dunnett, S.B., Wareham, A.T., & Torres, E.M. (1990). Cholinergic blockade in prefrontal cortex and hippocampus disrupts short-term memory in rats. *Neuroreport*, 1(1): 61-64.

Düzel, E., Penny, W. D., & Burgess, N. (2010). Brain oscillations and memory. *Current Opinion In Neurobiology*, 20(2): 143-149.

Echevarria, D., Brewer, A., Burk, J., & Brown, S. (2005). Construct validity of an operant signal detection task for rats. *Behavioral Brain Research*, 157: 283-290.

Ehlers, C.L., Wall, T.L., Schuckit, M.A. (1989). EEG spectral characteristics following ethanol administration in young men. *Electroencephalography and Clinical Neurophysiology*, 73(3): 179-187.

Ehlers, C.L., Wills, D.N., Havstad, J. (2012) Ethanol reduces the phase locking of neural activity in human and rodent brain. *Brain Research*, 1450: 67-79.

Eichenbaum, H., & Cohen, N.J. (2001). From conditioning to conscious recollection: *Memory systems of the brain*. Oxford University Press.

Ennaceur, A., & Aggleton, J. (1998). Analysis of the automated delayed nonmatching-to-position task: *Neuroscience Research Communications,* 22: 21-29.

Ericson, M., Sama, M.A., Yeh, H.H. (2009). Acute Ethanol Exposure Elevates Muscarinic Tone in the Septohippocampal System. *Journal of Neurophysiology*, 103: 290-296.

Fanselow, M., & Dong, H. (2010). Are the dorsal and ventral hippocampus functionally distinct structures. *Neuron*, 65(1): 7‑19.

Floresco, S.B., Seamans, J.K., Phillips, A.G. (1997). Selective Roles for Hippocampal, Prefrontal Cortical, and Ventral Striatal Circuits in Radial-Arm Maze Tasks With or Without a Delay. *The Journal of Neuroscience*, 17(5):1880-1890.

Fries, P., Nikolić, D., & Singer, W. (2007). The gamma cycle. *Trends in Neurosciences,* 30 (7): 309-316.

Fuentemilla, L., Penny, W. D., Cashdollar, N., Bunzeck, N., & Düzel, E. (2010). Theta-Coupled Periodic Replay in Working Memory. *Current Biology*, 20(7): 606-612.

Fujii, S., Yamazaki, Y., Sugihara, T., Wakabayashi, I. (2008). Acute and chronic ethanol exposure differentially affect induction of hippocampal LTP. *Brain Research*, 1211: 13-21.

Gandal, M.J., Edgar, J.C., Klook, K., Siegel, S.J. (2011). Gamma synchrony: Towards a translational biomarker for the treatment-resistant symptoms of schizophrenia. *Neuropharmacology*, 62: 1504-1518.

Gaykema, R.P.A., Luiten, P.G.M., Nyakas, C. & Traber, J. (1990). Cortical Projection Patterns of the Medial Septum-Diagonal Band Complex. *Journal of Comparative Neurology*, 293: 103-124.

Gemperle, A. Y., McAllister, K. H., & Olpe, H. (2003). Differential effects of iloperidone, clozapine, and haloperidol on working memory of rats in the delayed non-matching-to-position paradigm. *Psychopharmacology*, 169(3-4): 354-64.

Givens, B. (1995). Low doses of ethanol impair spatial working memory and reduce hippocampal theta activity. *Alcoholism: Clinical and Experimental Research*, 19(3): 763-767.

Givens, B. (1996). Stimulus-evoked resetting of the dentate theta rhythm: relation to working memory. *Neuroreport*, 8(1): 159-163.

Givens, B., & McMahon, K. (1997). Effects of ethanol on nonspatial working memory and attention in rats. *Behavioral Neuroscience*, 111(2): 275-82.

Givens, B., Williams, J., & Gill, T. (2000). Septohippocampal pathway as a site for the memory-impairing effects of ethanol. *Hippocampus*, 10: 111-121.

Givens, B., Williams, J., and Gill, T. M. (1998). Cognitive correlates of single neuron activity in task-performing animals: Applications to ethanol research. *Alcoholism: Clinical and Experimental Research*, 22: 23-31.

Goldman-Rakic, P. (1994). Working Memory Dysfunction in Schizophrenia. *Journal of Neuropsychiatry*, 6 (4): 348-357.

Gordon J.A. (2011) Oscillations and hippocampal-prefrontal synchrony. *Current Opinions in Neurobiology*, 21:486–491.

Goto, Y., & Grace, A. A. (2008). Dopamine Modulation of Hippocampal-Prefrontal Cortical Interaction Drives Memory-Guided Behavior. *Cerebral Cortex*, 18(6): 1407-1414.

Grastyan, E., Lissak K., Madarasz, I., & Donhoffer, H. (1959) . Hippocampal electrical activity during the development of conditioned reflexes. *Electroencephalogr Clin Neurophysiol*., 11(3): 409-430.

Hampson, R. E., Jarrard, L. E., & Deadwyler, S. A. (1999). Effects of Ibotenate Hippocampal and Extrahippocampal Destruction on Delayed-Match and -Nonmatch-to-Sample Behavior in Rats. *The Journal Of Neuroscience*, 19(4): 1495-1507.

Han, C., Pierre-Louis, J., Scheff, A., & Robinson, J. (2000). A performance-dependent adjustment of the retention interval in a delayed non-matching-to-position paradigm differentiates effects of amnestic drugs in rats. *European Journal Of Pharmacology*, 403(1-2): 87-93.

Hanslmayr, S., & Staudigl, T. (2014). How brain oscillations form memories — A processing based perspective on oscillatory subsequent memory effects. *Neuroimage*, 85: 648-655.

Hasselmo, M. E., & Stern, C. E. (2014). Theta rhythm and the encoding and retrieval of space and time. *Neuroimage*, 85: 656-66.

Hasselmo, M. E., Bodelón, C., & Wyble, B. (2002). A proposed function for hippocampal theta rhythm: separate phases of encoding and retrieval enhance reversal of prior learning. *Neural Computation*, 14: 793-817.

Hasselmo, M.E. & Eichenbaum, H. (2005). Hippocampal mechanisms for the context-dependent retrieval of episodes. *Neural Networks*, 18: 1172-1190.

Hasselmo M.E., Wyble B.P., Wallenstein G.V. (1996) Encoding and retrieval of episodic memories: role of cholinergic and GABAergic modulation in the hippocampus. *Hippocampus*, 6: 693–708.

Herremans, A.H.J., Hijzen, T.H., Welborn, P.F.E, Olivier B., & Slangen J.L. (1996). Effects of infusion of cholinergic drugs into the prefrontal cortex area on delayed matching to position performance in the rat. *Brain Research*, 711:102-111.

Heyser, C., Hampson, R. E., & Deadwyler, S. A. (1993). Effects of delta-9-tetrahydrocannabinol on delayed match to sample performance in rats: alterations in short-term memory associated with changes in task specific firing of hippocampal cells. *Journal Of Pharmacology and Experimental Therapeutics*, 264(1): 294-307.

Honig, W.K. (1978). Studies of working memory in the pigeon. Ins. H. Hulse, H. Fowler, and W.K Honig, eds., *Cognitive processes in animal behavior*. Hillsdale, NJ: Erlbaum.

Hoover, W., & Vertes, R. (2007). Anatomical analysis of afferent projections to the medial prefrontal cortex in the rat. *Brain Structure And Function* 212(2): 149-79.

Hyman, J. M., Zilli, E. A., Paley, A. M., & Hasselmo, M. E. (2010). Working memory performance correlates with prefrontal-hippocampal theta interactions but not with prefrontal neuron firing rates. *Frontiers In Integrative Neuroscience*, 4: 1-13.

Jacobson, T. K., Howe, M. D., Schmidt, B., Hinman, J. R., Escabi, M. A., & Markus, E. J. (2013). Hippocampal theta, gamma, and theta-gamma coupling: effects of aging, environmental change, and cholinergic activation. *Journal Of Neurophysiology*, 109(7): 1852-1865.

Jay, T. M., Burette, F., & Laroche, S. (1996). Plasticity of the hippocampal-prefrontal cortex synapses. *Journal Of Physiology-Paris*, 90(5-6): 361-6.

Jay, T. M., Burette, F., & Laroche, S. (2006). NMDA Receptor-Dependent Long-term Potentiation in the Hippocampal Afferent Fibre System to the Prefrontal Cortex in the Rat. *European Journal Of Neuroscience*, 7: 247-250.

Jay, T., & Witter, M. (1991). Distribution of hippocampal CA1 and subicular efferents in the prefrontal cortex of the rat studied by means of anterograde transport of Phaseolus vulgaris-. *Journal Of Comparative Neurology,* 313(4):574-86.

Jay, T., Burette, F., & Laroche, S. (1995). NMDA Receptor-dependent Long-term Potentiation in the Hippocampal Afferent Fibre System to the Prefrontal Cortex in the Rat. *European Journal of Neuroscience*, 7(2): 247–250.

Jay, T., Theirry, A., Wiklund, L., & Glowinski, J. (1992) Excitatory Amino Acid Pathway from the Hippocampus to the Prefrontal Cortex. Contribution of AMPA receptors in hippocampo-prefrontal cortex transmission. *European Journal of Neuroscience*, 4(12): 1285-1295.

Jensen, O. (2006). Maintenance of multiple working memory items by temporal segmentation. *Neuroscience*, 139(1): 237-49.

Jensen, O. Lisman, J.E. (2005). Hippocampal sequence encoding by a multi-item working memory buffer. *Trends in Neuroscience*, 28:67-72.

Jensen, O., & Colgin, L. L. (2007). Cross-frequency coupling between neuronal oscillations. *Trends In Cognitive Sciences*, 11(7): 267-269.

Jones, M. W. (2002). A comparative review of rodent prefrontal cortex and working memory. *Current Molecular Medicine*, 2(7): 639-47.

Jones, M. W., & Wilson, M. A. (2005). Theta rhythms coordinate hippocampal–prefrontal interactions in a spatial memory task. *PLoS Biology*, 3 (12): e402.

Jung, M.W., Qin, Y., McNaughton, B. L., & Barnes, C.A. (1998). Firing characteristics of deep layer neurons in prefrontal cortex in rats performing spatial working memory tasks. *Cerebral cortex*, 8: 437-450.

Kahana, M.J. (2006). The cognitive correlates of human brain oscillations. *Journal of Neuroscience*, 26: 1669-1672.

Kahana, M.J., Sekuler, R., Caplan, J.B., Kirschen, M., & Madsen, J.R. (1999). Human theta oscillations exhibit task dependence during virtual maze navigation. *Nature*, 399(6738): 781-784.

Kajikawa, Y., & Schroeder, C. (2011). How Local Is the Local Field Potential. *Neuron*, 72(5): 847-858.

Kesner, R. P., & Churchwell, J. C. (2011). An analysis of rat prefrontal cortex in mediating executive function. *Neurobiology Of Learning And Memory*, 96(3): 417-31.

Klinkenberg, I., Blokl, A., & Blokland, A. (2011). A comparison of scopolamine and biperiden as a rodent model for cholinergic cognitive impairment. *Psychopharmacology*, 215(3): 549-66.

Komisaruk, B.R. (1970). Synchrony between limbic system theta activity and rhythmical behavior in rats. *Journal of comparative and Physiological Psychology*, 70: 482-492.

Kovacevic, S., Azma, S., Irimia, A., Sherfey, J., Halgren, E., Marinkovic, K. (2012). Theta Oscillations are sensitive to both early and late conflict processing stages: effects of alcohol intoxication. *PLOS One,* 7(8):e4397-e43957.

Kunec, S., Hasselmo, M.E., & Kopell, N. (2005). Encoding and retrieval in the CA3 region of the hippocampus: a model of theta-phase separation. *Journal of Neurophysiology*, 94(1): 70-82.

Laroche, S., Davis, S., & Jay, T. M. (2000). Plasticity at hippocampal to prefrontal cortex synapses: dual roles in working memory and consolidation. *Hippocampus*, 10(4):438-46.

Lee, H., Simpson, G., Logothetis, N., & Rainer, G. (2005). Phase locking of single neuron activity to theta oscillations during working memory in monkey extrastriate visual cortex. *Neuron*, 45(1):147-56.

Lewis, D.A. (2012). Cortical circuit dysfunction and cognitive deficits in schizophrenia—implications for preemptive interventions. *European Journal of Neuroscience*, 35: 1871-1878.

Lisman, J., & Buzsáki, G. (2008). A neural coding scheme formed by the combined function of gamma and theta oscillations. *Schizophrenia Bulletin*, 34(5): 974–980.

Lisman, J., & Idiart, M. (1995). Storage of 7+/-2 short-term memories in oscillatory subcycles. *Science*, 267: 1512-1515.

Lisman, J., & Jensen, O. (2013). The Theta-Gamma Neural Code. *Neuron*, 77(6): 1002-1016.

Lopes da Silva, F.H., Kamp, A. (1969). Hippocampal theta frequency shifts and operant behavior. *Electroencephalogr Clin Neurophysiol*., 26(2): 133-143.

Lubenov, E. V., & Siapas, A. G. (2009). Hippocampal theta oscillations are travelling waves. *Nature*, 459: 534-539.

Ma, W.J., Husain, M., & Bays, P.M. (2014). Changing concepts of working memory. *Nature Neuroscience*, 17: 347-356.

Manns, J.R., Zilli, E.A., Ong, K.C., Hasselmo, M.E., & Eichenbaum, H. (2007). Hippocampal CA1 spiking during encoding and retrieval: relation to theta phase. *Neurobiology of Learning and Memory*, 87: 9-20.

Mao, J., & Robinson, J. (1998). Microinjection of GABA-A agonist muscimol into the dorsal but not the ventral hippocampus impairs non-mnemonic measures of delayed non-matching-to-position performance in rats. *Brain Research*, 784, 139-147.

Masouka, T., Fujii, Y., Kamei, C. (2006). Participation of the hippocampal theta rhythm in memory formation for an eight-arm radial maze task in rats. *Brain Research*,1103(1): 159-163.

Matthews, D. B., & Silvers, J. R. (2004). The use of acute ethanol administration as a tool to investigate multiple memory systems. *Neurobiology Of Learning And Memory*, 82(3): 299-308.

Maviel T, Durkin TP, Menzaghi F, Bontempi B (2004) Sites of neocortical reorganization critical for remote spatial memory. *Science*, 305:96–99.

McCool, B.A. (2011). Ethanol Modulation of Synaptic Plasticity. *Neuropharmacology*, 61(7): 1097-1108.

McCartney, H., Johnson, A., Weil, Z., & Givens, B. (2004). Theta rest produces optimal conditions for long-term potentiation. *Hippocampus*, 14: 684-687.

McKenna, J.T., Vertes, R.P. (2004) Afferent projections to nucleus reuniens of the thalamus. *J. Comp. Neurol*. 480: 115-142.

McNaughton, N., Kocis, B., Hajós, M. (2007). Elicited hippocampal theta rhythm: a screen for anxiolytic and precognitive drugs through changes in hippocampal function? *Behavioral Pharmacology*, 18 (5-6): 329-346.

Melia, K.R., Ryabinin, A.E., Corodimas, K.P, Wlson, M.C., and Ledoux, J.E.(1996). Hippocampal-dependent learning and experience-dependent activation of the hippocampus are preferentially disrupted by ethanol. *Neuroscience*, 74(2): 313-322.

Miller, G.A., Galanter, E., Pribram, K.H. (1960). *Plans and the structure of Behavior*. New York: Holt, Rinehart, & Winston.

Miller, G.A. (1956). The magical number seven, plus or minus two: Some limits on our capacity for processing information. *Psychological Review*, 63: 81-97.

Mizuhara, H., & Yamaguchi, Y. (2007). Human cortical circuits for central executive function emerge by theta phase synchronization. *Neuroimage*, 36(1): 232-44.

Moser, M., & Moser, E. (1998). Functional differentiation in the hippocampus. *Hippocampus*, 8 (6): 608–619.

Nutt, D.J., King, L.A., & Phillips, L.D. (2010). Drug harms in the UK: a multicriteria decision analysis. *Lancet*, 376(9752): 1558-1565.

Nyhus, E., Curran, T. (2010). Functional role of gamma and theta oscillations in episodic memory. *Neuroscience and Biobehavior Review*, 34: 1023-1035.

O'Neill, P., Gordon, J. A., & Sigurdsson, T. (2013). Theta Oscillations in the Medial Prefrontal Cortex Are Modulated by Spatial Working Memory and Synchronize with the Hippocampus through Its Ventral Subregion. *Journal Of Neuroscience*, 33(35): 14211-14224.

Onslow, A. C., Bogacz, R., & Jones, M. W. (2011). Quantifying phase–amplitude coupling in neuronal network oscillations. *Progress In Biophysics And Molecular Biology*, 105(1-2): 49-57.

Osipova, D., Takashima, A., & Oostenveld, R. (2006). Theta and gamma oscillations predict encoding and retrieval of declarative memory. *The Journal Of Neuroscience*. 26(28): 7523-7531.

Pache, D., Sewell, R., & Spencer, P. (1999). Detecting drug effects on short-term memory function using a combined delayed matching and non-matching to position task. *Journal of Pharmacological and Toxicological Methods*, 41: 135-141.

Parent, M. A., Wang, L., Su, J., Netoff, T., & Yuan, L. (2010). Identification of the Hippocampal Input to Medial Prefrontal Cortex In Vitro. *Cerebral Cortex*, 20(2): 393-403.

Park, J. Y., Jhung, K., Lee, J., & An, S. K. (2013). Theta–gamma coupling during a working memory task as compared to a simple vigilance task. *Neuroscience Letter*s, 532: 39-43.

Paxinos, G., and Watson, C. (2007). The rat brain in stereotaxic coordinates / George Paxinos, Charles Watson, Elsevier, Amsterdam: 2007.

Paz, R., Bauer, E. P., & Pare, D. (2008). Theta synchronizes the activity of medial prefrontal neurons during learning. *Learning & Memory*, 15(7): 524-531.

Petit, L., Courtney, S.M., Ungerleider, L.G., Haxby, J.V. (1998) Sustained activity in the medial wall during working memory delays. *Journal of Neuroscience*, 18(22): 9429-9437.

Poch, C., Campo, P. (2012). Neocortical-hippocampal dynamics of working memory in healthy and diseased brain states based on functional connectivity. *Frontiers in Human Neuroscience*, 6: 1-14.

Pontecorvo, M., Sahgal, A., & Steckler, T. (1996). Further developments in the measurement of working memory in rodents. *Cognitive Brain Res*earch, 3(3-4):205‑213.

Porjesz, B., Rangaswamy, M., Kamarajan, C., Jones, K. A., Padmanabhapillai, A., & Begleiter, H. (2005). The utility of neurophysiological markers in the study of alcoholism. *Clinical Neurophysiology*, 116(5): 993-1018.

Porter, M., Burk, J., & Mair, R. (2000). A comparison of the effects of hippocampal or prefrontal cortical lesions on three versions of delayed non-matching-to-sample based on positional or spatial cues. *Behavioural Brain Research*, 109(1): 69‑81.

Preston, A., & Eichenbaum, H. (2013). Interplay of Hippocampus and Prefrontal Cortex in Memory. *Current Biology*, 23(17): R764‑R773.

Raghavachari, S., Kahana, M. J., & Rizzuto, D. (2001). Gating of human theta oscillations by a working memory task. *The Journal Of Neuroscience*, 21(9): 3175-3183.

Raghavachari, S., Lisman, J., & Tully, M. (2006). Theta oscillations in human cortex during a working-memory task: evidence for local generators. *Journal of Neurophysiology,* 95(1): 1630-1638.

Rangaswamy, M., & Porjesz, B. (2008). Uncovering genes for cognitive (dys)function and predisposition for alcoholism spectrum disorders: A review of human brain oscillations as effective endophenotypes. *Brain Research*, 1235: 153-171.

Remondes, M., & Wilson, M. A. (2013). Cingulate-Hippocampus Coherence and Trajectory Coding in a Sequential Choice Task. *Neuron*, 80(5): 1277‑1289.

Rich, E.L. & Shapiro, M.L. (2007). Prelimbic/infralimbic inactivation impairs memory for multiple task switches, but not flexible selection of familiar tasks. *The Journal of Neuroscience*, 27(17): 4747-4755.

Rizzuto, D., Madsen, J., & Bromfield, E. (2006). Human neocortical oscillations exhibit theta phase differences between encoding and retrieval. *Neuroimage*, 31(3):1352‑1358.

Rizzuto, D.S., Madsen, J.R., Bromfield, E.B., Schulze-Bonhage, A., Seelig, D., Aschenbrenner-Scheibe, R., & Kahana, M.J. (2003). Reset of human neocortical oscillations during a working memory task. *PNAS Proceedings of the National Academy of Sciences of the United States of America*, 100(13): 7931-7936.

Robinson, J., & Mao, J. (1997). Differential effects on delayed non-matching-to-position in rats of microinjections of muscarinic receptor antagonist scopolamine or NMDA receptor antagonist MK-801. *Brain Research*, 765(1): 51‑60.

Robinson, J., Scheff, A., & Pierre-Louis, J. (2000). Specificity of memory measures in an adjusting delayed nonmatching-to-position task for rats. *Behavioral Brain Research*, 111, 107-113.

Sahgal, A. (1987). Contrasting effects of vasopressin, desglycinamide-vasopressin and amphetamine on a delayed matching to position task in rats. *Psychopharmacology*, 93: 243-249.

Sakimoto, Y., Takeda, K., Okada, K., Hattori, M., & Sakata, S. (2013). Transient decline in rats' hippocampal theta power relates to inhibitory stimulus-reward association. *Behavioural Brain Research*, 246: 132-138.

Santos, L. M., Dzirasa, K., Kubo, R., Silva, M. T., Ribeiro, S., Sameshima, K., et al. (2008). Baseline hippocampal theta oscillation speeds correlate with rate of operant task acquisition. *Behavioural Brain Research*, 190(1): 152-155.

Sarter, M., Bruno, J.P., Givens, B. (2003) Attentional functions of cortical cholinergic inputs: What does it mean for learning and memory? *Neurobiology of Learning and Memory*, 80: 245-256.

Saults, J.S., Cowan, N., Sher, K.J., & Moreno, M.V. (2007). Differential effects of alcohol on working memory: distinguishing multiple processes. *Experimental and Clinical Psychopharmacology*, 15(6): 576-587.

Sauseng, P., & Klimesch, W. (2008). What does phase information of oscillatory brain activity tell us about cognitive processes. *Neuroscience and Biobehavioral Reviews*, 32(5): 1001-13.

Sauseng, P., Griesmayr, B., Freunberger, R., & Klimesch, W. (2010). Control mechanisms in working memory: A possible function of EEG theta oscillations. *Neuroscience & Biobehavioral Reviews*, 34(7): 1015-1022.

Schnitzler, A., & Gross, J. (2005). Normal and pathological oscillatory communication in the brain. *Nature Reviews Neuroscience*, 6:2 85-296.

Schweizer, T.A. and Vogel-Sprott, M. (2008). Alcohol impaired speed and accuracy of cognitive functions: A review of acute tolerance and recovery of cognitive function. *Experimental and Clinical Psychopharmacology*, 16: 240-250.

Seamans, J.K., Floresco, S.B., Phillips, A.G. (1995). Functional differences between the prelimbic and anterior cingulate regions of the rat prefrontal cortex. *Behavioral Neuroscience*, 109(6):063-1073.

Sesack, S.R., Deutch, A.Y., Roth, R.H., & Bunney, B.S. (1989). Topographical organization of the efferent projections of the medial prefrontal cortex in the rat: an anterograde tract-tracing study with Phaseolus vulgaris leucoagglutinin. *Journal of comparative Neurology*, 290(2): 213-242.

Sederberg, P., Kahana, M. J., & Howard, M. (2003). Theta and gamma oscillations during encoding predict subsequent recall. *The Journal Of Neuroscience*, 23: 10809-10814.

Sederberg, P.B., Schulze-Bonhange, A., Madsen J.R., Bromfield, E.B., McCarthy, D.C., Brandt, A., Tully, M.S., and Kahana, M.J. (2007). Hippocampal and neocortical gamma oscillations predict memory formation in humans. *Cerebral Cortex*, 17: 1190-1196.

Shannon, H. E., & Yang, L. (2007). A non-spatial, stimulus-comparison working memory task in rats and disruption by scopolamine. *Neuroscience*, 145(3): 955-962.

Siggins, G.R., Bloom, F.E., French, E.D., Madamba, S.G., Mancillas, J., Pittman, Q.J., and Rogers, J. (1987) Electrophysiology of Ethanol on Central Neurons. *Annals of the New York Acadamy of Sciences*, 492: 350-366.

Shaw, C., & Aggleton, J. (1993). The effects of fornix and medial prefrontal lesions on delayed non-matching-to-sample by rats. *Behavioural Brain Research*, 54 (1): 91‑102.

Shibata, H. (1993). Efferent projections from the anterior thalamic nuclei to the cingulate cortex in the rat. *Journal of Comparative Neurology*, 330: 533-542.

Siapas, A. G., Lubenov, E. V., & Wilson, M. A. (2005). Prefrontal Phase Locking to Hippocampal Theta Oscillations. *Neuron*, 46(1): 141-151.

Sigurdsson, T., Stark, K., Karayiorgou, M., & Gogos, J. (2010). Impaired hippocampal–prefrontal synchrony in a genetic mouse model of schizophrenia. *Nature*, 464:763-767.

Sirota, A., Montgomery, S., Fujisawa, S., Isomura, Y., Zugaro, M., & Buzsáki, G. (2008). Entrainment of Neocortical Neurons and Gamma Oscillations by the Hippocampal Theta Rhythm. *Neuron*, 60(4): 683-697.

Sloan, H., Good, M., & Dunnett, S. (2006). Double dissociation between hippocampal and prefrontal lesions on an operant delayed matching task and a water maze reference memory task. *Behavioral Brain Research*, 171(1): 116-126.

Söderlund, H., Parker, E.S., Schwartz, B.L., & Tulving, E. (2005). Memory encoding and retrieval on the ascending and descending limbs of the blood alcohol concentration curve. *Psychopharmacology*, 182(2): 305-317.

Sohal, V.S, Zhang, F., Yizhar, O., & Deisseroth, K. (2009). Parvalbumin neurons and gamma rhythms enhance cortical circuit performance. *Nature*, 459 (7247): 698-702.

Spinetta, M.J., Woodlee, M.T., Feinberg, L.M., Stroud, C., Schallert, K., Cormack, L.K., & Schallert, T. (2008). Alcohol-induced retrograde memory impairment in rats: prevention by caffeine. *Psychopharmacology*, 201: 361-371.

Squire L.R., Clark R.E., Knowlton B.J. (2001) Retrograde amnesia. *Hippocampus* 11: 50–55.

Steele, C.M.; Josephs, R.A. (1988). Drinking Your Troubles Away II: An Attention-Allocation Model of Alcohol's Effect on Psychological Stress. *Journal of Abnormal Psychology*, 97(2): 196-205.

Steele, C.M.; Josephs, R.A. (1990). Alcohol Myopia: Its Prized and dangerous Effects. *American Psychologist*, 45(8): 921-933.

Steele, R., & Morris, R. (1999). Delay-dependent impairment of a matching-to-place task with chronic and intrahippocampal infusion of the NMDA-antagonist D-AP 5. *Hippocampus*, 9(2):118-36.

Steffensen, S.C., Yeckel, M.F., Miller, D.R., Henriksen, S.J. (1993). Ethanol-induced suppression of hippocampal long-term potentiation by lesion of the septohippocampal nucleus. *Alcohol Clin Exp Res*, 17: 655-699.

Sukhotina, I. A., Dravolina, O. A., Novitskaya, Y., Zvartau, E. E., Danysz, W., & Bespalov, A. Y. (2008). Effects of mGlu1 receptor blockade on working memory, time estimation, and impulsivity in rats. *Psychopharmacology*, 196(2): 211-20.

Thierry, A., Gioanni, Y., Dégénétais, E., & Glowinski, J. (2000). Hippocampo-prefrontal cortex pathway: anatomical and electrophysiological characteristics. *Hippocampus*, 10(4):411-9.

Timofeeva, O.A., Levin, E.D. (2011). Glutamate and Nicotinic Receptor Interactions in Working Memory: Importance for the cognitive impairment of schizophrenia. *Neuroscience*, 195, 21-36.

Tzambazis, K.; Stough, C. (2000). Alcohol impairs speed of information processing and simple and choice reaction time and differentially impairs higher-order cognitive abilities. *Alcohol and Acoholism*, 35(2): 197-201.

Van Hest, A. & Steckler, T. (1996). Effects of procedural parameters on response accuracy: lessons from delayed (non-) matching procedures in animals. *Cognitive Brain Research*, 3-4(3): 193-203.

Vanderwolf, C.H. (1969). "Hippocampal electrical activity and voluntary movement in the rat". *EEG Clin Neurophysiol*, 26 (4): 407–418.

Varela, C., Kumar, S., Yang, J., & Wilson, M. A. (2013). Anatomical substrates for direct interactions between hippocampus, medial prefrontal cortex, and the thalamic nucleus reuniens. *Brain Structure And Function*, 219(3): 911-929.

Vertes, R. (2006). Interactions among the medial prefrontal cortex, hippocampus and midline thalamus in emotional and cognitive processing in the rat. *Neuroscience*, 142(1):1-20.

Vertes, R.P., Hoover, W.B., & Viana Di Prisco, G. (2004). Theta Rhythm of the hippocampus: subcortical control and functional significance. *Behavioral and Cognitive Neuroscience Reviews*, 3(3): 173-200.

Wang, G., & Cai, J. (2006). Disconnection of the hippocampal–prefrontal cortical circuits impairs spatial working memory performance in rats. *Behavioural Brain Research*, 175(2): 329-36.

Weight, F.F., Aguayo, L.G., White, G., Lovinger, D.M., & Peoples, R.W. (1992). GABA- and glutamate-gated ion channels as molecular sites of alcohol and anesthetic action. *Advances in biochemical psychopharmacology*, 47: 335-347.

Wells, C.E., Amos, D.P., Jeewajee, A., Douchamps, V., Rodgers, J., O'Keefe, J., Burgess, N., & Lever, C. (2013). Novelty and Anxiolytic Drugs Dissociate two components of Hippocampal Theta in Behaving Rats. *Journal of Neuroscience*, 33(20): 8650-8667.

Whishaw, I.Q. (1976). The effects of alcohol and atropine on EEG and behavior in the rabbit. *Psychopharmacology*, 48: 83-90.

White, A., Matthews, D. B., & Best, P. (2000). Ethanol, Memory, and Hippocampal Function: A Review of Recent Findings. *Hippocampus*, 10(1): 88-93.

White, A., & Best, P. (2000). Effects of ethanol on hippocampal place-cell and interneuron activity. *Brain Research*, 876: 154-165.

White, T., Jansen, M., & Doege, K. (2012). Theta power during encoding predicts subsequent-memory performance and default mode network deactivation. *Human Brain*, 34(11): 2929-43.

Williams, J. M., & Givens, B. (2003). Stimulation-induced reset of hippocampal theta in the freely performing rat. *Hippocampus*, 13(1): 109-16.

Willmore, C., LaVecchia, K., & Wiley, J. (2001). NMDA antagonists produce site-selective impairment of accuracy in a delayed nonmatch-to-sample task in rats. *Neuropharmacology*, 41(8):916-27.

Wiltgen, B.J., Brown, R.A.M, Talton, L.E., & Silva, A.J. (2004) New Circuits for Old Memories: The Role of the Neocortex in Consolidation, *Neuron*, 44(1): 101-108.

Winters, B.D. & Dunnett, S.B. (2004). Selective lesioning of the cholinergic septo-hippocampal pathway does not disrupt spatial short-term memory: a comparison with the effects of fimbria-fornix lesions. *Behavioral Neuroscience*, 118: 546-562.

Wixted, J.T. (2005). A Theory About Why We Forget What We Once Knew. *Current Directions in Psychological Science*, 14(1): 6-9.

Womelsdorf T., Johnston K., Vinck, M., Everling, S. (2010) Theta-activity in anterior cingulate cortex predicts task rules and their adjustments following errors. *Proceedings of the National Acadamy of Sciences, U.S.A*., 107(11):5248-53.

Yoon, T., Okada, J., Jung, M.W., Kim, J. J. (2008). Prefrontal cortex and hippocampus subserve different components of working memory in rats. *Learning & Memory*, 15: 97-105.

Appendix A: Operant Working Memory Task Code

```
\  OPERANT WORKING MEMORY TASK
\   VARIABLE DELAYED NON-MATCH TO POSITION TASK
\  FOR MED-PC SOFTWARE AND HARDWARE
\=============================================================
\ WRITTEN BY K.E.S.
\ PROGRAM DESCRIPTION: VARIABLE DELAYED NON-MATCH TO POSITION
\ SAMPLE PHASE:  ONE LIGHT RANDOMLY ILLUMINATES ON RIGHT OR
\ LEFT SIDE. IF RAT PRESSES LEVER UNDER LIGHT THEN IT GETS A WATER
\ REWARD FOR .02 SECONDS. IF RAT PRESSES OTHER LEVER, OR OMITS
\ THEN TRIAL IS REPEATED WITH A NEW RANDOM SAMPLE.

\ DELAY PHASE:  RANDOMLY 5, 10, or 15 SECONDS

\ TEST PHASE:   BOTH SIGNAL LIGHTS ILLUMINATE.  THE FIRST RESPONSE
IS COUNTED CORRECT OR INCORRECT. THE RAT MUST PRESS THE
\ LEVER NOT CORRESPONDING TO THE LIGHT DURING THE SAMPLE
\  PHASE.  CORRECT RESPONSES ARE REWARDED WITH A .05" WATER
\  REWARD. RESPONSE WINDOW LASTS FOR 3 SECONDS ELSE OMISSION.
\ HOUSELIGHT ACTS AS SECONDARY CUE TO LET THE ANIMAL KNOW
\ WHEN "IN" TRIAL AND WHEN "OUT" OF TRIAL.  INCORRECT TEST PHASE
\ RESPONSE OR OMISSION  TURNS OFF HOUSELIGHT.  CORRECT RESPONSES
\ LEAVE HOUSELIGHT ON FOR 3 SECONDS TO ALLOW TIME TO CONSUME \
\ REWARD.
\ INTERTRIAL INTERVAL: 10 SECONDS
\ PROGRAM LASTS FOR 60 MINUTES OR 100 TRIALS

\ UPDATED BY KSE ON 3/5/12
\  * 15 SECOND DELAY OPTION COMMENTED OUT
\  * DELAY CHANGED FROM RANDD TO RANDI
\ UPDATED BY KSE ON 5/14/12
\  * REVERTED TO 15 SECOND DELAY INSTEAD OF 20 SECONDS
\  * ADDED OMISSION TRACKING
\  * ARRAY DIMS CHANGED FROM 299 TO 200
\  * ADDED MORE TRACKING BY TRIAL TYPE
\  * CHANGED REWARD TIMES FROM .3 TO.1 (SAMPLE)
```

```
\  AND .6 TO .5 SECONDS (CHOICE)
\ UPDATED BY KSE ON 5/27/12
\  * DELAY CHANGED BACK TO RANDD
\  * SESSION TIMER 45 MINUTES OR 100 TRIALS
\  * OMISSIONS NO LONGER COUNT AGAINST ACCURACY
\ UPDATED BY KSE ON 11/1/12
\  * DELAYS CHANGED TO 4, 8, 12 SECONDS
\  * HOUSELIGHT AS ATTENTIONAL CUE 1 SECOND BEFORE LIGHT ONSET,
\  3 SECONDS AFTER RESPONSE.
\ UPDATED BY KES ON 8/8/13
\   CHANGED SAMPLE PHASE RESPONSE WINDOW FROM 3 TO 4 SECONDS
\   CHANGED SESSION LENGTH FORM 120 TOTAL TO 100 VALID TRIALS
\   REDUCED ARRAY DIMENSIONS TO 101
\   SAMPLE OMIT OR MISS NOW LEADS TO SHORTED (5 SECONDS) ITI WITH
NEW RANDOM SAMPLE SIGNAL. ONLY VALID TRIALS ADD TO TRIAL
COUNT. UPDATED DISPLAY TO SHOW SAMPLE MISSES INSTEAD OF
NUMBER OF CORRECTIONS.
\MODIFIED FOR RECORDING ROOM CONFIGURATION

\====================
\Outputs s room
   ^LEFTLEVER    =1
   ^RIGHTLEVER  =2
   ^LEFTLIGHT    =3
   ^RIGHTLIGHT  =4
   ^TONE     =5
   ^DUMMY   =6
   ^WATER    =7
   ^HOUSELIGHT  =8
\Inputs
  ^LBAR   =1
  ^RBAR   =2
\=====================
\Defined Variables
\A= Calculations for accuracy
\  A(1)= PERCENT CORRECT OVERALL
\  A(2)= PERCENT CORRECT on SHORT  DELAY
\  A(3)= PERCENT CORRECT on MEDIUM  DELAY
\  A(4)= PERCENT CORRECT on LONG   DELAY
\  A(5)= PERCENT CORRECT on LONGEST DELAY
\  A(6)= NUMBER OF VALID TRIALS WITH CHOICE RESPONSE
\C= Counters
\  C(1)= CORRECT LEVER PRESS DURING SAMPLE PHASE [UNDER LIGHT]
\  C(2)= INCORRECT LEVER PRESS DURING SAMPLE PHASE
\  C(3)= DARK ITI PRESSES
```

\ C(4)= HOUSELIGHT ON ITI PRESSES
\ C(5)= ITI PRESS TOTAL
\ C(6)= OMISSIONS DURING SAMPLE PHASE
\ C(7)= OVERALL INCORRECT RESPONSES DURING TEST PHASE
\ C(8)= OVERALL CORRECT RESPONSES DURING TEST PHASE
\ C(9)= NUMBER OF CORRECTION TRIALS
\ C(10)= INCORRECT RESPONSES/ SAMPLE PHASE CORRECTION TRIALS
\ C(11)= CORRECT RESPONSES / TEST PHASE / CORRECTION TRIALS
\ C(12)= INCORRECT RESPONSES / TEST PHASE / CORRECTION TRIALS
\ C(13)= CORRECT RESPONSES / TEST PHASE / SHORT DELAY
\ C(14)= INCORRECT RESPONSES / TEST PHASE / SHORT DELAY
\ C(15)= CORRECT RESPONSES / TEST PHASE / MEDIUM DELAY
\ C(16)= INCORRECT RESPONSES / TEST PHASE / MEDIUM DELAY
\ C(17)= CORRECT RESPONSES / TEST PHASE / LONG DELAY
\ C(18)= INCORRECT RESPONSES / TEST PHASE / LONG DELAY
\ C(19)= CORRECT RESPONSES / TEST PHASE / LONGEST DELAY
\ C(20)= INCORRECT RESPONSES / TEST PHASE / LONGEST DELAY
\ C(21)= SAMPLE PHASE REACTION TIME TOTAL
\ C(22)= TEST PHASE REACTION TIME TOTAL
\ C(23)= CORRECT DELAY RESPONSES
\ C(24)= INCORRECT DELAY RESPONSES
\ C(25)= DELAY RESPONSE TOTAL
\ C(26)= OMISSIONS FOR SHORT DELAY TRIALS
\ C(27)= OMISSIONS FOR MEDIUM DELAY TRIALS
\ C(28)= OMISSIONS FOR LONG DELAY TRIALS
\ C(29)= OMISSIONS FOR LONGEST DELAY TRIALS
\ C(30)= MISS FROM LEFT SAMPLE
\ C(31)= MISS FROM RIGHT SAMPLE
\E= CUMULATIVE TRIALS
\F= SAMPLE LIGHT SELECTION
\G= DELAY PERIOD TRIAL COUNTERS
\M= MINUTES
\O= STORAGE OF SAMPLE LIGHT
\P= STORAGE OF RESPONSE TYPES
\Q= STORAGE OF MINUTES
\S= SAMPLE PHASE REACTION TIMES
\T= CHOICE PHASE REACTION TIMES

\Z= Z Pulses
\ Z(1)= DUMMY FOR INCORRECT RESPONSES [PHYSIOLOGY PROGRAM MARKER]
\ Z(2)= .02" WATER REWARD
\ Z(3)= .04" WATER REWARD
\ Z(5)= START SAMPLE REACTION TIME
\ Z(6)= STOP SAMPLE REACTION TIME

```
\  Z(7)= START TEST REACTION TIME
\  Z(8)= STOP  TEST REACTION TIME
LIST F= 1, 2   \SELECT SAMPLE SIDE: [1=LEFT, 2=RIGHT]
LIST B= 5",5",5",10",10",10",15",15",15"  \DELAY PERIODS
DIM A=10   \CALCULATIONS, SHOW
DIM C=35   \COUNTERS
DIM D=101  \DELAY STORAGE ARRAY
DIM G=6    \NUMBER OF TRIALS OF EACH DELAY TYPE
DIM O=101  \RIGHT OR LEFT SAMPLE STORAGE ARRAY
DIM P=101  \RESPONSE TYPE [1=HIT, 2=MISS, 3=OMIT]
DIM Q=101  \MINUTE STORAGE ARRAY
DIM S=101  \SAMPLE PHASE REACTION TIME ARRAY
DIM T=101  \TEST PHASE REACTION TIME ARRAY
\Unused Variables
\  H, I, J, K, L, N, R, U, V, W, X, Y
\============================================================
S.S.1,
  S1,    \START PROGRAM
  #START: ON^LEFTLEVER; ON^RIGHTLEVER --->S2
  S2,    \START 10 SECOND ITI PERIOD
  #R^LBAR: ADD C(3); ADD C(5) --->SX   \ADD DARK ITI PRESSES
  #R^RBAR: ADD C(3); ADD C(5) --->SX   \ADD DARK ITI PRESSES
  9":ON^HOUSELIGHT--->S3
  S3,    \HOUSELIGHT CUE PORTION OF ITI PERIOD
  1":Set H=0 --->S4
  #R^LBAR: ADD C(4); ADD C(5) --->SX   \ADD HOUSELIGHT ITI PRESSES
  #R^RBAR: ADD C(4); ADD C(5) --->SX   \ADD HOUSELIGHT ITI PRESSES
  S4,    \SESSION TIMER 100 TRIALS OR 60 MINUTES
  0.01": ADD E; SET Q(E)=M; IF E>=101 [@STOPTRIAL, @GO]
    @STOPTRIAL:--->STOPABORTFLUSH
    @GO: IF M>=60 [@STOPTIME, @GO]
    @STOPTIME: --->STOPABORTFLUSH
    @GO:--->S5
  S5,    \CHOOSE SAMPLE LIGHT AND DELAY PERIOD
  0.01":  RANDI O(E)=F; RANDD D(E)=B; IF O(E)=1 [@LEFT, @RIGHT]
    @LEFT: ON^LEFTLIGHT; Z5  --->S6
    @RIGHT: ON^RIGHTLIGHT; Z5 --->S10
  S6,    \SAMPLE PHASE, LEFT LIGHT ILLUMINATED
  #R^LBAR: OFF^LEFTLIGHT; Z2; Z6; ADD C(1) --->S14
  #R^RBAR: OFF^LEFTLIGHT; Z6; OFF^HOUSELIGHT; ADD C(2)--->S7
  4": OFF^LEFTLIGHT; OFF^HOUSELIGHT;Z6; ADD C(6)--->S7
  S7,  \REDO NEW RANDOM SAMPLE WITH SHORTENED ITI, SAME TRIAL
  4":ON^HOUSELIGHT--->S8
  #R^LBAR: ADD C(3); ADD C(5) --->SX   \ADD DARK ITI PRESSES
  #R^RBAR: ADD C(3); ADD C(5) --->SX   \ADD DARK ITI PRESSES
```

```
 S8,
 1":Set H=0 --->S5
 #R^LBAR: ADD C(4); ADD C(5) --->SX   \ADD HOUSELIGHT ITI PRESSES
 #R^RBAR: ADD C(4); ADD C(5) --->SX   \ADD HOUSELIGHT ITI PRESSES
 S10,  \SAMPLE PHASE, RIGHT LIGHT ILLUMINATED
 #R^LBAR: OFF^RIGHTLIGHT; Z6; OFF^HOUSELIGHT; ADD C(2)--->S7
 #R^RBAR: OFF^RIGHTLIGHT; Z2; Z6; ADD C(1) --->S15
 4": OFF^RIGHTLIGHT; OFF^HOUSELIGHT;Z6; ADD C(6)--->S7
\=============================================================
 S14,   \LEFT SAMPLE TRIALS
 .01": IF D(E)=5" [@SHORT, @OTHER]
  @SHORT:ADD G(1)   --->S16
  @OTHER: IF D(E)=10" [@MEDIUM, @OTHERMORE]
  @MEDIUM:ADD G(2)   --->S18
  @OTHERMORE:IF D(E)=15" [@LONG, @LONGEST]
  @LONG: ADD G(3)   --->S20
  @LONGEST: ADD G(4)   --->S22
 S15,   \RIGHT SAMPLE TRIALS
 .01": IF D(E)=5" [@SHORT, @OTHER]
  @SHORT:ADD G(1)   --->S24
  @OTHER: IF D(E)=10" [@MEDIUM, @OTHERMORE]
  @MEDIUM: ADD G(2)  --->S26
  @OTHERMORE:IF D(E)=15" [@LONG, @LONGEST]
  @LONG:ADD G(3)   --->S28
  @LONGEST:ADD G(4)   --->S30
\=============================================================
 S16,   \TEST PHASE, LEFT SAMPLE TRIALS, SHORT DELAY
 5": ON^LEFTLIGHT; ON^RIGHTLIGHT; Z7   --->S17
 #R^LBAR: ADD C(24); ADD C(25)   --->SX
 #R^RBAR: ADD C(23); ADD C(25)   --->SX
 S17,
 3":OFF^LEFTLIGHT; OFF^RIGHTLIGHT;OFF^HOUSELIGHT;
 Z8; ADD C(26); SET P(E)=3   --->S2
 #R^LBAR: OFF^LEFTLIGHT; OFF^RIGHTLIGHT; OFF^HOUSELIGHT;
 Z8; ADD C(7); ADD C(30); ADD C(14); Z1; SET P(E)=2 --->S2
 #R^RBAR: OFF^LEFTLIGHT; OFF^RIGHTLIGHT;
 Z8; Z3; ADD C(8); ADD C(13); SET P(E)=1   --->S30
 S18,  \TEST PHASE, LEFT SAMPLE TRIALS, MEDIUM DELAY
 10": ON^LEFTLIGHT; ON^RIGHTLIGHT;Z7  --->S19
 #R^LBAR: ADD C(24); ADD C(25)   --->SX
 #R^RBAR: ADD C(23); ADD C(25)   --->SX
 S19,
 3": OFF^LEFTLIGHT; OFF^RIGHTLIGHT; OFF^HOUSELIGHT;
 Z8; ADD C(27); SET P(E)=3     --->S2
 #R^LBAR: OFF^LEFTLIGHT; OFF^RIGHTLIGHT; OFF^HOUSELIGHT;
```

```
Z8; ADD C(7); ADD C(30); ADD C(16); Z1; SET P(E)=2--->S2
#R^RBAR: OFF^LEFTLIGHT; OFF^RIGHTLIGHT;
Z8; Z9; Z3; ADD C(8); ADD C(15); SET P(E)=1   --->S30
S20,   \TEST PHASE, LEFT SAMPLE TRIALS, LONG DELAY
15": ON^LEFTLIGHT; ON^RIGHTLIGHT; Z7    --->S21
#R^LBAR: ADD C(24); ADD C(25)    --->SX
#R^RBAR: ADD C(23); ADD C(25)    --->SX
S21,
3": OFF^LEFTLIGHT; OFF^RIGHTLIGHT; OFF^HOUSELIGHT;
Z8; ADD C(28); SET P(E)=3      --->S2
#R^LBAR: OFF^LEFTLIGHT; OFF^RIGHTLIGHT; OFF^HOUSELIGHT;
Z8; ADD C(7); ADD C(18); ADD C(30); Z1; SET P(E)=2--->S2
#R^RBAR: OFF^LEFTLIGHT; OFF^RIGHTLIGHT;
Z8; Z3; ADD C(8); ADD C(17); SET P(E)=1   --->S30
\=============================================================
S24,  \TEST PHASE, RIGHT SAMPLE TRIALS, SHORT DELAY
5": ON^LEFTLIGHT; ON^RIGHTLIGHT; Z7    --->S25
#R^LBAR: ADD C(23); ADD C(25)   --->SX
#R^RBAR: ADD C(24); ADD C(25)   --->SX
S25,
 3": OFF^LEFTLIGHT; OFF^RIGHTLIGHT; OFF^HOUSELIGHT;
  Z8; ADD C(26);  SET P(E)=3     --->S2
 #R^LBAR: OFF^LEFTLIGHT; OFF^RIGHTLIGHT;
  Z8; Z3; ADD C(8); ADD C(13); SET P(E)=1   --->S30
 #R^RBAR: OFF^LEFTLIGHT; OFF^RIGHTLIGHT; OFF^HOUSELIGHT;
  Z8; ADD C(7); ADD C(14); ADD C(31); Z1; SET P(E)=2--->S2
S26,  \TEST PHASE, RIGHT SAMPLE TRIALS, MEDIUM DELAY
 10": ON^LEFTLIGHT; ON^RIGHTLIGHT; Z7    --->S27
 #R^LBAR: ADD C(23); ADD C(25)   --->SX
 #R^RBAR: ADD C(24); ADD C(25)   --->SX
S27,
 3": OFF^LEFTLIGHT; OFF^RIGHTLIGHT; OFF^HOUSELIGHT;
  Z8; ADD C(27); SET P(E)=3      --->S2
 #R^LBAR: OFF^LEFTLIGHT; OFF^RIGHTLIGHT;
  Z8; Z3; ADD C(8); ADD C(15); SET P(E)=1   --->S30
 #R^RBAR: OFF^LEFTLIGHT; OFF^RIGHTLIGHT; OFF^HOUSELIGHT;
  Z8; ADD C(7); ADD C(16); ADD C(31);Z1; SET P(E)=2 --->S2
 S28,  \TEST PHASE, RIGHT SAMPLE TRIALS, LONG DELAY
15": ON^LEFTLIGHT; ON^RIGHTLIGHT; Z7    --->S29
#R^LBAR: ADD C(23); ADD C(25)    --->SX
#R^RBAR: ADD C(24); ADD C(25)    --->SX
S29,
 3": OFF^LEFTLIGHT; OFF^RIGHTLIGHT; OFF^HOUSELIGHT;
  Z8; ADD C(28); SET P(E)=3      --->S2
 #R^LBAR: OFF^LEFTLIGHT; OFF^RIGHTLIGHT;
```

```
   Z8; Z3; ADD C(8); ADD C(17); SET P(E)=1   --->S30
  #R^RBAR: OFF^LEFTLIGHT; OFF^RIGHTLIGHT; OFF^HOUSELIGHT;
   Z8; ADD C(7); ADD C(18); ADD C(31); Z1; SET P(E)=2--->S2

 S30,
  3": OFF^HOUSELIGHT --->S2
  #R^LBAR: ADD C(4); ADD C(5) --->SX   \ADD HOUSELIGHT ITI PRESSES
  #R^RBAR: ADD C(4); ADD C(5) --->SX   \ADD HOUSELIGHT ITI PRESSES
\============================================================
S.S.2,   \SESSION TIMER
 S1,
 #START:--->S2
 S2,
 1': ADD M; SET Q(E)=M --->S2
\============================================================
S.S.3,  \WATER REWARD FOR SAMPLE PHASE
 S1,
 #START:--->S2
 S2,
  #Z2: ON^WATER--->S3
 S3,
 0.02": OFF^WATER--->S2

S.S.4,  \WATER REWARD FOR TEST PHASE
 S1,
 #START:--->s2
 S2,
 #Z3: ON^WATER--->S3
 S3,
 0.04": OFF^WATER--->S2
\============================================================
S.S.5,  \SAMPLE PHASE REACTION TIMER
  S1,
 #Z5: --->S2
  S2,
 .01": SET S(E)=0--->S3
  S3,
 0.01": SET S(E)= S(E)+0.01; --->S3
 #Z6:--->S1
S.S.6,  \TEST PHASE REACTION TIMER
  S1,
 #Z7: --->S2
  S2,
 .01": SET T(E)=0--->S3
  S3,
```

```
 0.01": SET T(E)= T(E)+0.01; --->S3
 #Z8:--->S1
\=============================================================
S.S.7,  \DUMMY SIGNAL TO USE AS MARKER FOR MISSES ON SPIKE2
 S1,
 #START:                  --->S2
 S2,
 #Z1: ON^DUMMY  --->S3
 S3,
 .04": OFF^DUMMY   --->S2
\=============================================================
S.S.8,  \CALCULATIONS AND SCREEN DISPLAY
 S1,
 #START:--->S2
 S2,
 .25":SET A(1)=(C(8)/(C(7)+C(8)+.0001))*100,   \% CORRECT ALL
 A(2)=(C(13)/(C(13)+C(14)+.0001))*100,  \% SHORT DELAY
 A(3)=(C(15)/(C(15)+C(16)+.0001))*100,  \% MEDIUM DELAY
 A(4)=(C(17)/(C(17)+C(18)+.0001))*100,  \% LONG DELAY
 A(5)=(C(19)/(C(19)+C(20)+.0001))*100,  \% LONGEST DELAY
 A(6)= (C(7)+C(8))  --->S3    \# VALID TRIALS
 S3,
  .25":  SHOW 1, # TRIALS,                E;
   SHOW 2,% OVERALL,                     A(1);
   SHOW 3,% SHORT,                       A(2);
   SHOW 4,% MED,                         A(3);
   SHOW 5,% LONG,                        A(4);
   SHOW 6, #LEFTSMISS,                   C(30);
   SHOW 7, #RIGHTSMISS,                  C(31);
   SHOW 8, #OMIT SHORT,                  C(26);
   SHOW 9, #OMIT MED,                    C(27);
   SHOW 10,#OMIT LONG,                   C(28);
   SHOW 11, #SAMPLE OMITS,               C(6);
   SHOW 12, #DARK IT       I             C(3);
   SHOW 13, #LIGHT ITI,                  C(4);
   SHOW 14, #DELAY CORRECT,              C(23);
   SHOW 15, #DELAY INCORRECT,            C(24);
   SHOW 16, #SAMPLE MISSES,              C(2);
   SHOW 17, VALID TRIALS,                A(6) --->S2
\=============================================================
```